Science Advances
AAAS

advances.sciencemag.org/cgi/content/full/6/45/eabd1951/DC1

Supplementary Materials for

Selective valorization of lignin to phenol by direct transformation of C_{sp2}–C_{sp3} and C–O bonds

Jiang Yan, Qinglei Meng*, Xiaojun Shen, Bingfeng Chen, Yang Sun, Junfeng Xiang, Huizhen Liu, Buxing Han*

*Corresponding author. Email: mengqinglei@iccas.ac.cn (Q.M.); hanbx@iccas.ac.cn (B.H.)

Published 6 November 2020, *Sci. Adv.* **6**, eabd1951 (2020)
DOI: 10.1126/sciadv.abd1951

This PDF file includes:

Supplementary Test

4-(1-Hydroxypropyl)phenol (**1a**):

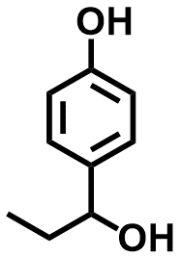

4-Hydroxybenzaldehyde (1.2 g, 10 mmol) was added into the solution of grignard reagent that was freshly prepared from bromoethane (3.3 g, 30 mmol) and magnesium turnings (0.7 g, 30 mmol) in anhydrous THF (20 mL) at 0 °C. The reaction mixture was stirred at room temperature for 1 h. After the reaction, the mixture was quenched with cold water (1 mL) and acidified with saturated NH_4Cl solution (20 mL). Ethyl acetate (50 mL) was added into the stirred organic layer at room temperature. The organic layer was then successively washed with deionized water (50 mL×3) and saturated brine (50 mL), dried by anhydrous $MgSO_4$. After the concentration in vacuum rotavap, 0.5 g of **1a** was obtained finally. ^{1}H NMR (400 MHz, DMSO-d6): δ 9.18 (s, 1H), 7.09~7.07 (d, 2H), 6.69~6.67 (d, 2H), 4.90~4.89 (d, 1H), 4.34~4.28 (q, 1H), 1.64~1.47 (m, 2H), 0.80~0.76 (t, 3H). ^{13}C NMR (101 MHz, DMSO-d6): δ 156.46, 136.87, 127.41, 115.06, 73.91, 32.51, 10.69.

1-(4-Methoxyphenyl)-1-propanol (**2a**):

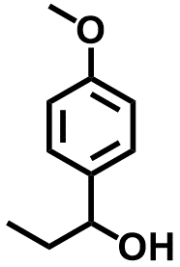

Sodium borohydride (3.8 g, 100 mmol) was added into the solution of 4'-methoxypropiophenone (16.4 g, 100 mmol) in THF/H_2O (100 mL/30 mL) at 0 °C. The reaction mixture was stirred at room temperature for 24 h. After the reaction, the mixture was sat for 10 min, and then the organic layer was separated. Ethyl acetate (50 mL) was added into the stirred organic layer at room temperature. The organic layer was then successively washed with deionized water (50 mL×3) and saturated brine (50 mL), dried by anhydrous $MgSO_4$. After the concentration in vacuum rotavap, 15.1 g of **2a** was obtained finally. ^{1}H NMR (400 MHz, DMSO-d6): δ 7.24~7.22 (d, 2H), 6.88~6.86 (d, 2H), 5.03~5.02 (d, 1H), 4.42~4.37 (q, 1H), 3.72 (s, 3H), 1.68~1.52 (m, 2H), 0.83~0.79 (t, 3H). ^{13}C NMR (101 MHz, DMSO-d6): δ 158.51, 138.62, 127.43, 113.70, 73.80, 55.38, 32.57, 10.58.

2-(2-Methoxyphenoxy)-1-(4-methoxyphenyl) propane-1, 3-diol (**3a**):

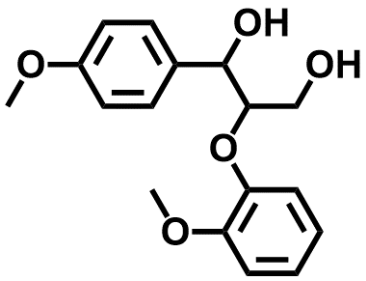

Bromine (33.6 g, 210 mmol) was added dropwise into the solution of 4'-methoxyacetophenone (30.1 g, 200 mmol) and $AlCl_3$ (667 mg, 5 mmol) in diethyl ether/tetrahydrofuran (50 mL/150 mL) at 0 °C~5 °C. The reaction mixture was then stirred at room temperature for 1h. After the reaction, the mixture was poured into ice water (1000 mL) and extracted by ethyl acetate (200 mL×2). The organic layer was then successively washed with deionized water (200 mL×3) and saturated brine (100 mL), dried by anhydrous $MgSO_4$ and concentrated in vacuum. Finally, 31.1 g of 2-bromo-1-(4-methoxyphenyl) ethanone was obtained by recrystallization process.

2-Methoxyphenol (16.4 g, 132 mmol) and K_2CO_3 (33.1 g, 240 mmol) were added into the solution of 2-bromo-1-(4-methoxyphenyl) ethanone (27.5 g, 120 mmol) in acetone (200 mL) at room temperature. The reaction mixture was stirred at room temperature for 24 h. After the reaction, the mixture was poured into 500 mL ice water and extracted by ethyl acetate (100 mL×2). The organic layer was then successively washed with deionized water (100 mL×3) and saturated brine (100 mL), dried by anhydrous $MgSO_4$ and concentrated in vacuum. Finally, 27.1 g of 2-(2-methoxyphenoxy)-1-(4-methoxyphenyl) ethanone was obtained by recrystallization process.

Formaldehyde solution (37%, 8.1 g, 99 mmol) and anhydrous K_2CO_3 (12.4 g, 90 mmol) were added into a solution of 2-(2-methoxyphenoxy)-1-(4-methoxyphenyl)-ethanone (24.5 g, 90 mmol) in acetone (200 mL) at room temperature. The reaction mixture was then stirred at room temperature for 1 h. After the reaction, the mixture was poured into 500 mL ice water and extracted by ethyl acetate (100 mL×2). The organic layer was then successively washed with deionized water (100 mL×3) and saturated brine (100 mL), dried by anhydrous $MgSO_4$ and concentrated in vacuum. Finally, 23.6 g of 3-hydroxy-2-(2-methoxyphenoxy)-1-(4-methoxyphenyl) propan-1-one was obtained by recrystallization process.

Sodium borohydride (2.3 g, 60 mmol) was added into the solution of 3-hydroxy-2-(2-methoxyphenoxy)-1-(4-methoxyphenyl) propan-1-one (18.1 g, 60 mmol) in THF/H_2O (100 mL/30 mL) at 0 °C. The reaction mixture was stirred at room temperature for 24 h. After the reaction, the mixture was sat for 10 min, and then the organic layer was separated. Ethyl acetate (50 mL) was added into the stirred organic layer at room temperature. The organic layer was then successively washed with deionized water (50 mL×3) and saturated brine (50 mL), dried by anhydrous $MgSO_4$. After the concentration in vacuum rotavap, 17.3 g of **3a** was obtained finally. ^{1}H NMR (400 MHz, DMSO-d6): δ 7.38~7.36 (m, 2H), 7.08~6.82 (m, 6H), 5.43~5.35 (q, 4H), 4.86~4.82 (m, 1H), 4.71~4.63 (m, 1H), 4.34~4.29 (m, 1H), 3.79~3.73 (m, 6H), 3.32~3.26 (m, 2H). ^{13}C NMR (101 MHz, DMSO-d6): δ 158.80, 158.78, 150.48, 150.41, 148.96, 148.57, 134.88, 134.52, 128.72, 128.39, 121.80, 121.75, 121.23, 121.19, 117.01, 116.89, 113.57, 113.50, 113.28, 113.20, 85.30, 84.65, 71.88, 71.38, 60.59, 60.49, 56.15, 55.43.

4-(1-Hydroxypropyl)-2-methoxyphenol (**4a**):

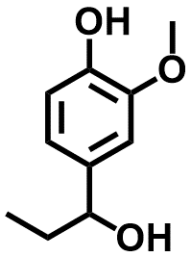

4-Hydroxy-3-methoxybenzaldehyde (1.5 g, 10 mmol) was added into the solution of grignard reagent that was freshly prepared from bromoethane (3.3 g, 30 mmol) and magnesium turnings (0.7 g, 30 mmol) in anhydrous THF (20 mL) at 0 °C. The reaction mixture was stirred at room temperature for 1 h. After the reaction, the mixture was quenched with cold water (1 mL) and acidified with saturated NH_4Cl solution (20 mL). Ethyl acetate (50 mL) was added into the stirred organic layer at room temperature. The organic layer was then successively washed with deionized water (50 mL×3) and saturated brine (50 mL), dried by anhydrous $MgSO_4$. After the concentration in vacuum rotavap, 0.9 g of **4a** was obtained finally. ^{1}H NMR (400 MHz, DMSO-d6): δ 8.69 (s, 1H), 6.90 (s, 1H), 6.72 (s, 2H), 4.95 (d, 1H), 4.36~4.35 (q, 1H), 3.77 (s, 3H), 1.67~1.55 (m, 2H), 0.85~0.81 (t, 3H). ^{13}C NMR (101 MHz, DMSO-d6): δ 147.72, 145.65, 137.71, 118.77, 115.36, 110.63, 74.18, 56.04, 32.55, 10.70.

1-(3, 4-Dimethoxyphenyl)propan-1-ol (**5a**):

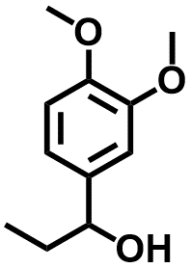

3, 4-Dimethoxybenzaldehyde (1.7 g, 10 mmol) was added into the solution of grignard reagent, freshly prepared from bromoethane (1.6 g, 15 mmol) and magnesium turnings (0.4 g, 15 mmol) in anhydrous THF (20 mL) at 0 °C. The reaction mixture was stirred at room temperature for 1 h. After the reaction, the mixture was quenched with cold water (1 mL) and acidified with saturated NH_4Cl solution (20 mL). Ethyl acetate (50 mL) was added into the stirred organic layer at room temperature. The organic layer was then successively washed with deionized water (50 mL×3) and saturated brine (50 mL), dried by anhydrous $MgSO_4$. After the concentration in vacuum rotavap, 1.7 g of **5a** was obtained finally. ^{1}H NMR (400 MHz, DMSO-d6): δ 6.91 (s, 1H), 6.88~6.86 (d, 1H), 6.81~6.79 (d, 1H), 4.99~4.98 (d, 1H), 4.39~4.34 (q, 1H), 3.74 (s, 3H), 3.72 (s, 3H), 1.65~1.53 (m, 2H), 0.83~0.79 (t, 3H). ^{13}C NMR (101 MHz, DMSO-d6): δ 148.99, 148.03, 139.31, 118.36, 111.96, 110.30, 73.96, 55.89, 32.53, 10.64.

1-(3,4-dimethoxyphenyl)-2-phenoxypropane-1,3-diol (**6a**):

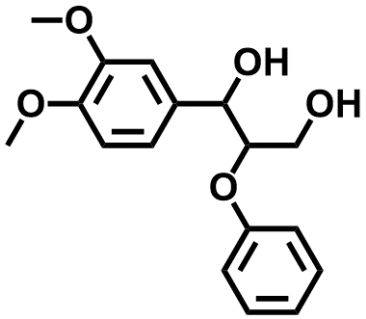

Bromine (33.6 g, 210 mmol) was added dropwise into the solution of 3', 4'-dimethoxyacetophenone (36.4 g, 200 mmol) and $AlCl_3$ (667 mg, 5 mmol) in diethyl ether/tetrahydrofuran (50 mL/150 mL) at 0 °C~5 °C. The reaction mixture was then stirred at room temperature for 1 h. After the reaction, the mixture was poured into ice water (1000 mL) and extracted by ethyl acetate (200 mL×2). The organic layer was then successively washed with deionized water (200 mL×3) and saturated brine (100 mL), dried by anhydrous $MgSO_4$ and concentrated in vacuum. Finally, 34.2 g of 2-bromo-1-(3, 4-dimethoxyphenyl)ethanone was obtained by recrystallization process.

Phenol (12.4 g, 132 mmol) and K_2CO_3 (33.1 g, 240 mmol) were added into the solution of 2-bromo-1-(3, 4-dimethoxyphenyl)ethanone (31.1 g, 120 mmol) in acetone (200 mL) at room temperature. The reaction mixture was stirred at room temperature for 24 h. After the reaction, the mixture was poured into 500 mL ice water and extracted by ethyl acetate (100 mL×2). The organic layer was then successively washed with deionized water (100 mL×3) and saturated brine (100 mL), dried by anhydrous $MgSO_4$ and concentrated in vacuum. Finally, 27.7 g of 1-(3,4-dimethoxyphenyl)-2-phenoxyethanone was obtained by recrystallization process.

Formaldehyde solution (37%, 8.9 g, 110 mmol) and anhydrous K_2CO_3 (13.8 g, 100 mmol) were added into a solution of 1-(3, 4-dimethoxyphenyl)-2-phenoxyethanone (27.2 g, 100 mol) in acetone (200 mL) at room temperature. The reaction mixture was then stirred at room temperature for 1 h. After the reaction, mixture was poured into 500 mL ice water and extracted by ethyl acetate (50 mL×2). The organic layer was then successively washed with deionized water (100 mL×3) and saturated brine (100 mL), dried by anhydrous $MgSO_4$ and concentrated in vacuum. Finally, 28.1 g of 1-(3, 4-dimethoxyphenyl)-3-hydroxy-2-phenoxypropan-1-one was obtained by recrystallization process.

Sodium borohydride (3.0 g, 80 mmol) was added into the solution of 1-(3, 4-dimethoxyphenyl)-3-hydroxy-2-phenoxypropan-1-one (24.2 g, 80 mmol) in THF/H_2O (100 mL/30 mL) at 0 °C. The reaction mixture was stirred at room temperature for 24 h. After the reaction, the mixture was sat for 10 min, and then the organic layer was separated. Ethyl acetate (50 mL) was added into the stirred organic layer at room temperature. The organic layer was then successively washed with deionized water (50 mL×3) and saturated brine (50 mL), dried by anhydrous $MgSO_4$. After the concentration in vacuum rotavap, 22.3 g of **6a** was obtained finally. ^{1}H NMR (400 MHz, DMSO-d6): δ 7.28~7.20 (m, 2H), 7.01~6.85 (m, 6H), 5.51~5.46 (q, 1H), 4.83~4.77 (m, 2H), 4.43~ 4.37 (m, 1H), 3.73 (m, 6H), 3.71~3.33 (m, 2H). ^{13}C NMR (101 MHz, DMSO-d6): δ 159.53, 159.25, 148.74, 148.71, 148.34, 148.31, 135.31, 129.76, 129.68, 120.85, 119.68, 119.23, 116.56, 116.38, 111.72, 111.68, 111.47, 111.11, 83.38, 71.95, 71.44, 60.55, 55.96, 55.94, 55.87, 55.85.

4-(1-Hydroxypropyl)-2, 6-dimethoxyphenol (**7a**):

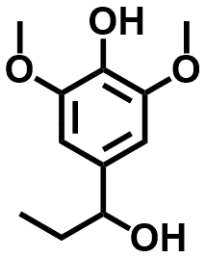

4'-Hydroxy-3', 5'-dimethoxybenzaldehyde (1.8 g, 10 mmol) was added into the solution of grignard reagent that was freshly prepared from bromoethane (3.3 g, 30 mmol) and magnesium turnings (0.7 g, 30 mmol) in anhydrous THF (20 mL) at 0 °C. The reaction mixture was stirred at room temperature for 1 h. After the reaction, the mixture was quenched with cold water (1 mL) and acidified with saturated NH_4Cl solution (20 mL). Ethyl acetate (50 mL) was added into the stirred organic layer at room temperature. The organic layer was then successively washed with deionized water (50 mL×3) and saturated brine (50 mL), dried by anhydrous $MgSO_4$. After the concentration in vacuum rotavap, 1.3 g of **7a** was obtained finally. ^{1}H NMR (400 MHz, DMSO-d6) δ 8.06 (s, 1H), 6.57 (s, 2H), 4.96 (d, 1H), 4.36~4.32 (q, 1H), 3.76 (s, 6H), 1.63~1.56 (m, 2H), 0.85~0.81 (t, 3H). ^{13}C NMR (101 MHz, DMSO-d6) δ 148.14, 136.91, 134.67, 103.91, 74.38, 56.42, 32.60, 10.71.

1-(3, 4, 5-Trimethoxyphenyl) propan-1-ol (**8a**):

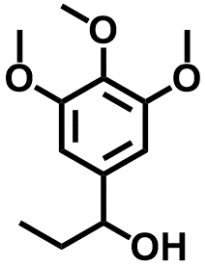

3, 4, 5-Trimethoxybenzaldehyde (2.0 g, 10 mmol) was added into the solution of grignard reagent that was freshly prepared from bromoethane (1.6 g, 15 mmol) and magnesium turnings (0.4 g, 15 mmol) in anhydrous THF (20 mL) at 0 °C. The reaction mixture was stirred at room temperature for 1 h. After the reaction, the mixture was quenched with cold water (1 mL) and acidified with saturated NH_4Cl solution (20 mL). Ethyl acetate (50 mL) was added into the stirred organic layer at room temperature. The organic layer was then successively washed with deionized water (50 mL×3) and saturated brine (50 mL), dried by anhydrous $MgSO_4$. After the concentration in vacuum rotavap, 2.0 g of **8a** was obtained finally. ^{1}H NMR (400 MHz, DMSO-d6): δ 6.62 (s, 2H), 5.07 (d, 1H), 4.39~4.36 (q, 1H), 3.76 (s, 6H), 3.63 (s, 3H), 1.63~1.56 (m, 2H), 0.86~0.83 (t, 3H). ^{13}C NMR (101 MHz, DMSO-D6): δ 153.01, 142.52, 136.59, 103.52, 74.24, 60.40, 56.24, 32.52, 10.69.

2-(2-Methoxyphenoxy)-1-(3, 4, 5-trimethoxyphenyl) propane-1, 3-diol (**9a**):

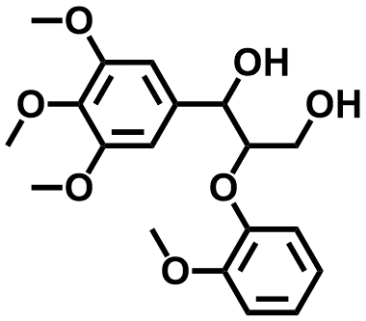

Bromine (33.6 g, 210 mmol) was added dropwise into the solution of 3', 4', 5'-trimethoxyacetophenone (42.0 g, 200 mmol) and $AlCl_3$ (667 mg, 5 mmol) in diethyl ether/tetrahydrofuran (50 mL/150 mL) at 0 °C~5 °C. The reaction mixture was then stirred at room temperature for 1h. After the reaction, the mixture was poured into ice water (1000 mL) and extracted by ethyl acetate (200 mL×2). The organic layer was then successively washed with deionized water (200 mL×3) and saturated brine (100 mL), dried by anhydrous $MgSO_4$ and concentrated in vacuum. Finally, 41.6 g of 2-bromo-1-(3, 4, 5-trimethoxyphenyl) ethanone was obtained by recrystallization process.

2-Methoxyphenol (16.4 g, 132 mmol) and K_2CO_3 (33.1 g, 240 mmol) were added into the solution of 2-bromo-1-(3, 4, 5-trimethoxyphenyl) ethanone (34.7 g, 120 mmol) in acetone (200 mL) at room temperature. The reaction mixture was stirred at room temperature for 24 h. After the reaction, the mixture was poured into 500 mL ice water and extracted by ethyl acetate (100 mL×2). The organic layer was then successively washed with deionized water (100 mL×3) and saturated brine (100 mL), dried by anhydrous $MgSO_4$ and concentrated in vacuum. Finally, 32.6 g of 2-(2-methoxy-phenoxy)-1-(3, 4, 5-trimethoxyphenyl) ethanone was obtained by recrystallization process.

Formaldehyde solution (37%, 7.1 g, 88 mmol) and anhydrous K_2CO_3 (12.1 g, 88 mmol) were added into a solution of 2-(2-methoxyphenoxy)-1-(3, 4, 5-trimethoxy-phenyl) ethanone (29.0 g, 80mol) in acetone (200 mL) at room temperature. The reaction mixture was then stirred at room temperature for 1 h. After the reaction, the mixture was poured into 500 mL ice water and extracted by ethyl acetate (100 mL×2). The organic layer was then successively washed with deionized water (100 mL×3) and saturated brine (100 mL), dried by anhydrous $MgSO_4$ and concentrated under vacuum. Finally, 24.1 g of 3-hydroxy-2-(2-methoxyphenoxy)-1-(3, 4, 5-trimethoxyphenyl) propan-1-one was obtained by recrystallization process.

Sodium borohydride (1.9 g, 50 mmol) was added into the solution of 3-hydroxy-2-(2-methoxyphenoxy)-1-(3, 4, 5-trimethoxyphenyl) propan-1-one (18.1 g, 50 mmol) in THF/H_2O (100 mL/30 mL) at 0 °C. The reaction mixture was stirred at room temperature for 24 h. After the reaction, the mixture was sat for 10 min, and then the organic layer was separated. Ethyl acetate (50 mL) was added into the stirred organic layer at room temperature. The organic layer was then successively washed with deionized water (50 mL×3) and saturated brine (50 mL), dried by anhydrous $MgSO_4$. After the concentration in vacuum rotavap, 17.3 g of **9a** was obtained finally. ^{1}H NMR (400 MHz, DMSO-d6): δ 7.05~6.79 (m, 4H), 6.74~6.72 (d, 2H), 5.46~5.42 (q, 1H), 4.81~4.76 (m, 1H), 4.75~4.63 (m, 1H), 4.37~4.33 (m, 1H), 3.76~3.27 (m, 14H). ^{13}C NMR (101 MHz, DMSO-d6): δ 152.78, 152.72, 150.16, 148.65, 148.48, 138.47, 138.14, 136.92, 136.84,

121.58, 121.44, 121.14, 121.06, 116.27, 116.14, 113.02, 112.98, 105.04, 104.42, 84.28, 83.80, 72.40, 71.38, 60.66, 60.53, 60.42, 60.39, 56.16, 56.13, 56.01, 55.98.

1-(4-Methoxyphenyl)ethanol (**10a**):

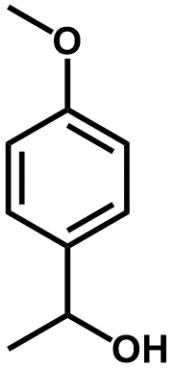

Sodium borohydride (0.4 g, 10 mmol) was added into the solution of 4'-methoxyacetophenone (1.5 g, 10 mmol) in THF/H_2O (10 mL/3 mL) at 0 °C. The reaction mixture was stirred at room temperature for 24 h. After the reaction, the mixture was sat for 10 min, and then the organic layer was separated. Ethyl acetate (50 mL) was added into the stirred organic layer at room temperature. The organic layer was then successively washed with deionized water (50 mL×3) and saturated brine (50 mL), dried by anhydrous $MgSO_4$. After the concentration in vacuum rotavap, 1.4 g of **10a** was obtained finally. ^{1}H NMR (400 MHz, DMSO-d6): δ 7.28~7.26 (d, 2H), 6.88~6.86 (d, 2H), 5.08~5.07 (d, 1H), 4.71~4.69 (q, 1H), 3.72 (s, 3H), 1.33~1.32 (t, 3H). ^{13}C NMR (101 MHz, DMSO-d6): δ 158.51, 139.91, 126.92, 113.79, 68.24, 55.39, 26.39.

1-(4-Methoxyphenyl)butan-1-ol (**11a**):

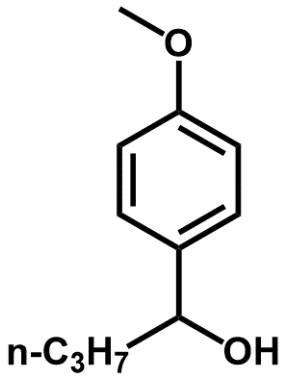

Sodium borohydride (0.4 g, 10 mmol) was added into the solution of 4'-methoxybutyrophenone (1.8 g, 10 mmol) in THF/H_2O (10 mL/3 mL) at 0 °C. The reaction mixture was stirred at room temperature for 24 h. After the reaction, the mixture was sat for 10 min, and then the organic layer was separated. Ethyl acetate (50 mL) was added into the stirred organic layer at room temperature. The organic layer was then successively washed with deionized water (50 mL×3) and saturated brine (50 mL), dried by anhydrous $MgSO_4$. After the concentration in vacuum rotavap, 1.4 g of **11a** was obtained finally. ^{1}H NMR (400 MHz, DMSO-d6): δ 7.24~7.22 (d, 2H), 6.87~6.85 (d, 2H), 4.99~4.97 (d, 1H), 4.97~4.45 (q, 1H), 3.72 (s, 3H), 1.66~1.46 (m, 2H),

1.40~1.16 (m, 2H), 0.88~0.84 (t, 3H). ^{13}C NMR (101 MHz, DMSO-d6): δ 158.50, 138.97, 127.36, 113.73, 72.16, 55.40, 42.09, 19.06, 14.35.

1-(4-Methoxyphenyl)heptan-1-ol (**12a**):

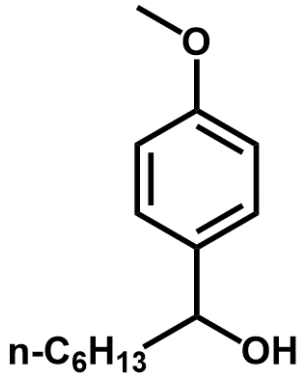

4'-Methoxybenzaldehyde (1.4 g, 10 mmol) was added into the solution of grignard reagent that was freshly prepared from 1-bromohexane (3.3 g, 20 mmol) and magnesium turnings (0.5 g, 20 mmol) in anhydrous THF (20 mL) at 0 °C. The reaction mixture was stirred at room temperature for 1 h. After the reaction, the mixture was quenched with cold water (1 mL) and acidified with saturated NH_4Cl solution (20 mL). Ethyl acetate (50 mL) was added into the stirred organic layer at room temperature. The organic layer was then successively washed with deionized water (50 mL×3) and saturated brine (50 mL), dried by anhydrous $MgSO_4$. After the concentration in vacuum rotavap, 1.8 g of **12a** was obtained finally. ^{1}H NMR (400 MHz, DMSO-d6): δ 7.23~7.21 (d, 2H), 6.87~6.85 (d, 2H), 4.98~4.97 (d, 1H), 4.47~4.45 (q, 1H), 3.72 (s, 3H), 1.63~1.53 (m, 2H), 1.40~1.04 (m, 8H), 0.85~0.82 (t, 3H). ^{13}C NMR (101 MHz, DMSO-d6): δ 158.50, 138.97, 127.33, 113.69, 72.47, 39.90, 31.85, 29.24, 25.85, 22.57, 14.32.

1-(4-Methoxyphenyl)tridecan-1-ol (**13a**):

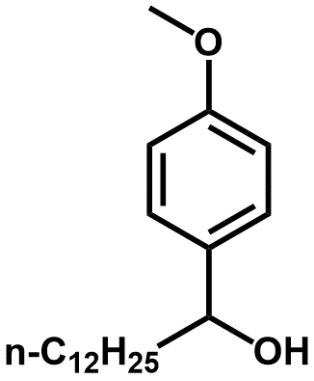

4'-Methoxybenzaldehyde (1.4 g, 10 mmol) was added into the solution of grignard reagent that was freshly prepared from 1-bromododecane (5.0 g, 20 mmol) and magnesium turnings (0.5 g, 20 mmol) in anhydrous THF (20 mL) at 0 °C. The reaction mixture was stirred at room temperature for 1 h. After the reaction, the mixture was quenched with cold water (1 mL) and acidified with saturated NH_4Cl solution (20 mL). Ethyl acetate (50 mL) was added into the stirred organic layer at room temperature. The organic layer was then successively washed with deionized

water (50 mL×3) and saturated brine (50 mL), dried by anhydrous $MgSO_4$. After the concentration in vacuum rotavap, 2.4 g of **13a** was obtained finally. ^{1}H NMR (400 MHz, DMSO-d6): δ 7.22~7.20 (d, 2H), 6.85~6.83 (d, 2H), 4.98~4.97 (d, 1H), 4.46~4.42 (q, 1H), 3.72 (s, 3H), 1.66~1.51 (t, 2H), 1.43~0.96 (m, 22H), 0.86~0.83 (t, 3H). ^{13}C NMR (101 MHz, DMSO-d6): δ 158.46, 138.93, 127.34, 113.72, 72.38, 55.43, 31.77, 29.52, 29.49, 29.47, 29.18, 25.80, 22.56, 14.38.

1-(4-Methoxy-phenyl)-3-phenylpropan-1-ol (**14a**):

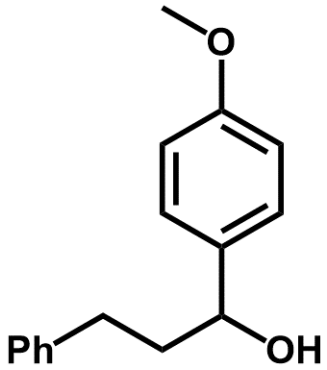

4'-Methoxybenzaldehyde (1.4 g, 10 mmol) was added into the solution of grignard reagent that was freshly prepared from 1-bromo-2-phenylethane (3.7 g, 20 mmol) and magnesium turnings (0.5 g, 20 mmol) in anhydrous THF (20 mL) at 0 °C. The reaction mixture was stirred at room temperature for 1 h. After the reaction, the mixture was quenched with cold water (1 mL) and acidified with saturated NH_4Cl solution (20 mL). Ethyl acetate (50 mL) was added into the stirred organic layer at room temperature. The organic layer was then successively washed with deionized water (50 ml×3) and saturated brine (50 mL), dried by anhydrous $MgSO_4$. After the concentration in vacuum rotavap, 1.9 g of **14a** was obtained finally. ^{1}H NMR (400 MHz, DMSO-d6): δ 7.29~7.25 (m, 4H), 7.19~7.15 (m, 3H), 6.91~6.89 (d, 2H), 5.21~5.20 (d, 1H), 4.52~4.51 (d, 1H), 3.74 (s, 3H), 2.67~2.54 (m, 2H), 1.95~1.87 (m, 2H). ^{13}C NMR (101 MHz, DMSO-d6): δ 158.55, 142.63, 138.58, 128.72, 128.69, 127.42, 126.04, 113.85, 71.75, 55.47, 41.52, 32.08.

1-(4-Methoxyphenyl)-4-phenylbutan-1-ol (**15a**):

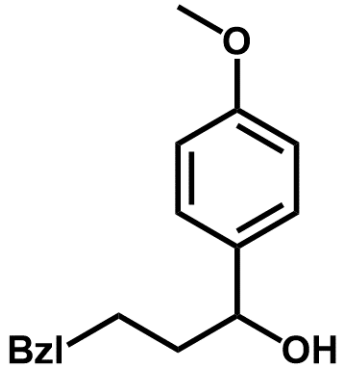

4'-Methoxybenzaldehyde (1.4 g, 10 mmol) was added into the solution of grignard reagent that was freshly prepared from 1-bromo-3-phenylpropane (4.0 g, 20 mmol) and magnesium turnings (0.5 g, 20 mmol) in anhydrous THF (20 mL) at 0 °C. The reaction mixture was stirred at

room temperature for 1 h. After the reaction, the mixture was quenched with cold water (1 mL) and acidified with saturated NH_4Cl solution (20 ml). Ethyl acetate (50 mL) was added into the stirred organic layer at room temperature. The organic layer was then successively washed with deionized water (50 mL×3) and saturated brine (50 mL), dried by anhydrous $MgSO_4$. After the concentration in vacuum rotavap, 1.7 g of **15a** was obtained finally. ^{1}H NMR (400 MHz, DMSO-d6): δ 7.28~7.23 (m, 4H), 7.16~7.14 (m, 3H), 6.89~6.87 (d, 2H), 5.10~5.09 (d, 1H), 4.53~4.52 (d, 1H), 3.73 (s, 3H), 2.57~2.55 (t, 2H), 1.71~1.47 (m, 2H). ^{13}C NMR (101 MHz, DMSO-d6): δ 158.49, 142.76, 138.83, 128.71, 128.66, 127.35, 126.04, 113.78, 72.19, 55.46, 35.55, 27.90.

2-(4-Methoxyphenyl)propan-2-ol (**16a**):

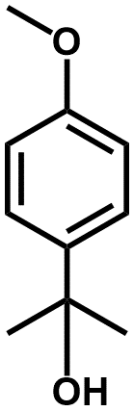

Methylmagnesium chloride solution (3.0 M in THF, 10 mL) was added into the solution of 4'-methoxyacetophenone (1.4 g, 10 mmol) in THF (20 mL) at 0 °C. The reaction mixture was stirred at room temperature for 1 h. After the reaction, the mixture was quenched with cold water (1 mL) and acidified with saturated NH_4Cl solution (20 mL). Ethyl acetate (50 mL) was added into the stirred organic layer at room temperature. The organic layer was then successively washed with deionized water (50 mL×3) and saturated brine (50 mL), dried by anhydrous $MgSO_4$. After the concentration in vacuum rotavap, 1.5 g of **16a** was obtained finally. ^{1}H NMR (400 MHz, DMSO-d6): δ 7.39~7.36 (d, 2H), 6.86~6.84 (d, 2H), 4.93 (s, 1H), 3.72 (s, 6H), 1.41 (s, 3H). ^{13}C NMR (101 MHz, DMSO-d6): δ 157.92, 143.12, 126.07, 113.45, 70.75, 55.41, 32.53.

1-(4-Methoxyphenyl)propan-2-ol (**18a**):

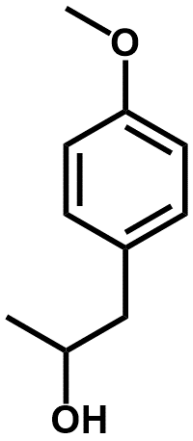

Sodium borohydride (0.4 g, 10 mmol) was added into the solution of 4'-methoxybutyrophenone (1.6 g, 10 mmol) in THF/H_2O (10 mL/3 mL) at 0 °C. The reaction mixture was stirred at room temperature for 24 h. After the reaction, the mixture was sat for 10 min, and then the organic layer was separated. Ethyl acetate (50 mL) was added into the stirred organic layer at room temperature. The organic layer was then successively washed with deionized water (50 mL×3) and saturated brine (50 mL), dried by anhydrous $MgSO_4$. After the concentration in vacuum rotavap, 1.6 g of **18a** was obtained finally. ^{1}H NMR (400 MHz, DMSO-d6): δ 7.15~7.13 (d, 2H), 6.86~6.84 (d, 2H), 4.58~4.57 (d, 1H), 3.88~3.79 (q, 1H), 3.73 (s, 3H), 2.73~2.51 (m, 2H), 1.09~1.07 (t, 3H). ^{13}C NMR (100MHz, DMSO-d6): δ 158.00, 131.92, 130.66, 113.87, 67.98, 55.29, 45.04, 23.38.

1-(1-Chloropropyl)-4-methoxybenzene (**19a**):

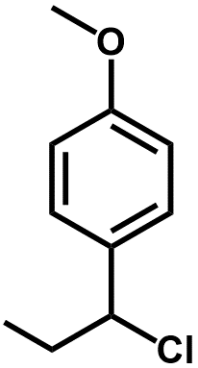

Thionyl chloride (4.2 g, 35 mmol) was added into the solution of 1-(4-methoxyphenyl) propan-1-ol (**2a**) (1.7 g, 10 mmol) in ethyl ether (50 mL) at 0 °C. The reaction mixture was stirred at 0 °C for 30 min. After the reaction, the mixture were then successively washed with ice water (50 mL×3) and saturated brine (50 mL), dried by anhydrous $MgSO_4$. Finally, 0.9 g of **19a** was obtained by silica gel column chromatography. ^{1}H NMR (400 MHz, DMSO-d6): δ 7.37~ 7.35 (d, 2H), 6.94~6.92 (d, 2H), 5.03~4.99 (t, 1H), 3.76 (s, 3H), 2.13~1.96 (m, 2H), 0.93~0.90 (t, 3H). ^{13}C NMR (101 MHz, DMSO-d6): δ 159.54, 134.01, 128.76, 114.29, 65.95, 55.53, 32.93, 12.03.

1-(1-Bromopropyl)-4-methoxybenzene (**20a**):

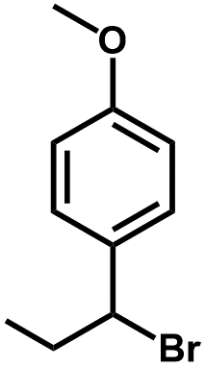

Phosphorus tribromide (9.5 g, 35 mmol) was added into the solution of 1-(4-methoxyphenyl) propan-1-ol (**2a**) (1.7 g, 10 mmol) in ethyl ether (50 mL) at 0 °C. The reaction mixture was stirred at 0 °C for 30 min. After the reaction, the mixture was successively washed with ice water (50 mL×3) and saturated brine (50 mL), dried by anhydrous $MgSO_4$. Finally, 0.9 g of **20a** was obtained by silica gel column chromatography. ^{1}H NMR (400 MHz, DMSO-d6): δ 7.37~7.35 (d, 2H), 6.94~6.92 (d, 2H), 5.02~4.99 (t, 3H), 3.76 (s, 3H), 2.15~1.96 (m, 2H), 0.93~0.90 (t, 3H). ^{13}C NMR (101 MHz, DMSO-d6): δ 159.54, 134.01, 128.75, 114.28, 65.94, 55.52, 32.94, 12.01.

1-(4-Methoxyphenyl)propyl acetate (**21a**):

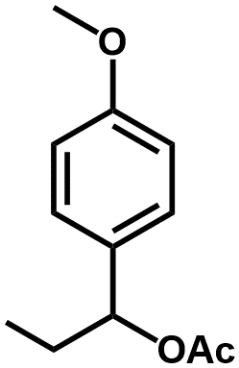

Triethylamine (1.5 g, 15 mmol) was added into the solution of 1-(4-methoxyphenyl) propan-1-ol (**2a**) (1.7 g, 10 mmol) and acetic anhydride (1.5 g, 15 mmol) in ethyl acetate (20 mL) at 0 °C. The reaction mixture was stirred at room temperature for 2 h. After the reaction, the mixture was poured into 100 mL ice water and extracted by ethyl acetate (20 mL×2). The organic layer was then successively washed with deionized water (20 mL×3) and saturated brine (20 mL), dried by anhydrous $MgSO_4$. Finally, 1.9 g of **21a** was obtained by silica gel column chromatography. ^{1}H NMR (400 MHz, DMSO-d6): δ 7.28~7.25 (q, 2H), 6.92~6.90 (m, 1H), 5.57~5.54 (t, 1H), 3.75 (s, 3H), 2.02 (s, 3H) 1.90~1.69 (m, 2H), 0.83~0.79 (t, 3H). ^{13}C NMR (100MHz, DMSO-d6): δ 170.15, 159.27, 132.91, 128.17, 114.14, 76.71, 55.47, 29.09, 21.32, 10.23.

1-(4-Methoxyphenyl)propyl benzoate (**22a**):

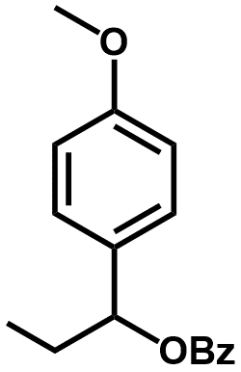

Benzoyl chloride (2.1 g, 15 mmol) was added into the solution of 1-(4-methoxyphenyl) propan-1-ol (**2a**) (1.7 g, 10 mmol) in pyridine (10 mL) at 0 °C. The reaction mixture was stirred at room temperature for 2 h. After the reaction, the mixture was poured into 100 mL ice water and extracted by ethyl acetate (20 mL×2). The organic layer was then successively washed with deionized water (20 mL×3) and saturated brine (20 mL), dried by anhydrous $MgSO_4$. Finally, 2.5 g of **22a** was obtained by silica gel column chromatography. ^{1}H NMR (400 MHz, DMSO-d6): δ 8.05~8.03 (d, 2H), 7.63~7.59 (t, 1H), 7.52~7.48 (t, 2H), 7.38~7.36 (d, 2H), 6.94~6.92 (d, 2H), 5.87~5.83 (t, 1H), 3.72 (s, 3H), 2.03~1.81 (m, 2H), 0.88~0.85 (t, 3H). ^{13}C NMR (101 MHz, DMSO-d6): δ 165.51, 159.38, 133.62, 132.85, 130.52, 129.58, 129.10, 128.15, 114.20, 77.59, 55.40, 29.35, 10.22.

Supplementary Figures

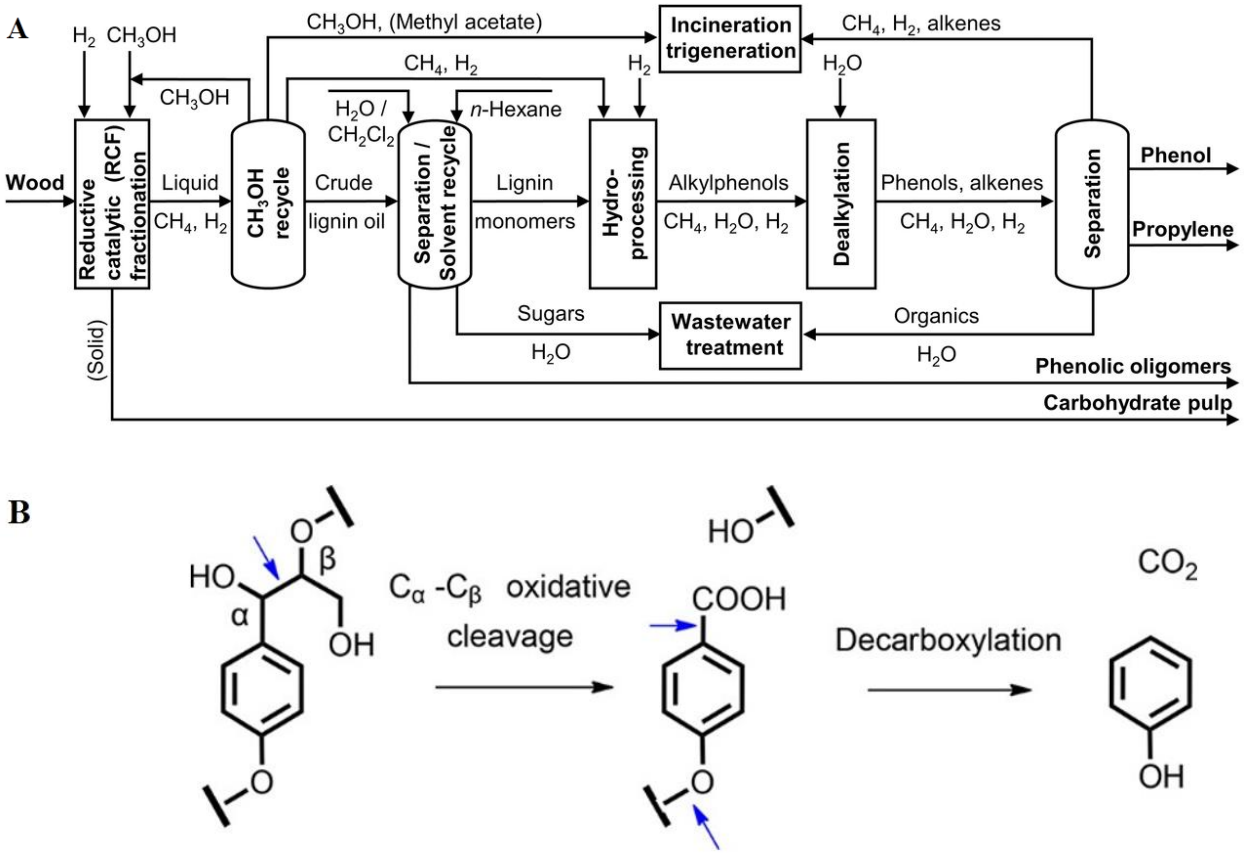

Fig. S1. Sustainable routes for phenol production. (**A**) Proposed integrated biorefinery process for phenol production from wood via sequential hydrogenolysis C-O bond and catalytic cracking of C-C bond (Ref. *12*). (**B**) Production of phenol from lignin via multiple oxidation cleavage of C-C bond and hydrogenolysis C-O bond (Ref. *13*).

A

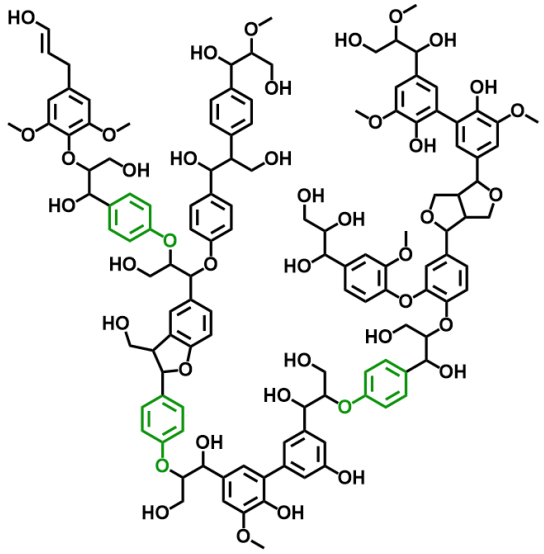

B

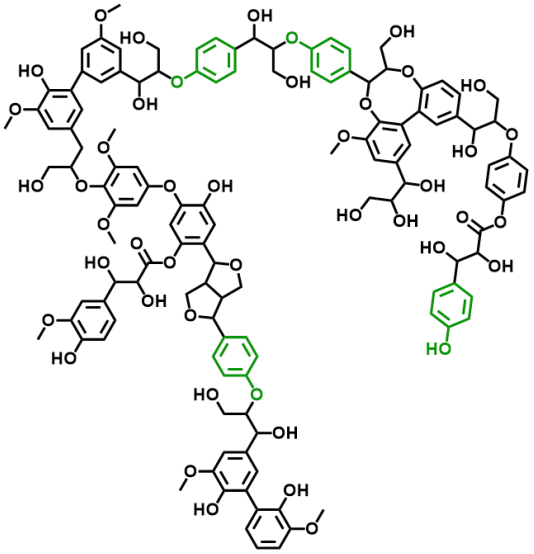

C

TABLE II
FUNCTIONAL GROUP CONTENT OF EAL AND MWL AS DETERMINED BY QUANTITATIVE ^{31}P-NMR[a]

Functional Group	Integrated Chemical Shift Range (ppm)	Poplar		Black Spruce	
		EAL	MWL	EAL	MWL
Aliphatic –OH	149.2–146.0	3.91	4.53	4.92	4.13
Guaiacyl –OH	140.0–138.8	0.33	0.37	0.72	0.67
p-Hydroxyl –OH	138.2–137.4	0.14	0.17	0.06	0.09
Syringyl –OH	143.1–142.38	0.23	0.24		
Ratio of G:H:S[b]		1.44:0.61:1	1.54:0.71:1		
Ratio of H:G[b]		0.43	0.48	0.09	0.13
Total Uncondensed Phenolic –OH		0.70	0.72	0.78	0.76
Condensed –OH	144.5–143.1 142.38–141.5	0.29	0.22	0.30	0.44
Total phenolic –OH		1.00 (0.21/C_9)	1.00 (0.21/C_9)	1.09 (0.21/C_9)	1.20 (0.23/C_9)
Total –OH		4.90	5.56	6.00	5.33
Carboxylic acids	135.5–134.5	0.11	0.14	0.09	0.11

(a) In mmol/g; error ±0.02.
(b) Refers to units bearing free phenolic OH; standardized by expressing the syringyl phenolics as unity.

D

Table 4 Molar ratio of syringaldehyde and *p*-hydroxybenzaldehyde to vanillin in the biomass samples studied as determined by alkaline nitrobenzene oxidation

Family	Sample number	Species	Lignin (g kg^{-1})	Vanillin	Syringaldehyde	*p*-Hydroxybenzaldehyde
Cupressaceae (softwood)	1	Japanese cedar	331	1	0	0.05
Fagaceae (hardwood)	2	Japanese beech	240	1	2.00	0
Haloragaceae	3	Parrot feather (aquatic plant)	175	1	1.00	0.76
Poaceae	4	Bamboo	206	1	1.28	0.45
(Gramineae)	5	Rice straw	202	1	0.67	0.52
	6	Rice husk	241	1	0.15	0.23
	7	Wheat straw	200	1	0.49	0.11
	8	Corn leaves	151	1	0.65	0.56
	9	Corn cob	180	1	0.64	0.77
	10	Erianthus	254	1	0.66	0.13
	11	Miscanthus	223	1	0.63	0.42
	12	Bagasse	224	1	0.80	0.19
	13	Sugarcane leaves	197	1	0.74	0.09
	14	Common reed	202	1	1.03	0.14
	15	Giant reed	249	1	1.09	0.23
Aracaceae	16	Oil palm trunk	282	1	3.50	0.00
(Palmae)	17	Nipa frond	196	1	1.20	0.03
	18	Sugar palm frond	209	1	1.56	0.13
Pontederiaceae (aquatic plants)	19	Water Hyacinth	101	1	0.84	0.67
Potamogetonaceae (aquatic plants)	20	Sennin-mo	149	1	1.43	2.47
Hydrocharitaceae (aquatic plants)	21	Okanada-mo	71	1	1.15	2.01
	22	Kuro-mo	79	1	1.26	1.76
	23	Kokanada-mo	76	1	0.70	0.93
Sargassaceae (brown algae)	24	Akamoku	142	1	0.23	2.70
	25	Sargassum	73	1	0.44	2.40
Ulvaceae (green algae)	26	Sea lettuce	33	1	1.36	0.11
	27	Chladophora	0	0	0	0
Caulerpaceae (green algae)	28	Caulerpa	37	1	1.25	1.95
	29	Sea grape	26	1	1.13	1.78
Chlorellaceae (green algae)	30	Chlorella	0	0	0	0
Solieraceae (red algae)	31	Eucheumia	18	1	1.24	0.90
Pseudanabaenaceae (blue-green algae)	32	Spirulina	0	0	0	0

Fig. S2. H (p-hydroxyphenl) unit in lignin. (**A**) Representative lignin structure of poplar (Ref. *57*). (**B**) Representative lignin structure of sugarcane bagasse (Ref. *58*). (**C**) The proportion of H unit in poplar lignin (Ref. *59*). (**D**) The proportion of H unit in herbaceous plant lignin (Ref. *60*).

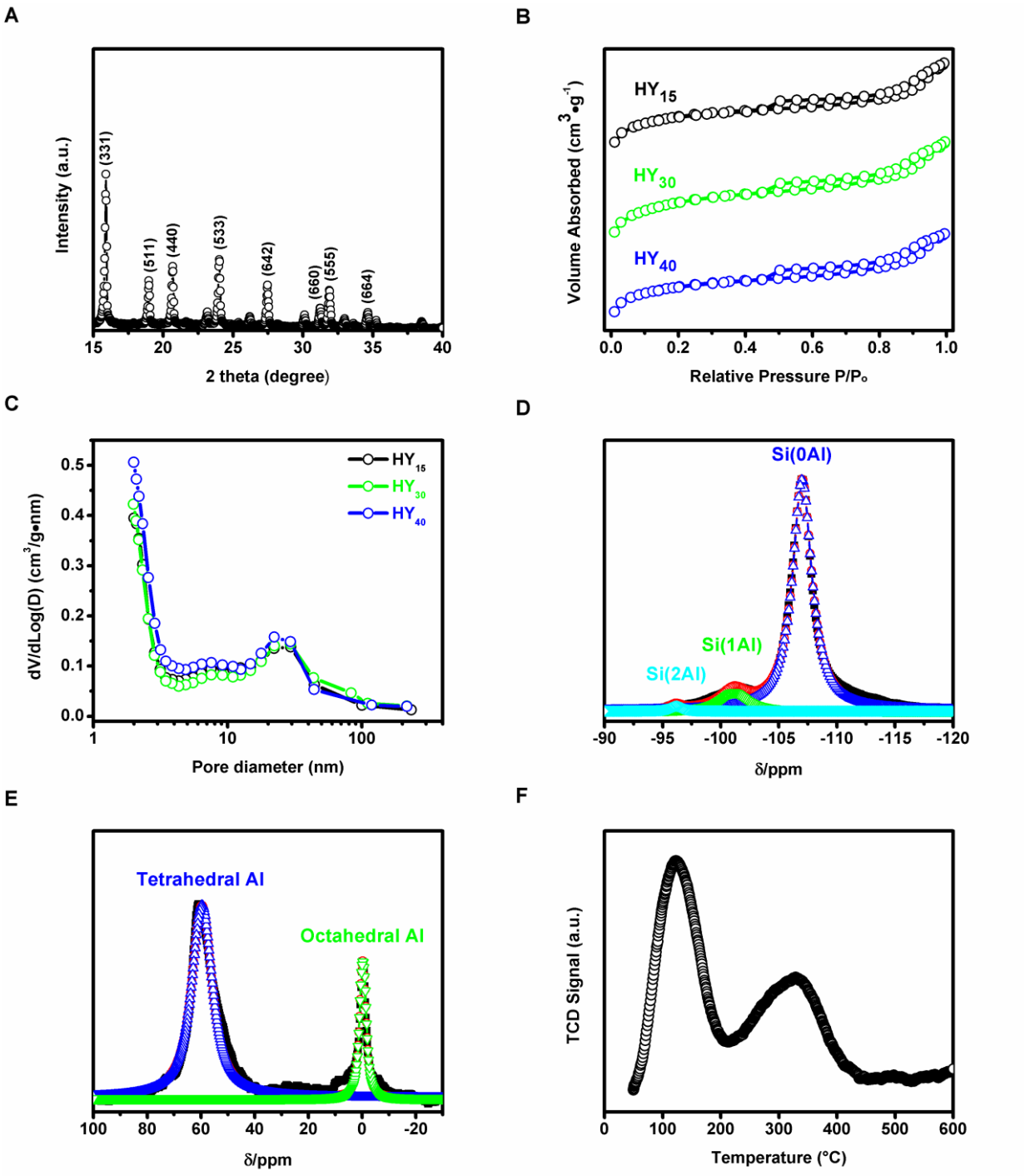
A
Intensity (a.u.)
(331)
(511)
(440)
(533)
(642)
(660)
(555)
(664)
2 theta (degree)
B
Volume Absorbed (cm3•g-1)
HY15
HY30
HY40
Relative Pressure P/Po
C
dV/dLog(D) (cm3/g•nm)
HY15
HY30
HY40
Pore diameter (nm)
D
Si(0Al)
Si(1Al)
Si(2Al)
δ/ppm
E
Tetrahedral Al
Octahedral Al
δ/ppm
F
TCD Signal (a.u.)
Temperature (°C)

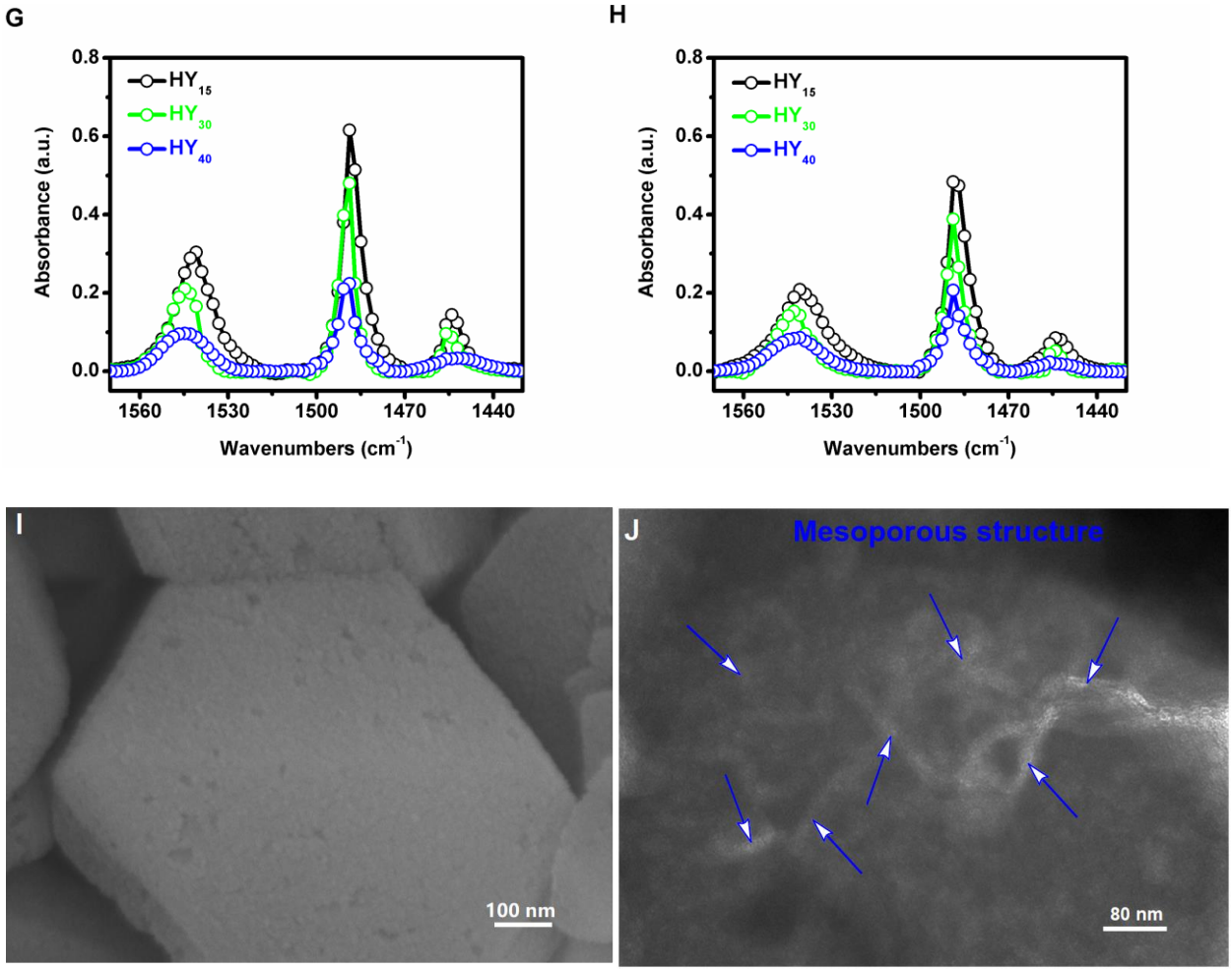

Fig. S3. Characterization of the HY_{30} zeolite. (**A**) X-ray diffraction. (**B**) Nitrogen adsorption–desorption isotherm. (**C**) Pore size distribution curve. (**D**) ^{29}Si MAS NMR spectra, black solid square (■) represents the observed intensities, red circle marks (○) is the total fitting curve, blue regular triangle upward (△), green regular triangle downward (▽) and cyan diamond (◇) represent the fitting curves of Si(0Al), Si(1Al) and Si(2Al), respectively. (**E**) ^{27}Al MAS NMR spectra, black solid square (■) represents the observed intensities, red circle marks (○) is the total fitting curve, blue regular triangle upward (△) and green regular triangle downward (▽) represent the fitting curves of tetrahedral Al and octahedral Al, respectively. (**F**) NH_3-TPD curve. (**G**) Py-FTIR spectrum (200 °C); (**H**) Py-FTIR spectrum (350 °C). (**I**) SEM image. (**J**) TEM image.

XRD patterns (Fig. S3A) showed that the HY_{30} zeolite was highly crystalline and exhibited typical characteristic peaks of faujasite structure. The nitrogen adsorption-desorption isotherms (Fig. S3B) exhibited Type IV isotherm which is characteristic of mesoporous structure with H-IV hysteresis loops in the HY_{30} zeolite with broad size distribution around 5-50 nm diameter. The micro/mesopore surface areas and volumes of HY_{15}, HY_{30} and HY_{40} zeolites are summarized in Table S2. ^{29}Si NMR spectrum (Fig. S3D) of the HY_{30} zeolite showed the presence of respective Si (0Al), Si (1Al), Si (2Al) species at -108, -103, -96 ppm, which was depending on the number of aluminum atoms connected to the silicon atom. ^{27}Al NMR spectrum (Fig. S3E) of the HY_{30} zeolite

shows the presence of octahedrally coordinated and tetrahedrally coordinated Al species at 0 ppm and 59.7 ppm, respectively. The NH_3-TPD profiles (Fig. S3F) of the HY_{30} zeolite is characteristic of two distinct NH_3 desorption peaks at lower (120 °C) and higher (310 °C) temperature, suggesting the weak and strong acid sites in the zeolite. The Py-FTIR analyses (Fig. S3G and S3H) were used to characterize the Brønsted and Lewis acid sites, which cannot be achieved by NH_3-TPD. The bands at 1540 cm^{-1} and 1450 cm^{-1} are assigned to the Brønsted and Lewis acid sites in the zeolite, respectively. The quantities of the Brønsted and Lewis acid sites in the HY_{15}, HY_{30} and HY_{40} zeolites were evaluated and summarized in Table S2, according to the equations in the literature 48. The SEM and TEM images are shown in Fig. S3I and S3J. The mesoporous structures in the HY_{30} zeolite can be observed in the TEM image (Fig. S3J).

A

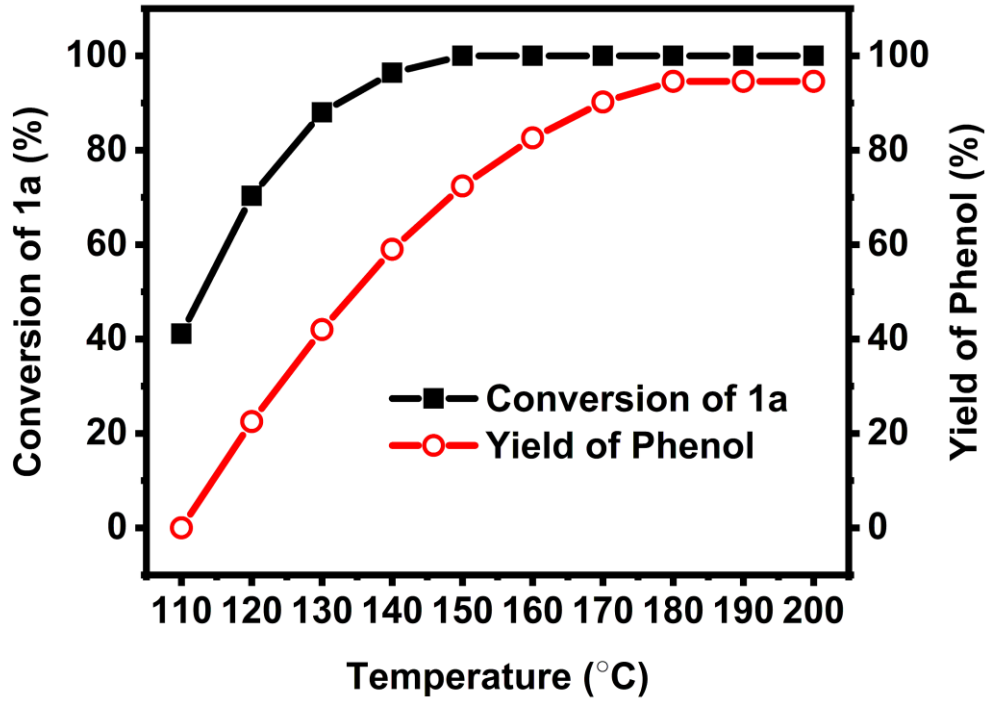
Conversion of 1a (%)
Yield of Phenol (%)
Conversion of 1a
Yield of Phenol
Temperature (°C)
0
20
40
60
80
100
110 120 130 140 150 160 170 180 190 200

B

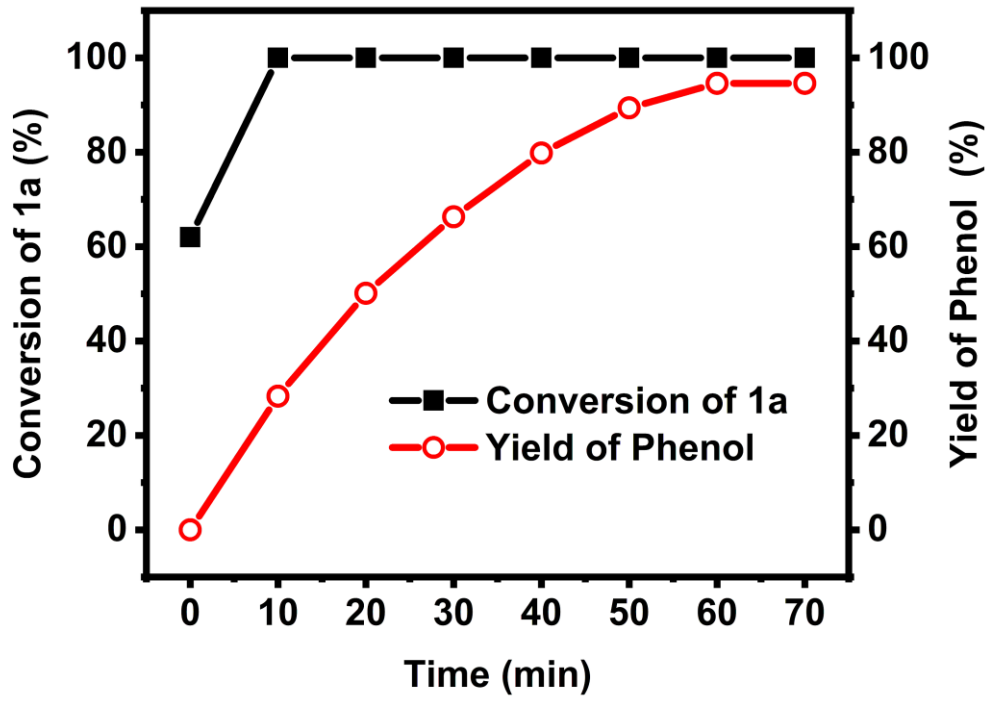
Conversion of 1a (%)
Yield of Phenol (%)
Conversion of 1a
Yield of Phenol
Time (min)
0
20
40
60
80
100
0 10 20 30 40 50 60 70

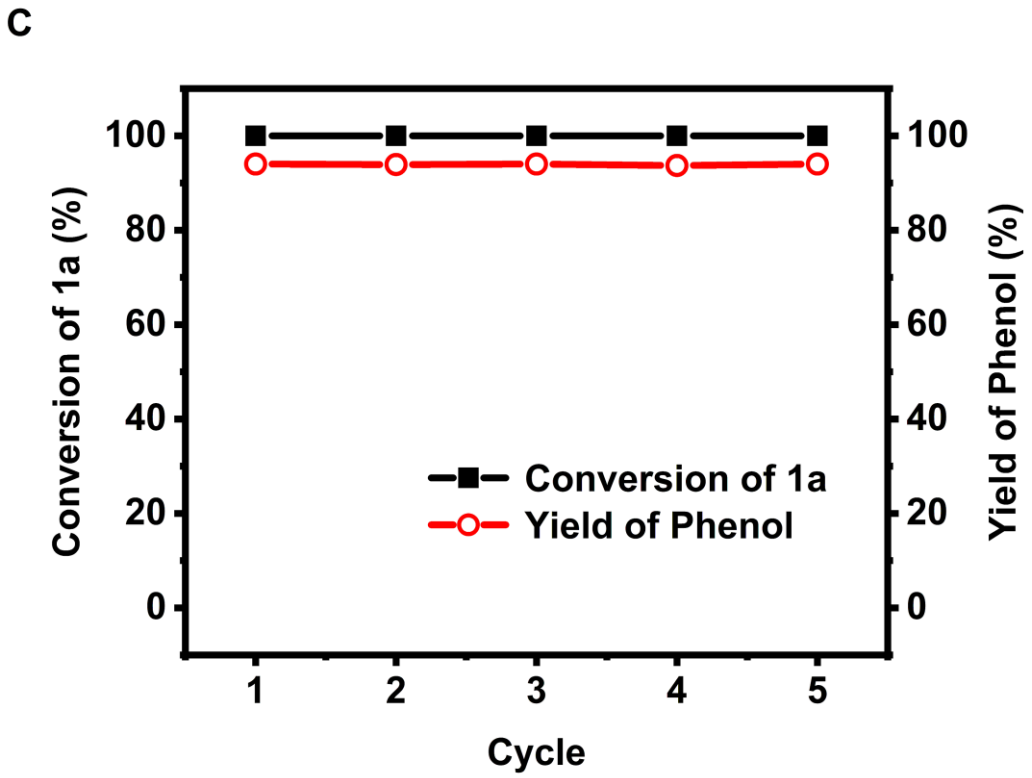

Fig. S4. Optimization of reaction conditions and reusability of the catalyst. (**A**) Effect of reaction temperature on the conversion of **1a** and yield of phenol over the HY_{30} catalyst. (**B**) Effect of reaction time on the conversion of **1a** and yield of phenol over the HY_{30} catalyst. (**C**) Reusability of the HY_{30} catalyst.

Reaction conditions: (**A**) **1a** (1 mmol), HY_{30} (0.3 g), H_2O (4.0 mL), 1 h, 0.5 MPa Ar, 800 rpm; (**B**) **1a** (1 mmol), HY_{30} (0.3 g), H_2O (4.0 mL), 180 °C, 0.5 MPa Ar, 800 rpm; (**C**) **1a** (1 mmol), HY_{30} (0.3 g, original dosage), H_2O (4.0 mL), 180 °C, 1 h, 0.5 MPa Ar, 800 rpm.

The effect of temperature and reaction time on the catalytic reaction over the HY_{30} catalyst, reusability of the HY_{30} catalyst are shown in fig. S4. As shown in Fig. S4A, HY_{30} catalyst could promote the transformation of **1a** even at lower temperatures ranging between 110 and 150 °C, but only low yield of phenol was observed. With further increase of temperature, HY_{30} catalyst gave increased yield of phenol at full conversion of **1a**, affording highest yield at 180 °C. The reaction was subsequently performed at 180 °C to study the effect of reaction time on the conversion and yield of the reaction (Fig. S4B). It can be found that the conversion of **1a** increased with extending the reaction time at beginning and became independent of reaction time when the time was longer than 10 min. However, the yield of phenol increased more slowly, and became independent of reaction time when the time was longer than 1 h. The conversion of **1a** and yield to phenol did not change notably after the HY_{30} catalyst was reused five times (Fig. S4C), which indicates the excellent stability of the HY_{30} catalyst.

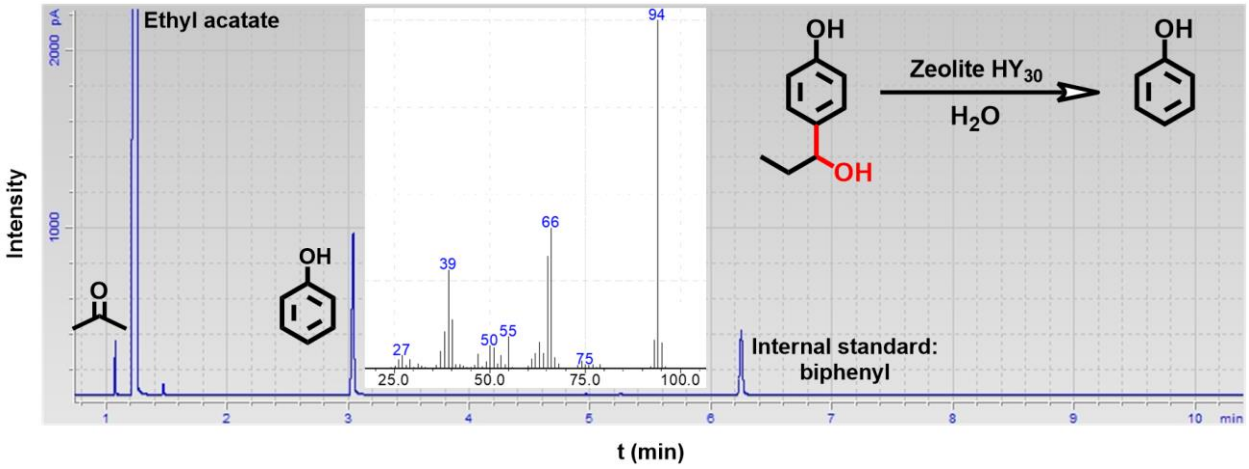

Fig. S5. GC trace of the liquid products generated from the transformation of the 4-(1-hydroxypropyl)phenol (1a).

Reaction conditions: **1a** (1 mmol), HY_{30} (0.3 g), H_2O (4.0 mL), 180 °C, 1 h, 0.5 MPa Ar, 800 rpm.

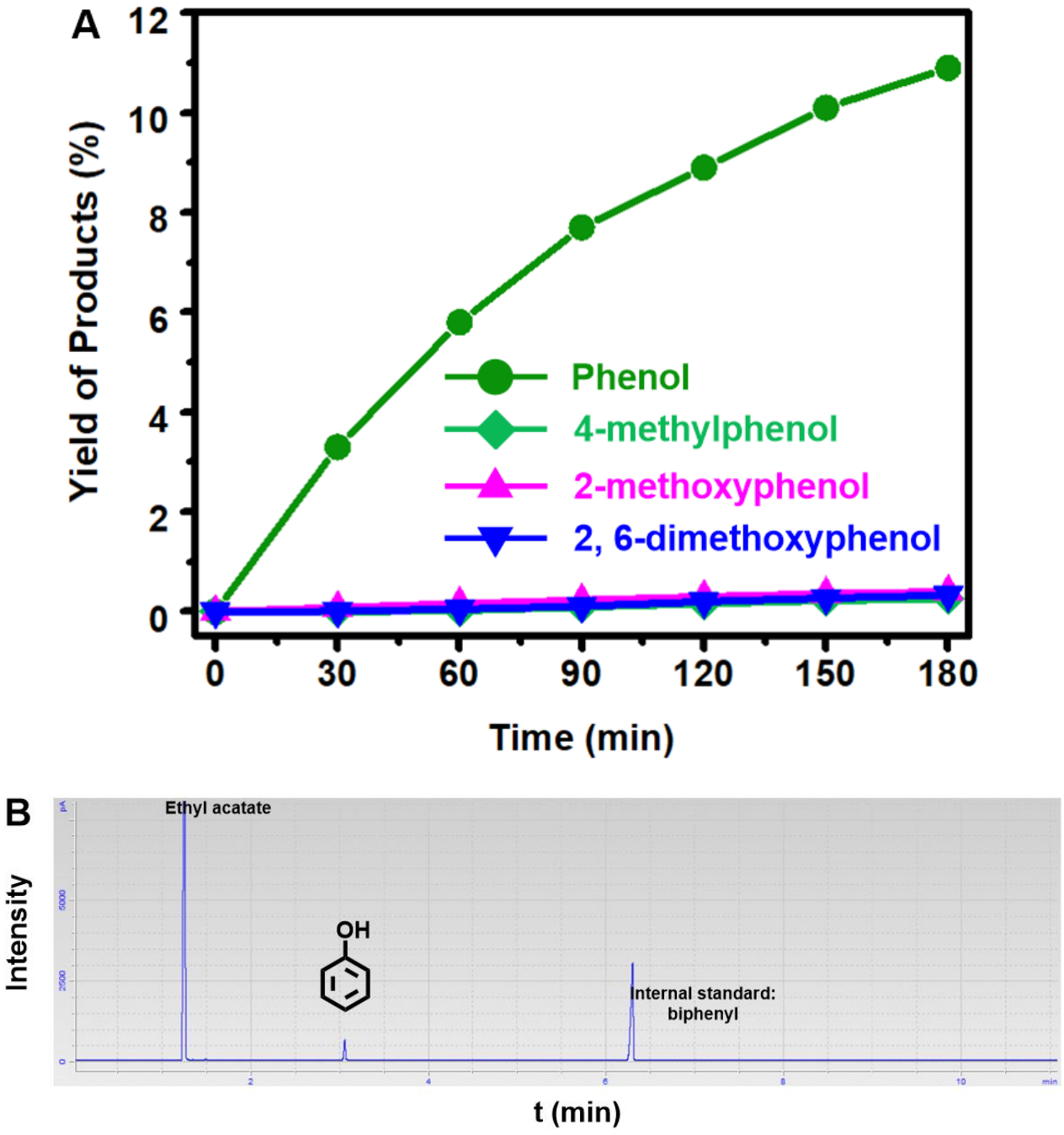
A
Yield of Products (%)
0
2
4
6
8
10
12
0
30
60
90
120
150
180
Time (min)
Phenol
4-methylphenol
2-methoxyphenol
2, 6-dimethoxyphenol
B
Intensity
Ethyl acatate
OH
Internal standard:
biphenyl
t (min)

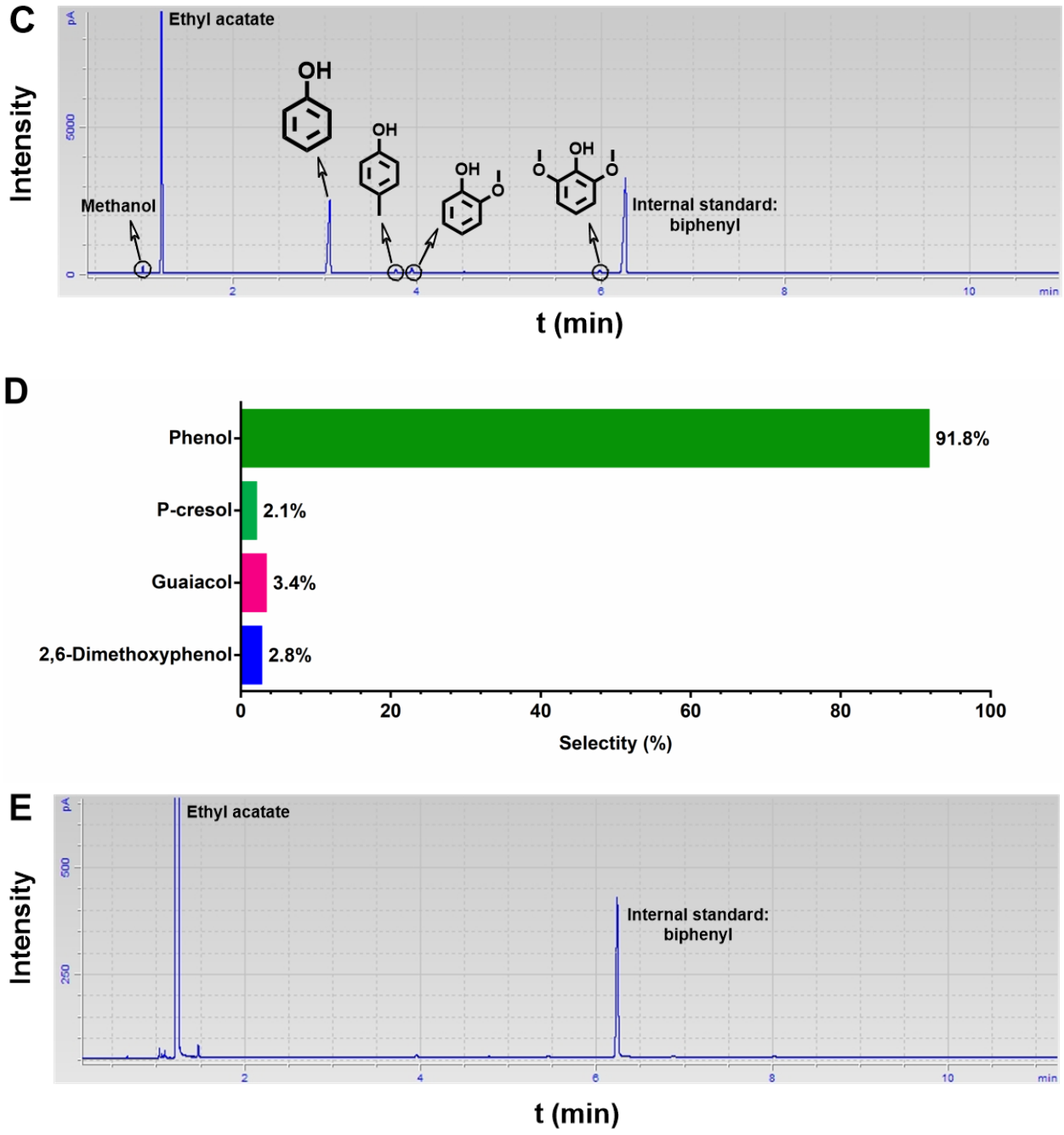

Fig. S6. Distribution of liquid products generated from the transformation of poplar lignin. (A) Time course of lignin depolymerization. (B) GC trace of the liquid products from lignin transformation over the HY_{30} catalyst in 30 min. (**C**) GC trace of the liquid products from lignin transformation over the HY_{30} catalyst in 3 h. (D) Selectivities of the liquid product from lignin

transformation over the HY_{30} catalyst. (**E**) GC trace of the liquid products from lignin transformation without catalyst.

Reaction conditions: (A) lignin (0.4 g), HY_{30} (0.4 g), H_2O (5.0 mL), 200 °C, 0.5 MPa Ar, 800 rpm. (B) lignin (0.4 g), HY_{30} (0.4 g), H_2O (5.0 mL), 200 °C, 30 min, 0.5 MPa Ar, 800 rpm. (**C**) and (**D**) lignin (0.4 g), HY_{30} (0.4 g), H_2O (5.0 mL), 200 °C, 3 h, 0.5 MPa Ar, 800 rpm. (**E**) lignin (0.4 g), H_2O (5.0 mL), 200 °C, 3 h, 0.5 MPa Ar, 800 rpm.

Based on the time course (Fig. S6A) and GC results (Fig. S6B), the intermediates bearing the benzylalcohol structure or alkyl side-chain were not detected, which confirmed that the phenol product could be obtained directly from the lignin structure via the simultaneous deconstruction of the C_{sp2}-C_{sp3} bonds and hydrolysis of the aliphatic C_β-O bonds. As shown in Fig. S6C, phenol, 2-methoxyphenol and 2, 6-methoxyphenol were yielded from lignin, with selectivities of 91.8%, 3.4% and 2.8%, respectively (Fig. S6D). Besides, it is reasonable to deduce that 4-methylphenol, with a selectivity of 2.1%, should be generated from the methylation of the yielded phenol, using the methoxy group-derived methyl in lignin (*32*). For comparison, the reaction of the lignin was also performed without the catalyst under the same conditions, which could not yield any low-molecular weight products (Fig. S6E).

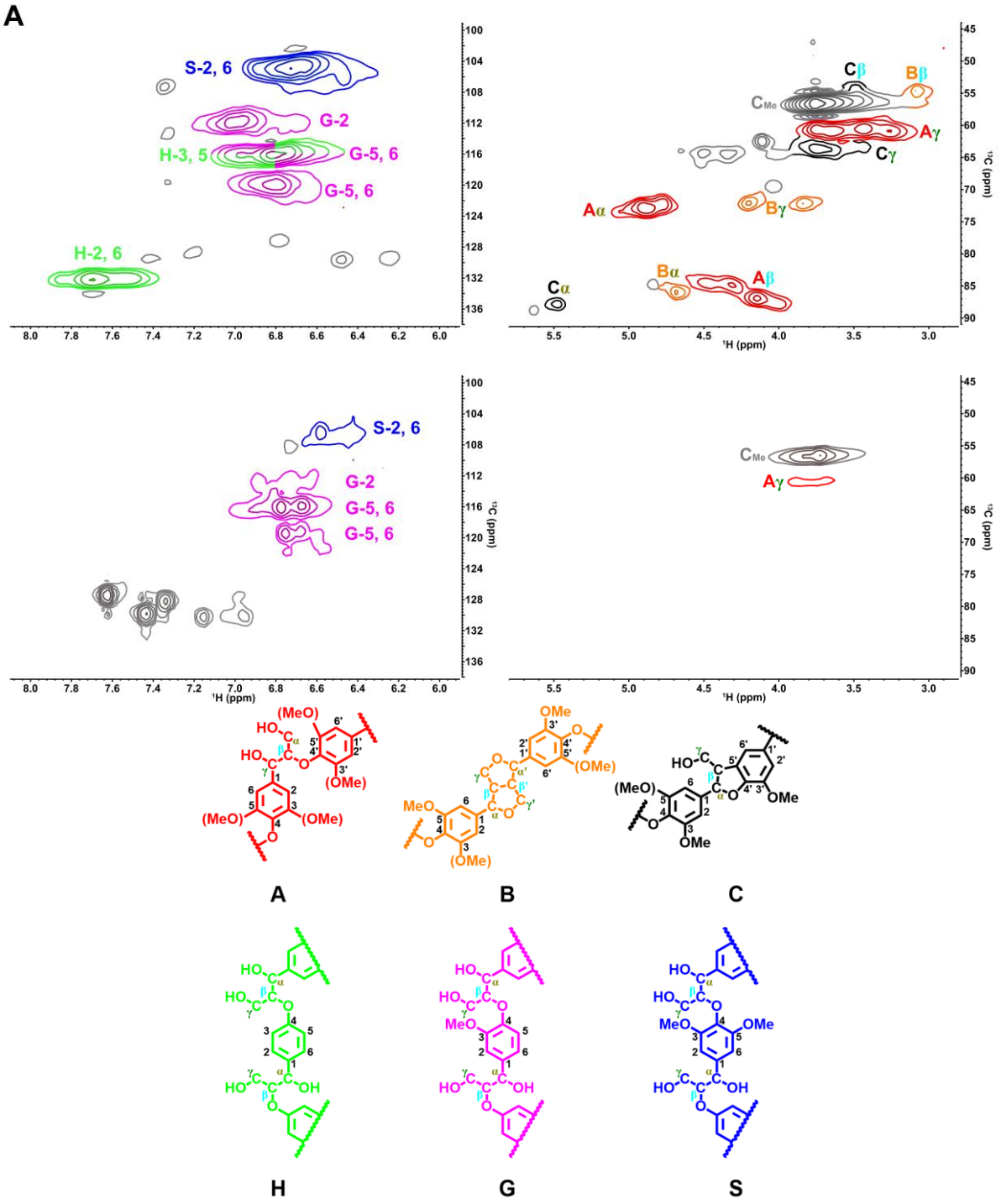

Fig. S7. $^{1}H/^{13}C$ 2D-HSQC NMR spectra of the poplar lignin. (**A**) The extracted poplar lignin before the transformation. (**B**) the residual solid after the transformation.

(A) β-aryl ether (β-O-4); (B) resinol (β-β); (C) phenylcoumaran (β-5); (H) p-hydroxyphenl unit; (G) guaiacyl unit; (S) syringyl unit; C_{Me}, the C atom in the methoxy group.

Reaction conditions: lignin (0.4 g), HY_{30} (0.4 g), H_2O (5.0 mL), 200 °C, 3 h, 0.5 MPa Ar, 800 rpm.

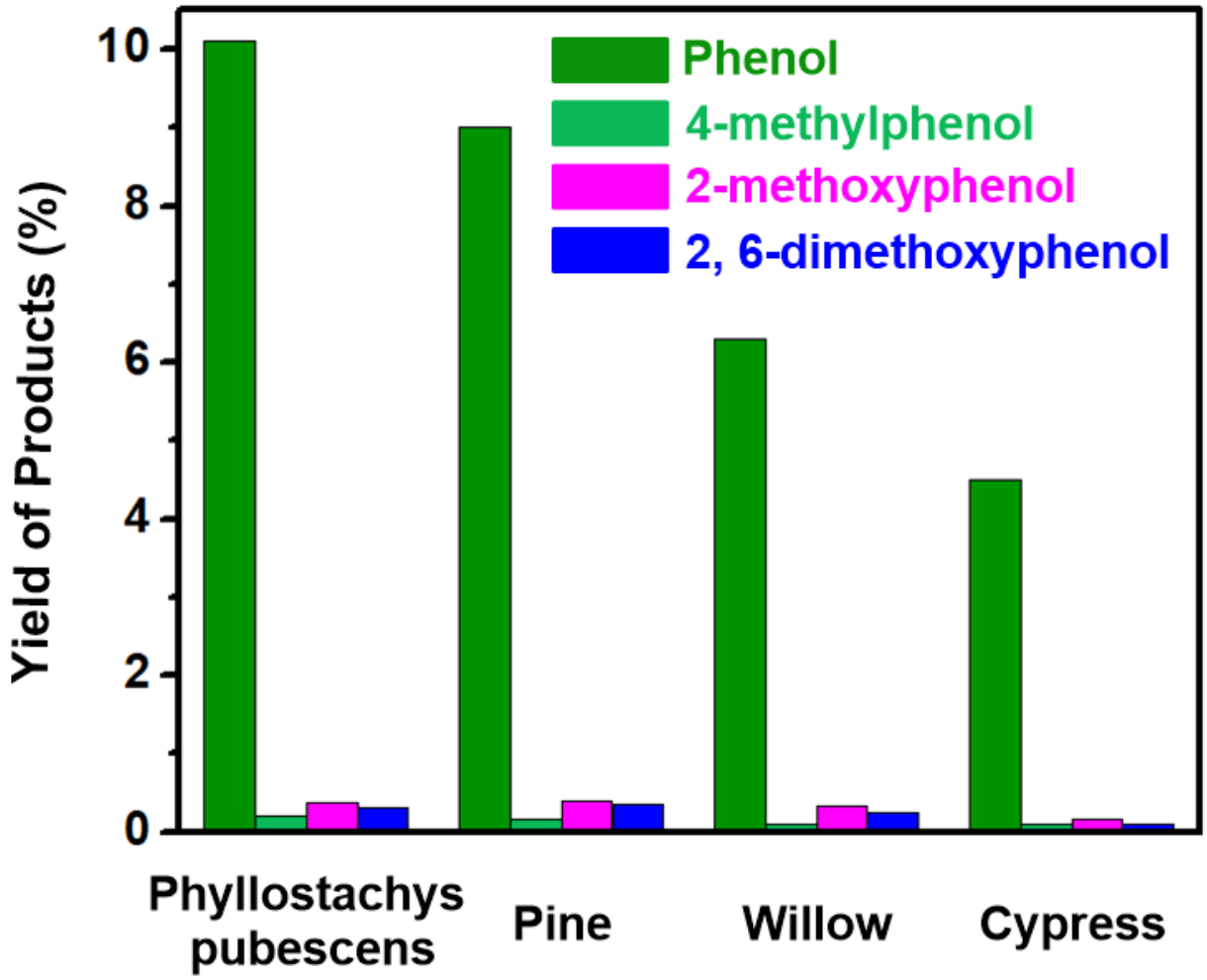

Fig. S8. Distribution of liquid products generated from the different kinds of lignin.

Reaction conditions: lignin (0.4 g), HY_{30} (0.4 g), H_2O (5.0 mL), 200 °C, 3 h, 0.5 MPa Ar, 800 rpm.

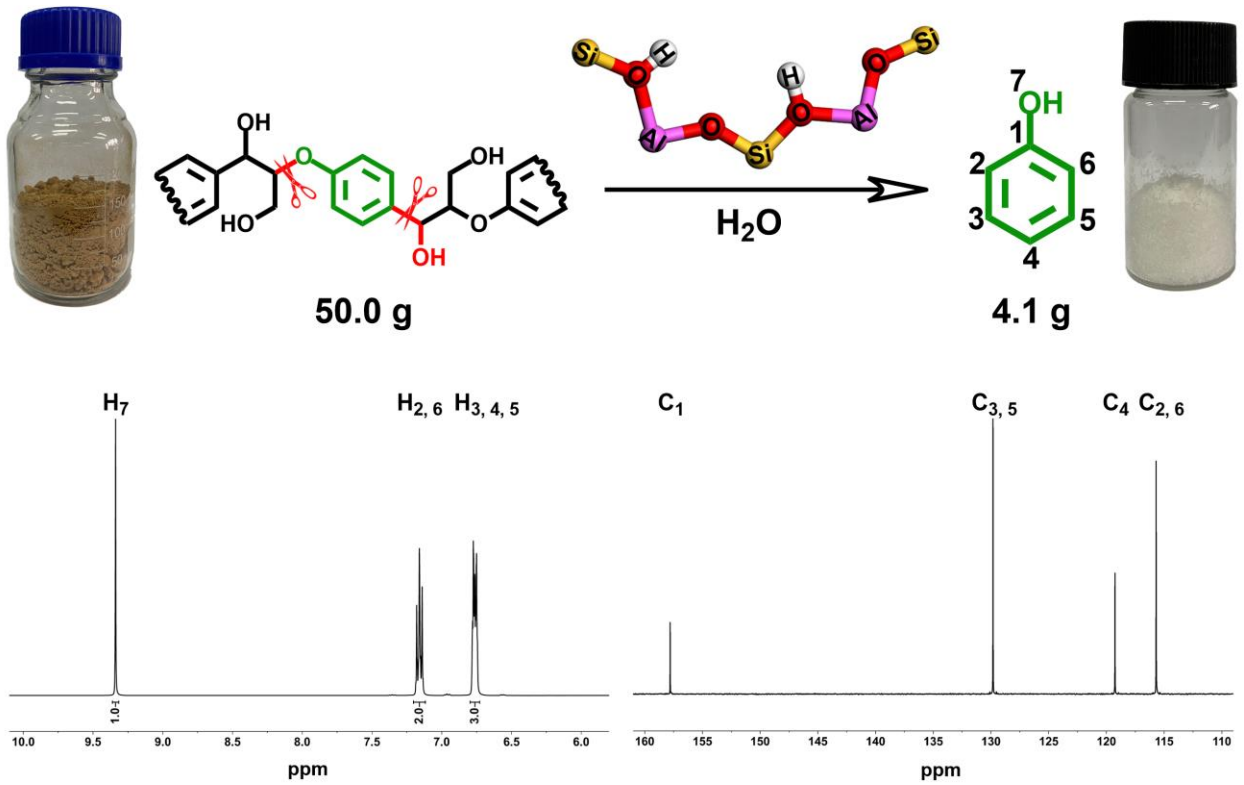

Fig. S9. The scale-up experiment of the poplar lignin transformation.

Reaction conditions: lignin (50.0 g), HY_{30} (50.0 g), H_2O (600 mL), 200 °C, 3 h, 0.5 MPa Ar, 800 rpm. Photo Credit: Qinglei Meng, Institute of Chemistry, Chinese Academy of Sciences.

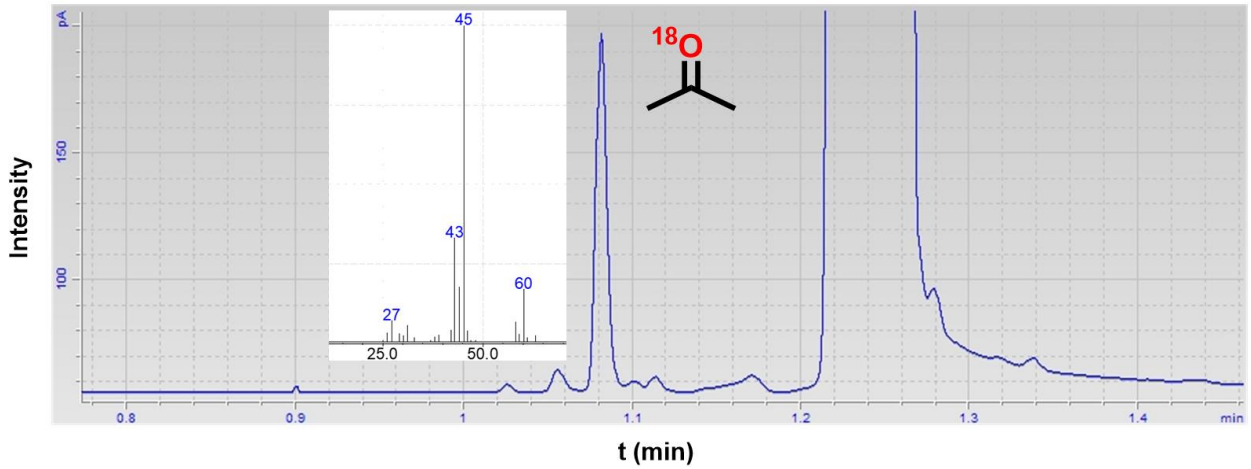

Fig. S10. Isotope labelling test of 4-(1-hydroxypropyl)phenol (1a) transformation in $H_2{}^{18}O$.

Reaction conditions: **1a** (1 mmol), HY_{30} (0.3 g), $H_2{}^{18}O$ (4.0 mL), 180 °C, 1 h, 0.5 MPa Ar, 800 rpm.

A

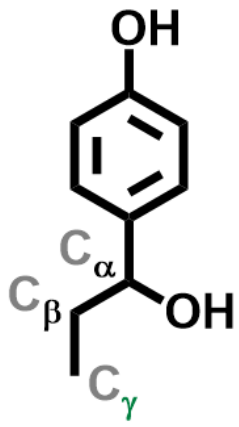

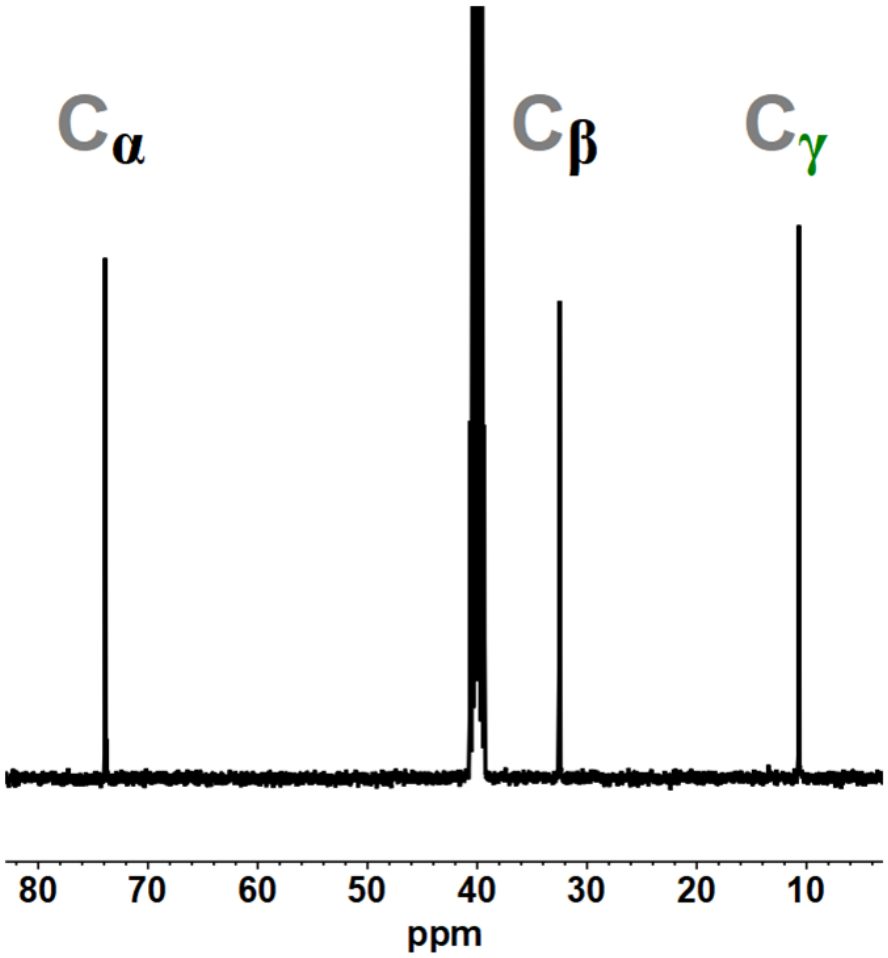

B

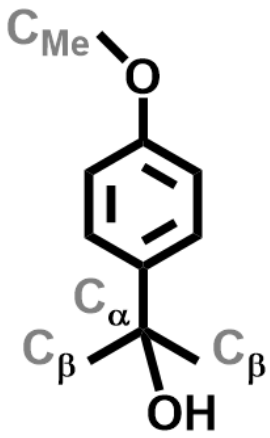

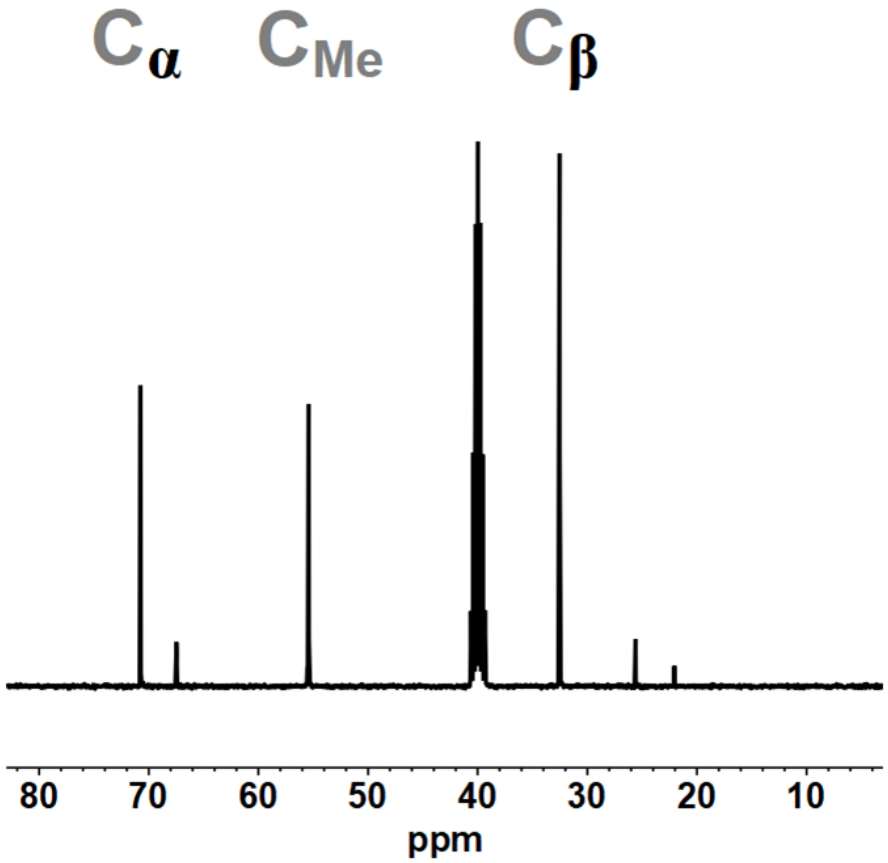

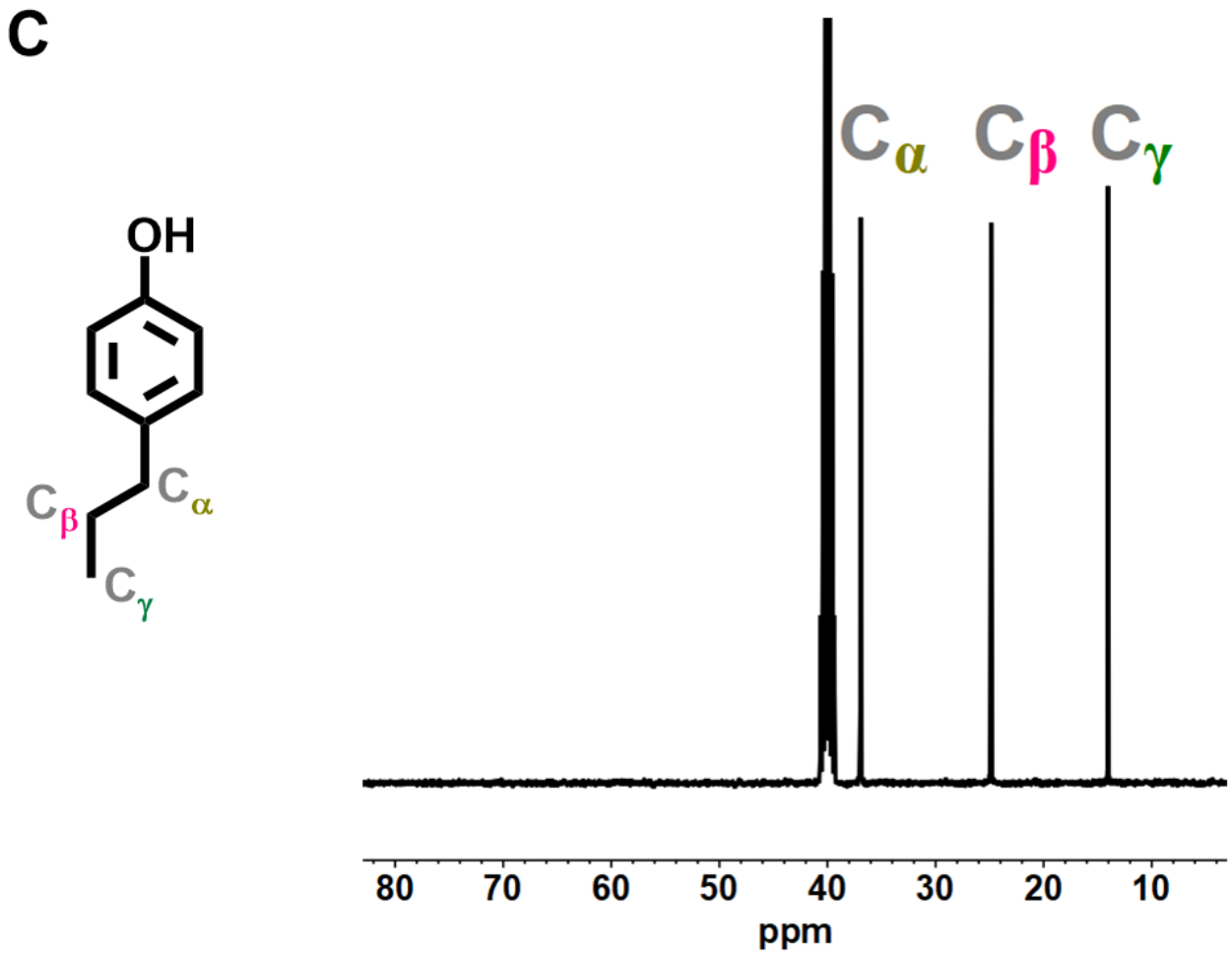

Fig. S11. ^{13}C NMR spectra of the model compounds in aliphatic region. (**A**) 4-(1-hydroxypropyl)phenol (**1a**). (**B**) 2-(4-methoxyphenyl) propan-2-ol (**16a**). (**C**) 4-n-propylphenol. C_α, C_β and C_γ represent the C atoms at the aliphatic α-C, β-C and γ-C positions, respectively.

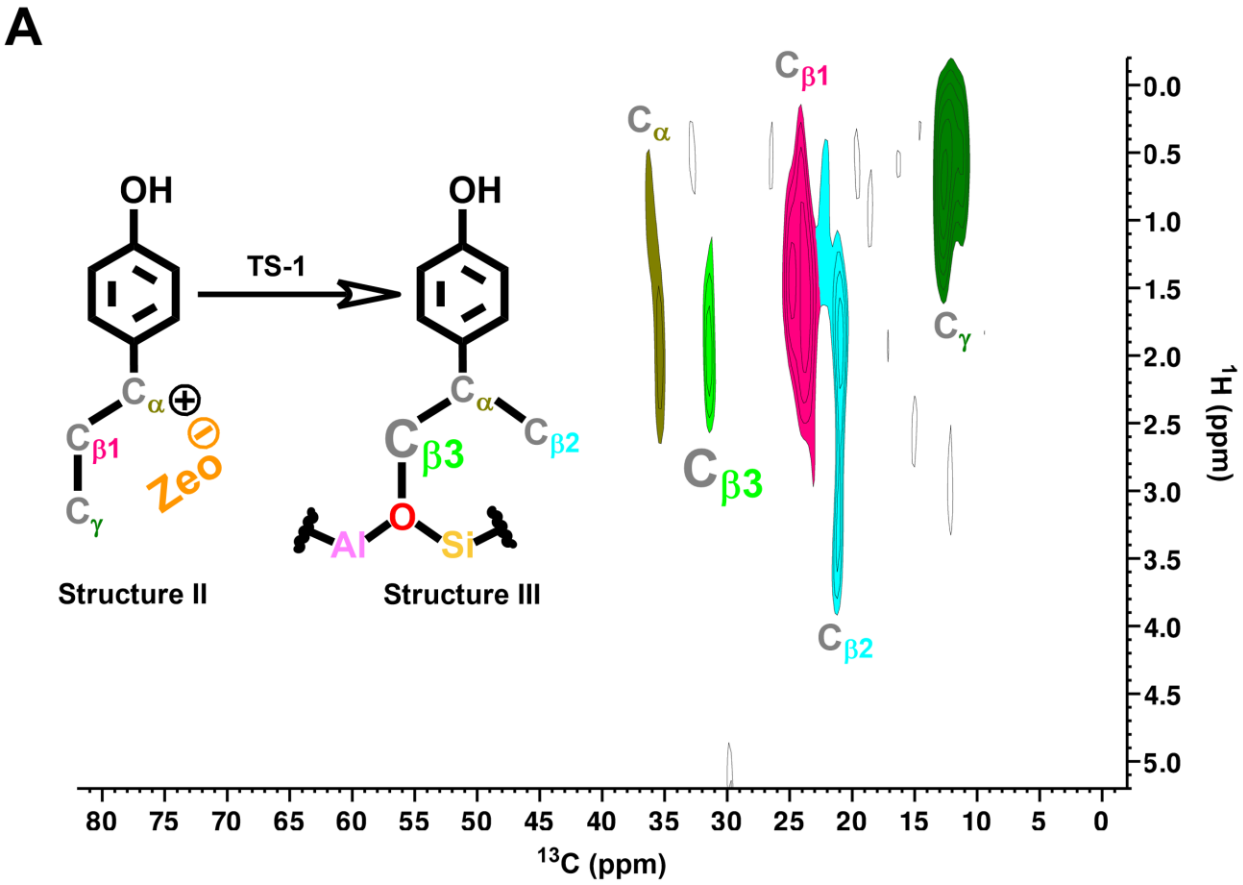
A
OH
TS-1
OH
Cα
Cβ1
Zeo
Cγ
Cα
Cβ3
Cβ2
Al
O
Si
Structure II
Structure III
Cβ1
Cα
Cβ3
Cβ2
Cγ
0.0
0.5
1.0
1.5
2.0
2.5
3.0
3.5
4.0
4.5
5.0
1H (ppm)
80 75 70 65 60 55 50 45 40 35 30 25 20 15 10 5 0
13C (ppm)

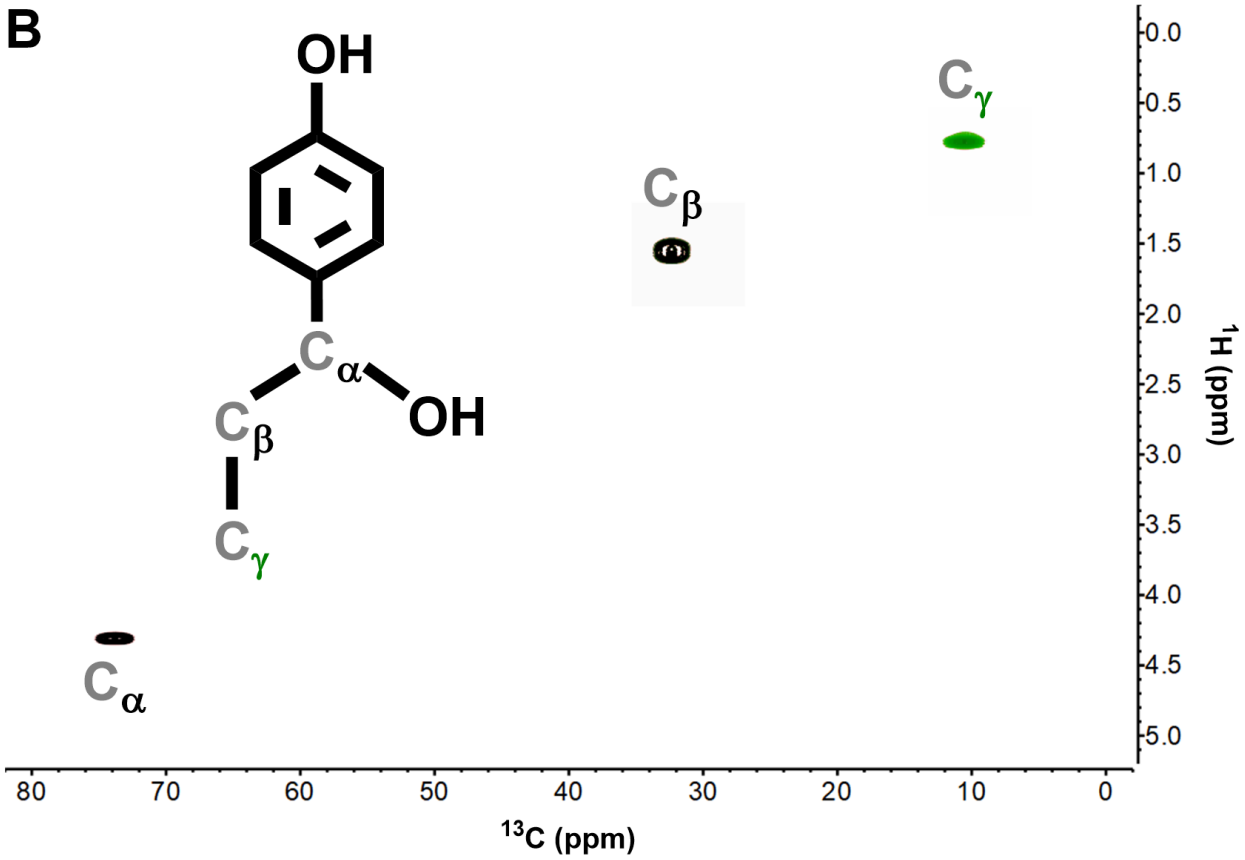
B
OH
Cγ
Cβ
Cα
OH
Cβ
Cγ
Cα
0.0
0.5
1.0
1.5
2.0
2.5
3.0
3.5
4.0
4.5
5.0
1H (ppm)
80
70
60
50
40
30
20
10
0
13C (ppm)

C

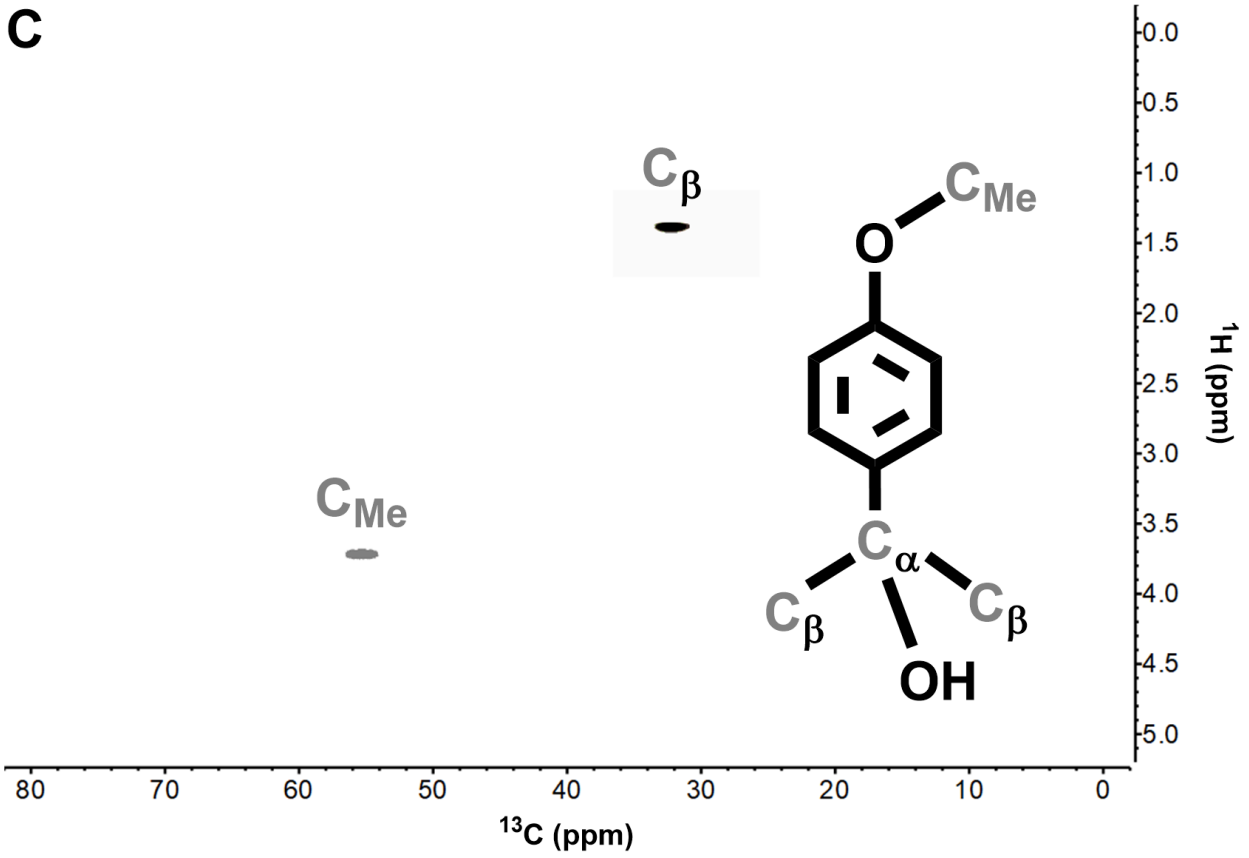
Cβ
CMe
O
CMe
Cα
Cβ
Cβ
OH
0.0
0.5
1.0
1.5
2.0
2.5
3.0
3.5
4.0
4.5
5.0
1H (ppm)
80
70
60
50
40
30
20
10
0
13C (ppm)

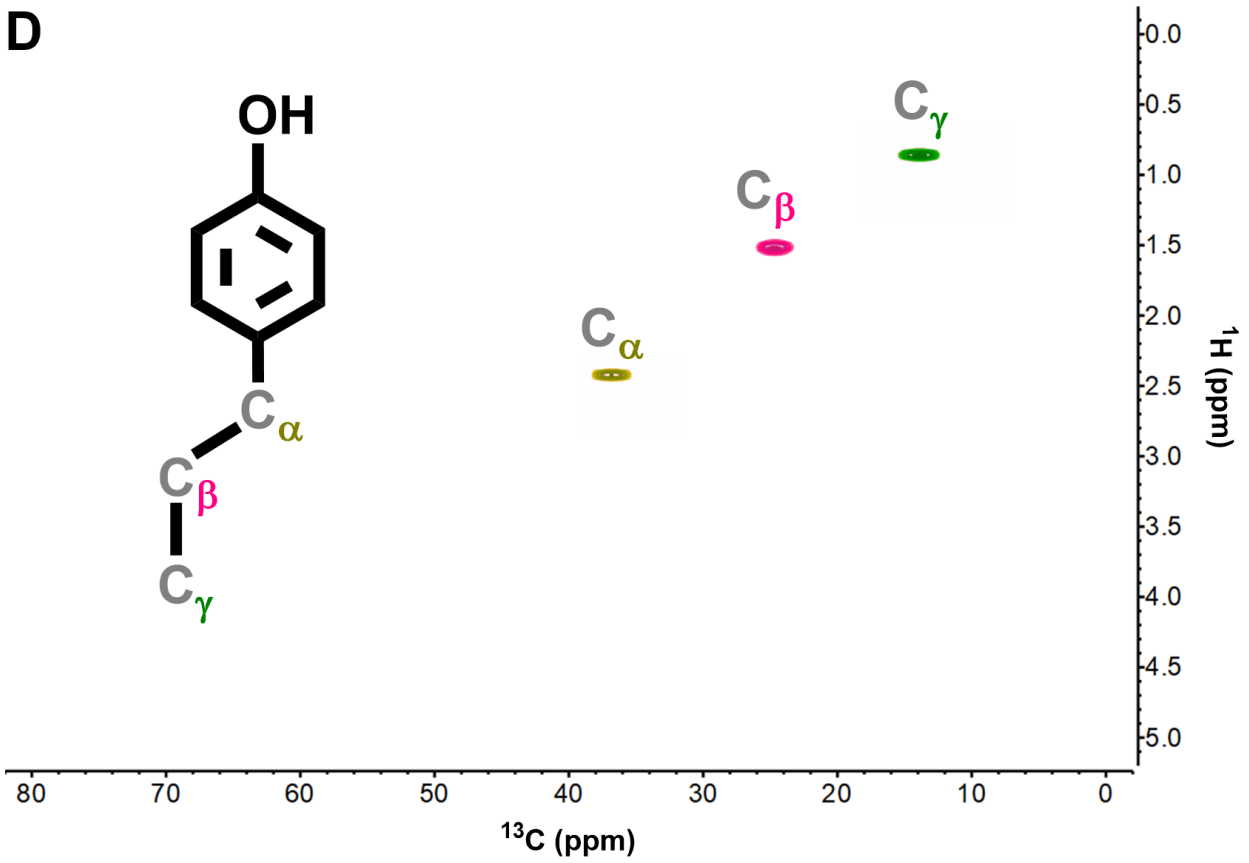

Fig. S12 2D $^{13}C\{^{1}H\}$ HETCOR and HSQC NMR spectra. (**A**) Solid-state 2D $^{13}C\{^{1}H\}$ HETCOR NMR spectrum of the intermediates in the reaction of 4-(1-hydroxypropyl)phenol (**1a**). (**B**) 2D HSQC NMR spectrum of **1a**. (**C**) 2D HSQC NMR spectrum of 2-(4-methoxyphenyl)propan-2-ol (**16a**). (**D**) 2D HSQC NMR spectrum of 4-n-propylphenol.

Reaction conditions: 1a (1 mmol), HY_{30} (0.3 g), H_2O (4.0 ml), 180 ºC, 10 min, 0.5 MPa Ar, 800 rpm.

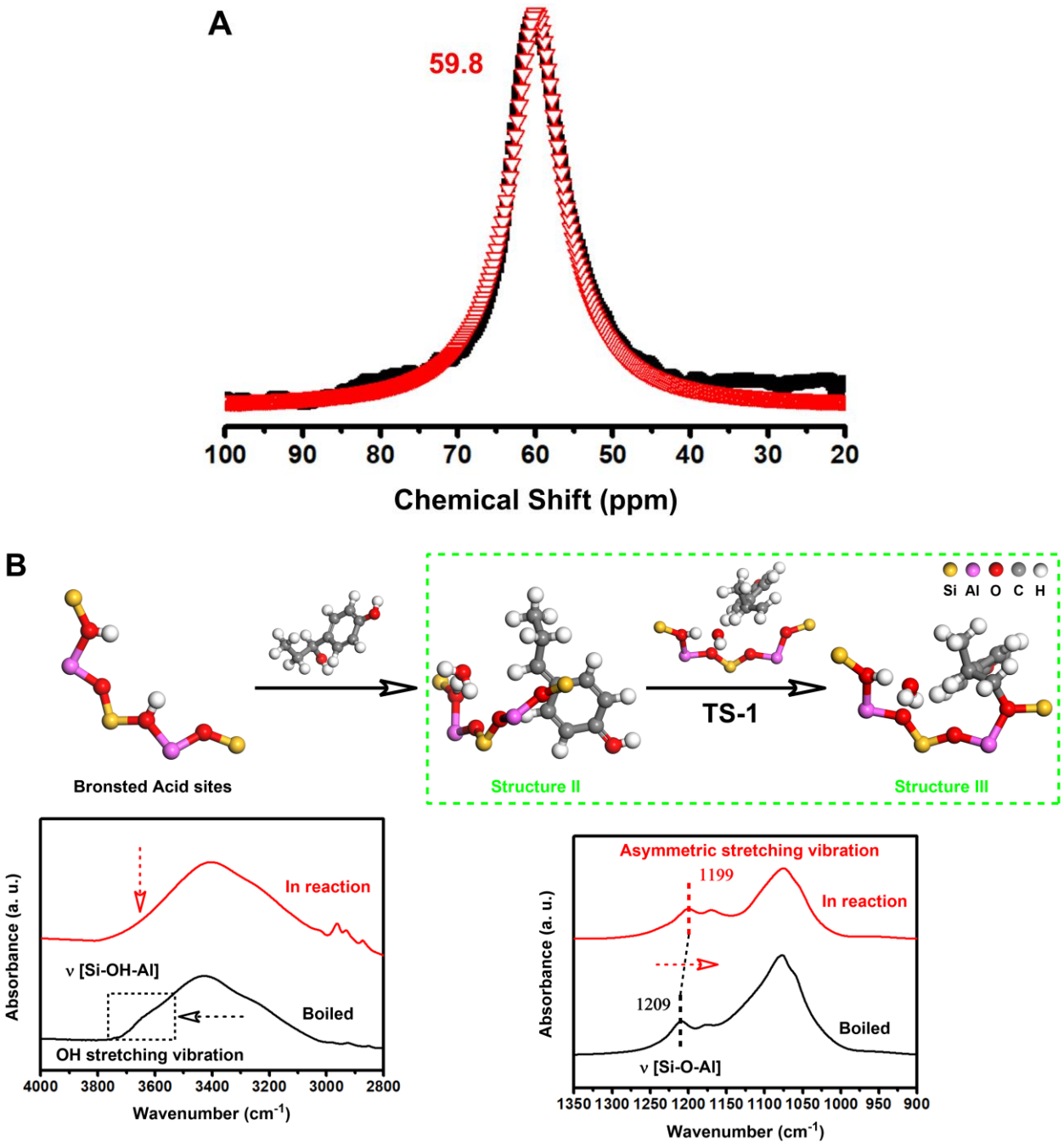

Fig. S13 ^{27}Al NMR and FTIR spectra of HY_{30} zeolite. (**A**) ^{27}Al NMR spectrum of the boiled HY_{30} zeolite, black solid square (■) represents the observed intensities, red inverted triangle (▽) is the fitting curve of framework Al(IV). (**B**) FTIR spectra of the HY_{30} zeolite, black line represents the boiled HY_{30} zeolite, red line represents the HY_{30} zeolite in the reaction.

Reaction conditions: (A) HY_{30} (0.3 g), H_2O (4.0 ml), 180 ºC, 10 min, 0.5 MPa Ar, 800 rpm. (B) 1a (1 mmol), HY_{30} (0.3 g), H_2O (4.0 ml), 180 ºC, 10 min, 0.5 MPa Ar, 800 rpm.

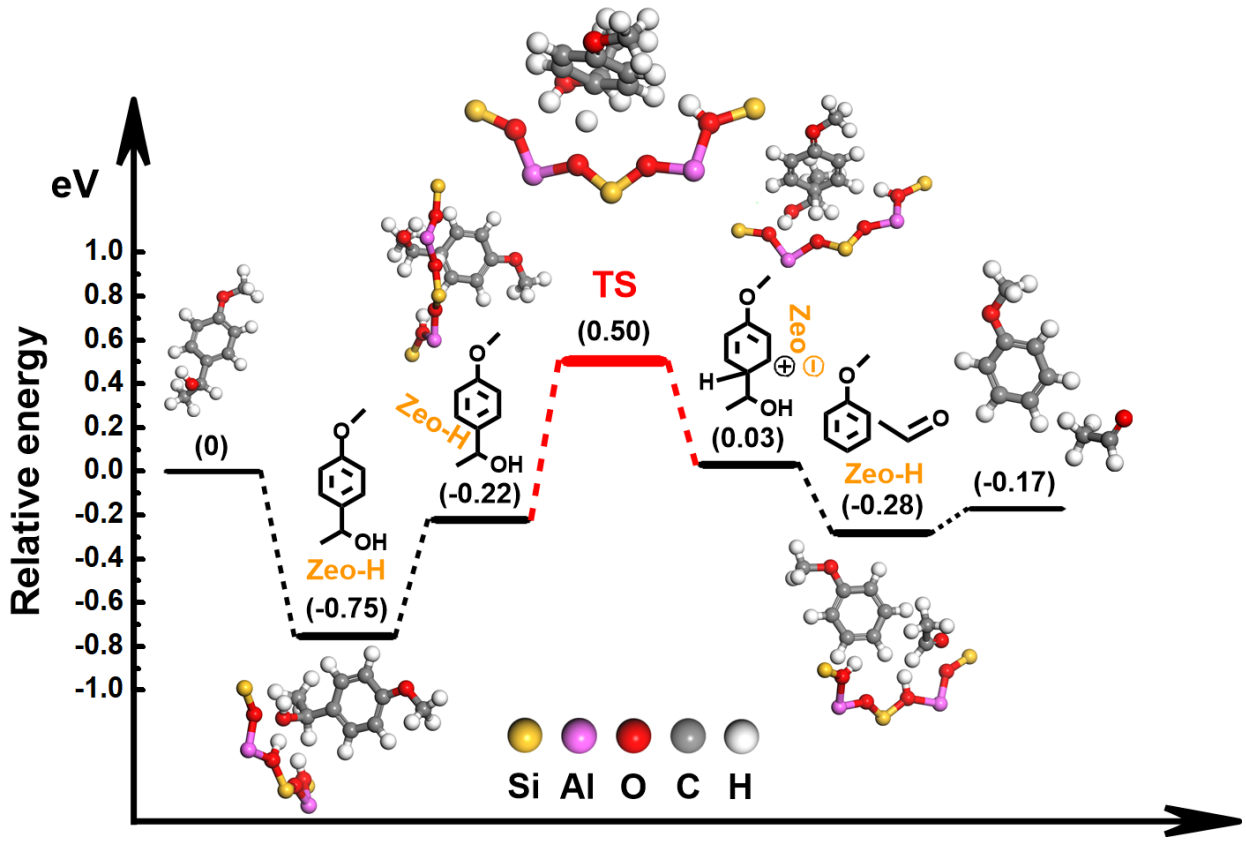

Fig. S14. Reaction pathway of 1-(4-methoxyphenyl)ethanol (10a).

Reaction conditions: 1-(4-Methoxyphenyl)ethanol (**10a**) (1 mmol), HY_{30} (0.3 g), H_2O (4.0 mL), 180 ºC, 1 h, 0.5 MPa Ar, 800 rpm.

A

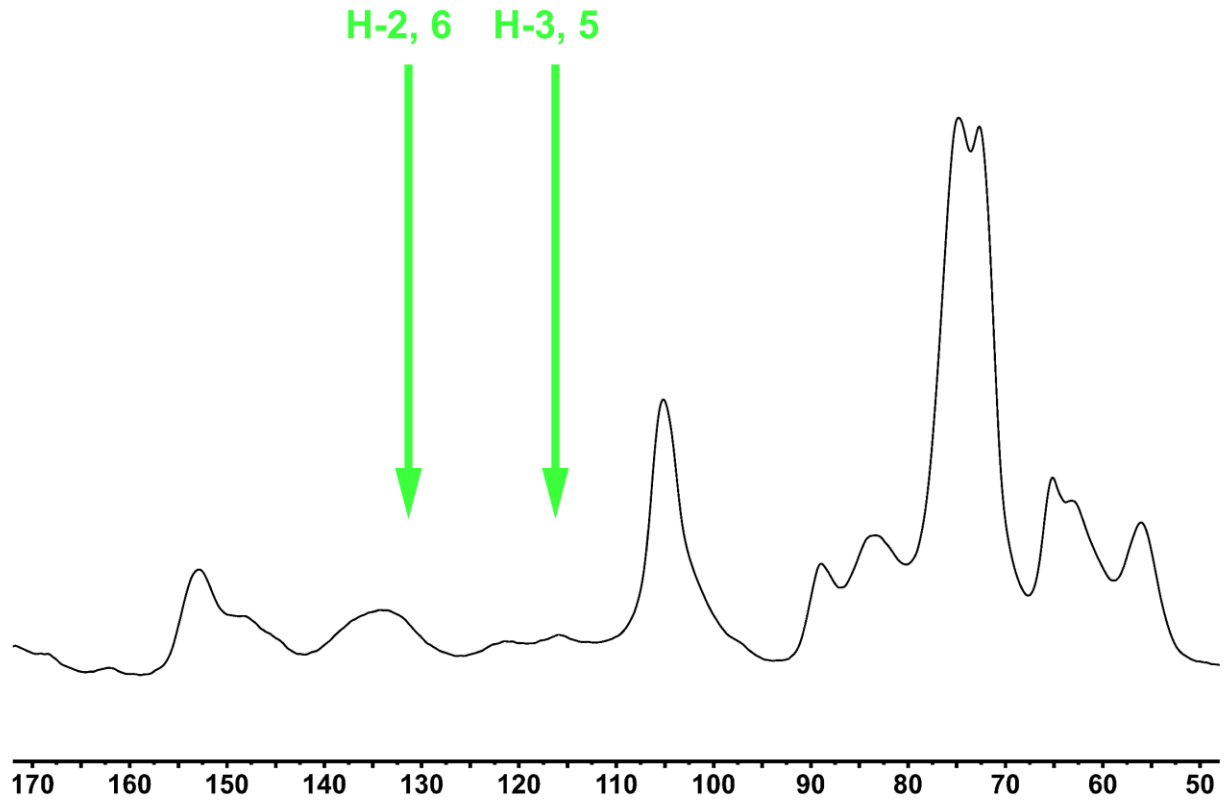

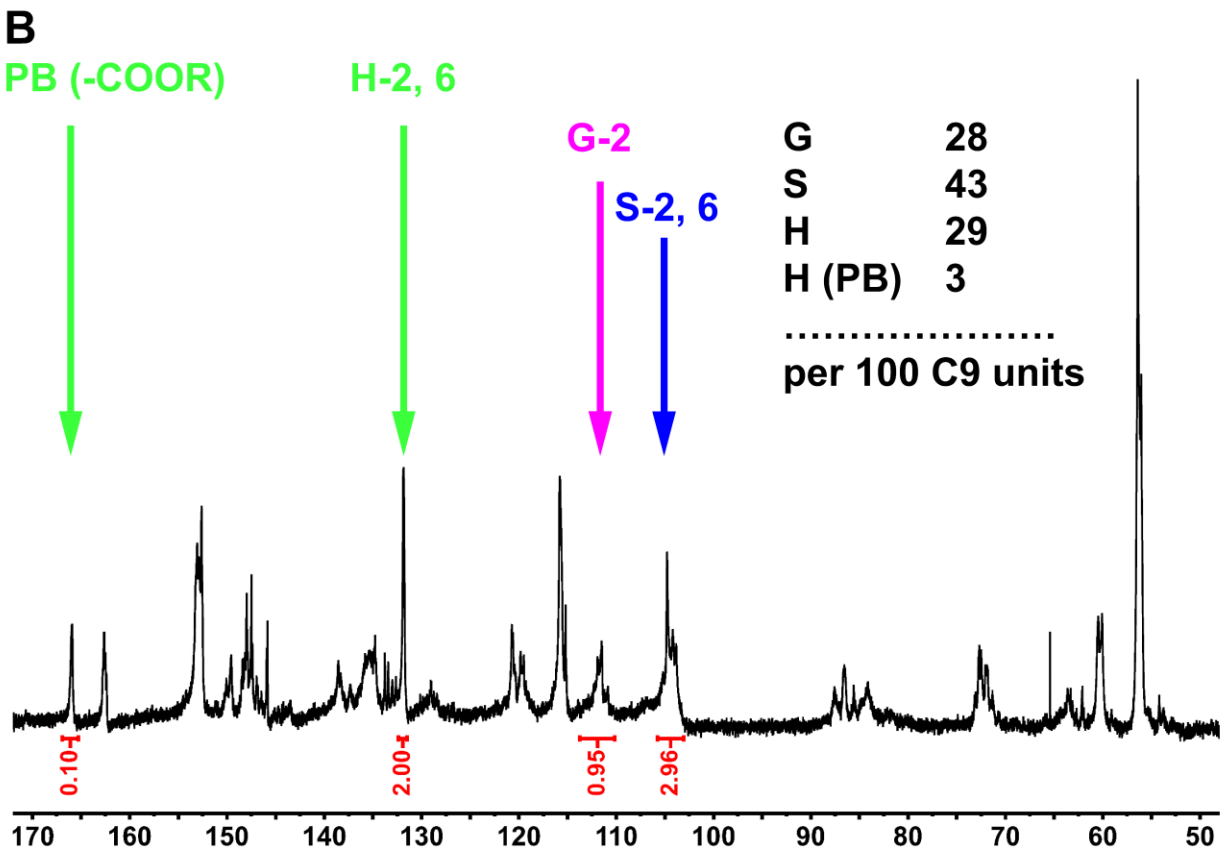
B
PB (-COOR)
H-2, 6
G-2
S-2, 6
G 28
S 43
H 29
H (PB) 3
.....
per 100 C9 units
0.10
2.00
0.95
2.96
170
160
150
140
130
120
110
100
90
80
70
60
50

C

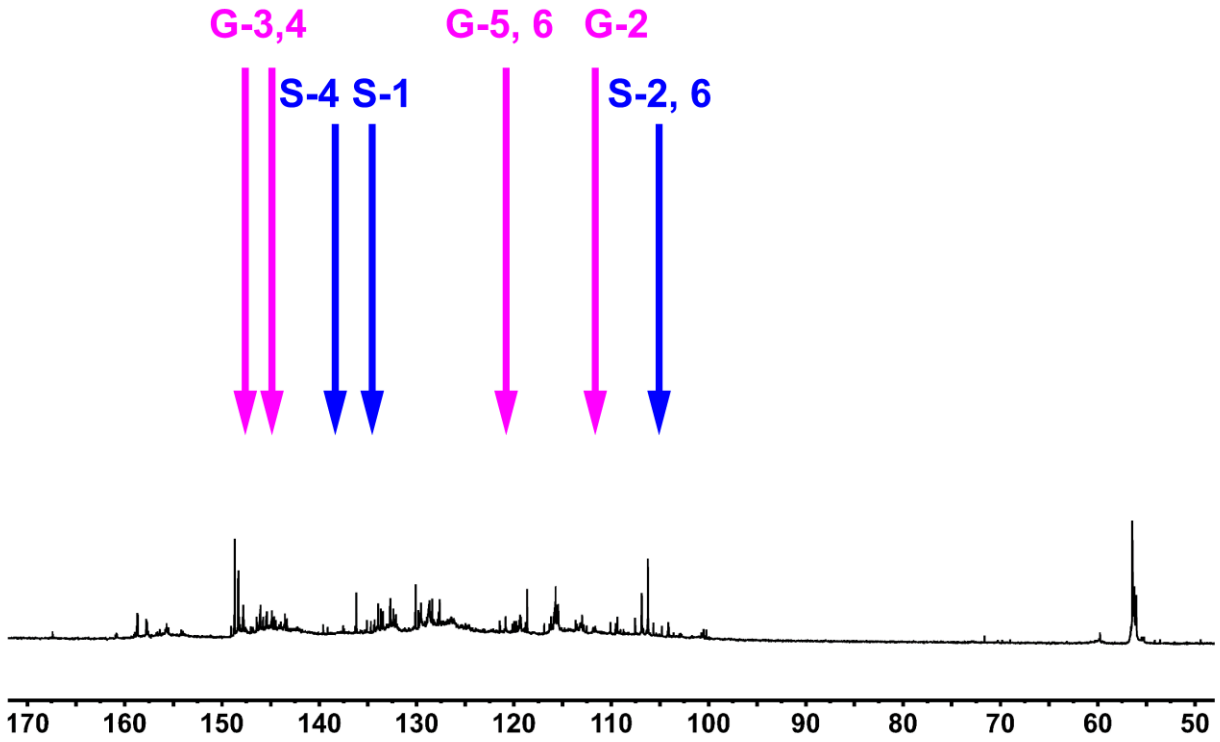

Fig. S15. ^{13}C NMR spectra of the poplar powder and the extracted lignin. (**A**) Poplar powder. (**B**) Quantitative ^{13}C NMR spectra of the extracted poplar lignin. (**C**) Quantitative ^{13}C NMR spectra of the residual solid after the transformation of the poplar lignin.

Reaction conditions: lignin (0.4 g), HY_{30} (0.4 g), H_2O (5.0 mL), 200 °C, 3 h, 0.5 MPa Ar, 800 rpm.

As shown in Fig. S15A, the resonance signals in the solid state ^{13}C NMR spectrum of poplar powder demonstrated that H units are originally existed in the lignin component of the poplar powder.

Supplementary Tables

Table S1 Results for the transformation of 1a over different catalysts.

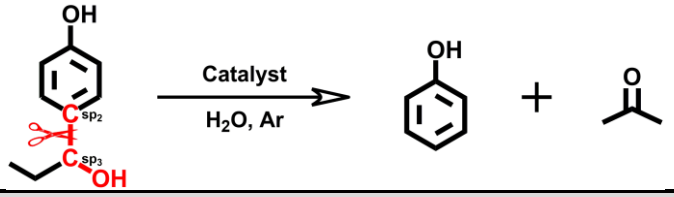

Entry*	Catalyst	Dosage (g)	H_2O (mL)	Yield of Phenol (%)	Yield of Acetone (%)
1	HY_3	0.3	4	0	0
2	HY_{15}	0.3	4	8.7	6.0
3	HY_{30}	0.3	4	94.6	69.5
4	HY_{40}	0.3	4	51.9	37.8
5	ZSM-5_9	0.3	4	0	0
6	ZSM-5_{30}	0.3	4	0	0
7	ZSM-5_{63}	0.3	4	0	0
8	ZSM-5_{235}	0.3	4	11.3	7.7
9	$Mordenite_{10}$	0.3	4	0	0
10	$Mordenite_{13}$	0.3	4	0	0
11	$Beta_{13}$	0.3	4	0	0
12	$Beta_{30}$	0.3	4	0	0
13	$Beta_{50}$	0.3	4	0	0
14	MCM-41	0.3	4	0	0
15	Ru/SiO_2†	0.3	4	0	0
16	Ni/SiO_2†	0.3	4	0	0
17	W/SiO_2†	0.3	4	0	0
18	SO_4^{2-}/ZrO_2‡	0.3	4	5.3	3.8
19	WO_3/ZrO_2§	0.3	4	0	0
20	WO_3/Al_2O_3§	0.3	4	0	0
21	Nb_2O_5/Al_2O_3‖	0.3	4	0	0
22	Silicotungstic acid	0.3	4	0	0
23	Phosphotungstic acid	0.3	4	0	0
24	Phosphomolybdic acid	0.3	4	0	0
25	Hydrochloric acid (37%)	0.039	4	0	0
26	Sulfuric acid (98%)	0.040	4	0	0
27	Phosphoric acid (85%)	0.046	4	0	0

*Reaction results are the averages of three experiments conducted in parallel. Reaction conditions: **1a** (1.0 mmol), 0.5 MPa Ar, 180 °C, 1 h, 800 rpm.

†Ru/SiO_2 (5.0 wt% Ru), Ni/SiO_2 (5.0 wt% Ni), W/SiO_2 (5.0 wt% W). The content of metal is based on support and determined by ICP.

‡SO_4^{2-}/ZrO_2 (7.0% wt% SO_4^{2-}).

§WO_3/ZrO_2 (20 wt% WO_3), WO_3/Al_2O_3 (20 wt% WO_3).

‖Nb_2O_5/Al_2O_3 (30 wt% WO_3).

Table S2 Textural and acid properties of HY zeolite

Textural and Acid Properties			HY_{15}	HY_{30}	HY_{40}
Texture Properties		Micropore Surface Area (m^2g^{-1})*	491	355	293
		Mesopore Surface Area (m^2g^{-1})†	321	431	482
		Micropore Volume (cm^3g^{-1})‡	0.191	0.143	0.110
		Mesopore Volume (cm^3g^{-1})§	0.140	0.188	0.219
Acid Properties	Total Acid	Brønsted ($\mu mol \cdot mg^{-1}$)	175	97	82
		Lewis ($\mu mol \cdot mg^{-1}$)	60	27	13
		B + L ($\mu mol \cdot mg^{-1}$)‖	235	124	95
		B/L¶	2.92	3.59	6.31
	Strong Acid	Brønsted ($\mu mol \cdot mg^{-1}$)	107	74	65
		Lewis ($\mu mol \cdot mg^{-1}$)	35	13	9
		B + L ($\mu mol \cdot mg^{-1}$)	142	87	74
		B/L	2.94	5.69	7.22
	Ratio of Strong Acid / Total Acid	Brønsted (%)	61.1	76.3	79.3
		Lewis (%)	58.3	48.1	69.2
		B + L (%)	60.4	70.2	77.9

*The t-plot micropore surface area.
†The t-plot mesopore surface area.
‡The t-plot micropore volume.
§BJH mesopore volume.
‖"B+L" represents the sum of the amounts of Bronsted acid and Lewis acid sites.
¶"B/L" denotes the ratio of the amounts of Bronsted acid and Lewis acid sites.

Table S3 Optimization of reaction conditions for the phenol production from poplar lignin

Entry*	Lignin (g)	HY_{30} (g)	H_2O (mL)	t (h)	T (°C)	Yield (wt%)†
1	0	0.4	5.0	3.0	200	0
2	0.4	0	5.0	3.0	200	0
3	0.4	0.1	5.0	3.0	200	1.1
4	0.4	0.2	5.0	3.0	200	5.3
5	0.4	0.3	5.0	3.0	200	8.9
6	0.4	0.4	5.0	3.0	200	10.9
7	0.4	0.5	5.0	3.0	200	10.9
8	0.4	0.4	5.0	0.5	200	3.3
9	0.4	0.4	5.0	1	200	5.8
10	0.4	0.4	5.0	1.5	200	7.7
11	0.4	0.4	5.0	2	200	8.9
12	0.4	0.4	5.0	2.5	200	10.1
13	0.4	0.4	5.0	3.0	200	10.9
14	0.4	0.4	5.0	4.0	200	10.9
15	0.4	0.4	5.0	5.0	200	10.9
16	0.4	0.4	5.0	3.0	150	0
17	0.4	0.4	5.0	3.0	160	3.2
18	0.4	0.4	5.0	3.0	170	6.2
19	0.4	0.4	5.0	3.0	180	8.3
20	0.4	0.4	5.0	3.0	190	10.1
21	0.4	0.4	5.0	3.0	210	10.9

*Reaction results are the averages of three experiments conducted in parallel. Reaction conditions: 0.5 MPa Ar, 800 rpm.

†The yield of phenol was calculated as follows:

$$\text{Yield} = \frac{m_{\text{phenol}}}{m_{\text{lignin}}} \times 100\%$$

Table S4 ^{13}C NMR chemical shifts of the model compounds

Model compounds	C_α*	C_β†	C_γ‡	C_{Me}§
4-(1-hydroxypropyl)phenol (**1a**)	73.9	32.5	10.7	—
2-(4-methoxyphenyl)propan-2-ol (**16a**)	70.8	32.5	—	55.4
4-n-propylphenol	36.9	24.9	14.0	—

*C_α, the C atom at the aliphatic α-C position.
†C_β, the C atom at the aliphatic β-C position.
‡C_γ, the C atom at the aliphatic γ-C position.
§C_{Me}, the C atom in the methoxy group.

Table S5 Solid-state 2D $^{13}C\{^{1}H\}$ HETCOR NMR chemical shifts of the intermediates in the reaction of 4-(1-hydroxypropyl)phenol (1a)

Samples	C_{α}‡	C_{β}§	$C_{\beta1}$‖	$C_{\beta2}$¶	$C_{\beta3}$**	C_{γ}††	C_{Me}‡‡
4-(1-hydroxypropyl)phenol*	36.3{2.0}	—	24.5{1.5}	21.0{1.9}	31.2{2.0}	12.7{0.7}	—
4-(1-hydroxypropyl)phenol†	73.8{4.3}	32.4{1.6}	—	—	—	10.6{0.8}	—
2-(4-methoxyphenyl)propan-2-ol†	—‡	32.3{1.4}	—	—	—	—	55.2{3.7}
4-n-propylphenol†	36.9{2.4}	24.6{1.5}	—	—	—	13.9{0.9}	—

*$^{13}C\{^{1}H\}$ HETCOR NMR chemical shifts of the intermediates in the reaction of 4-(1-hydroxypropyl)phenol (**1a**). Reaction conditions: **1a** (1 mmol), HY_{30} (0.3 g), H_2O (4.0 ml), 180 ºC, 10 min, 0.5 MPa Ar, 800 rpm.

†$^{13}C/^{1}H$ 2D HSQC NMR chemical shifts of the model compounds.

‡C_{α}, the C atom at the aliphatic α-C position. No signal for the C atom without H atom at C_{α} position of 2-(4-methoxyphenyl)propan-2-ol (**16a**).

§C_{β}, the C atom at the aliphatic β-C position of the model compounds.

‖$C_{\beta1}$, the C atom at the aliphatic β_1-C position of the intermediates in the reaction of **1a**.

¶$C_{\beta2}$, the C atom at the aliphatic β_2-C position of the intermediates in the reaction of **1a**.

$C_{\beta3}$, the C atom at the aliphatic β_3-C position of the intermediates in the reaction of **1a.

††C_{γ}, the C atom at the aliphatic γ-C position.

‡‡C_{Me}, the C atom in the methoxy group.

NMR spectra

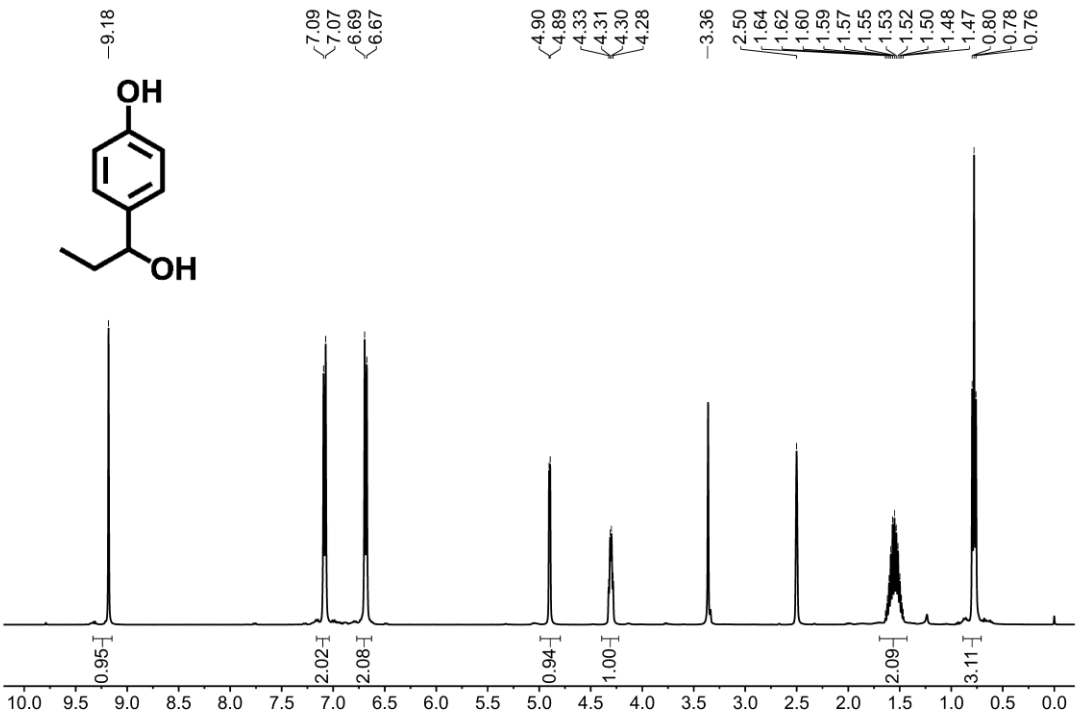
9.18
7.09
7.07
6.69
6.67
4.90
4.89
4.33
4.31
4.30
4.28
3.36
2.50
1.64
1.62
1.60
1.59
1.57
1.55
1.53
1.52
1.50
1.48
1.47
0.80
0.78
0.76
OH
OH
0.95
2.02
2.08
0.94
1.00
2.09
3.11
10.0 9.5 9.0 8.5 8.0 7.5 7.0 6.5 6.0 5.5 5.0 4.5 4.0 3.5 3.0 2.5 2.0 1.5 1.0 0.5 0.0

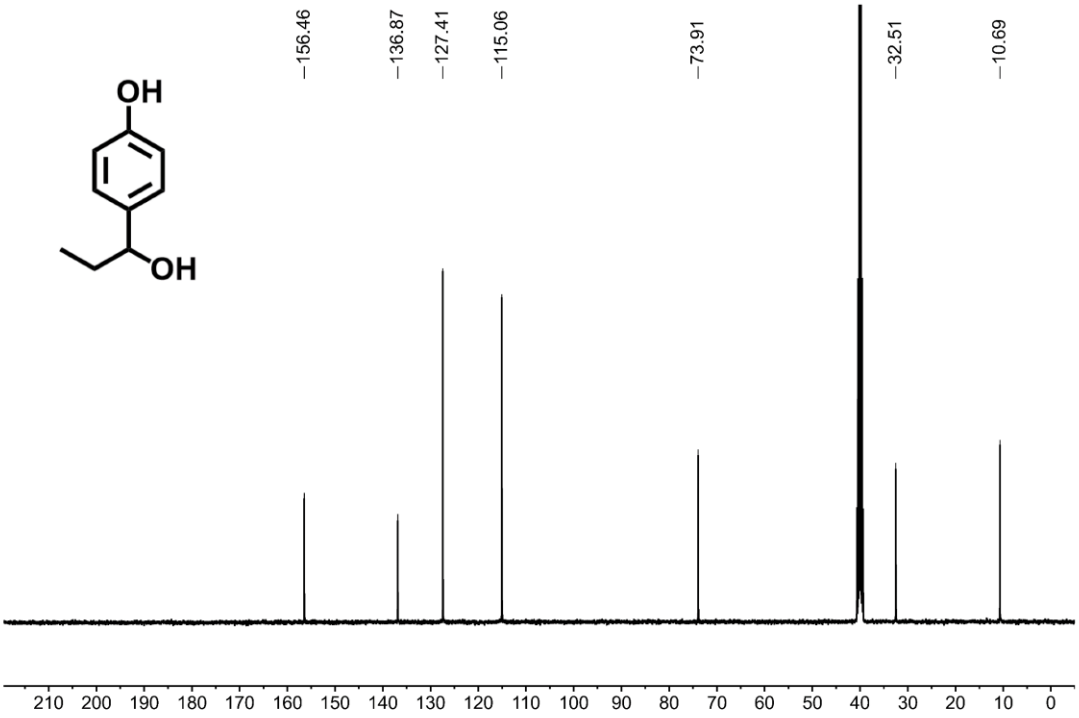
156.46
136.87
127.41
115.06
73.91
32.51
10.69
OH
OH
210 200 190 180 170 160 150 140 130 120 110 100 90 80 70 60 50 40 30 20 10 0

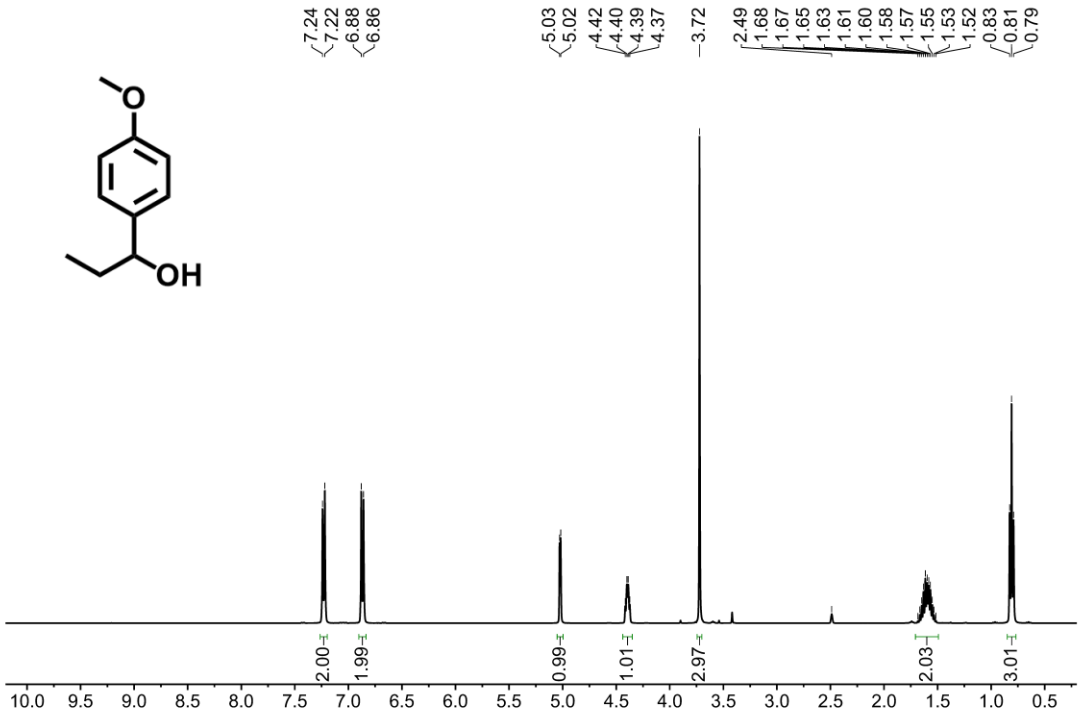
7.24
7.22
6.88
6.86
5.03
5.02
4.42
4.40
4.39
4.37
3.72
2.49
1.68
1.67
1.65
1.63
1.61
1.60
1.58
1.57
1.55
1.53
1.52
0.83
0.81
0.79
O
OH
2.00
1.99
0.99
1.01
2.97
2.03
3.01
10.0 9.5 9.0 8.5 8.0 7.5 7.0 6.5 6.0 5.5 5.0 4.5 4.0 3.5 3.0 2.5 2.0 1.5 1.0 0.5

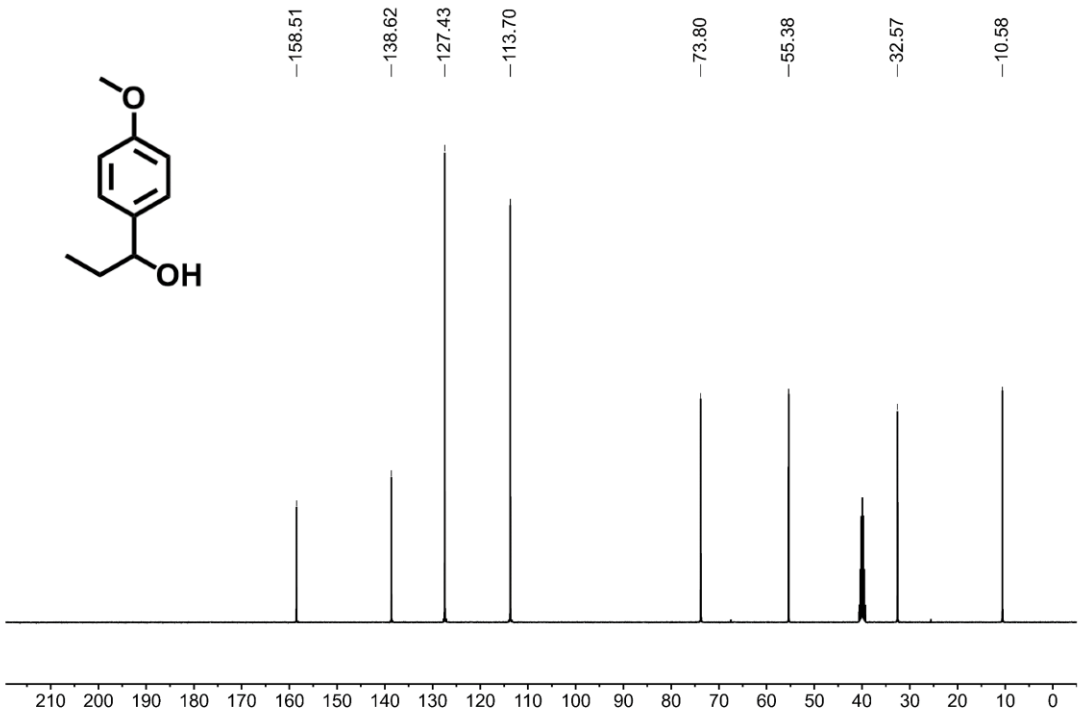
158.51
138.62
127.43
113.70
73.80
55.38
32.57
10.58
O
OH
210 200 190 180 170 160 150 140 130 120 110 100 90 80 70 60 50 40 30 20 10 0

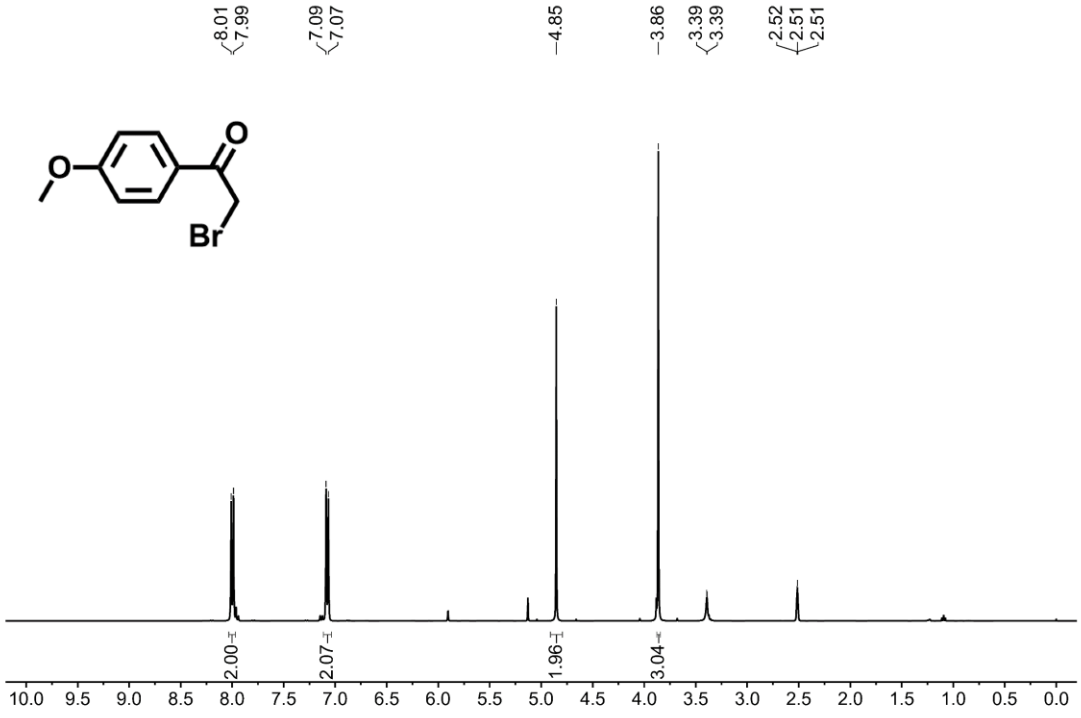
8.01
7.99
7.09
7.07
4.85
3.86
3.39
3.39
2.52
2.51
2.51
O
O
Br
2.00
2.07
1.96
3.04
10.0 9.5 9.0 8.5 8.0 7.5 7.0 6.5 6.0 5.5 5.0 4.5 4.0 3.5 3.0 2.5 2.0 1.5 1.0 0.5 0.0

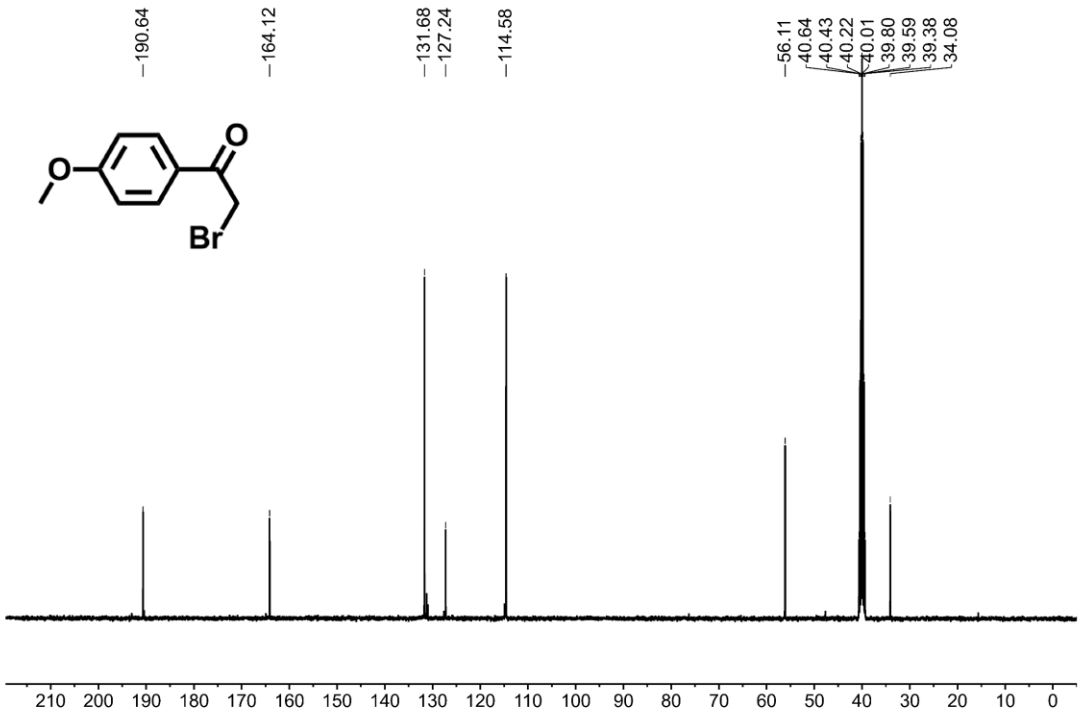
190.64
164.12
131.68
127.24
114.58
56.11
40.64
40.43
40.22
40.01
39.80
39.59
39.38
34.08
O
O
Br
210 200 190 180 170 160 150 140 130 120 110 100 90 80 70 60 50 40 30 20 10 0

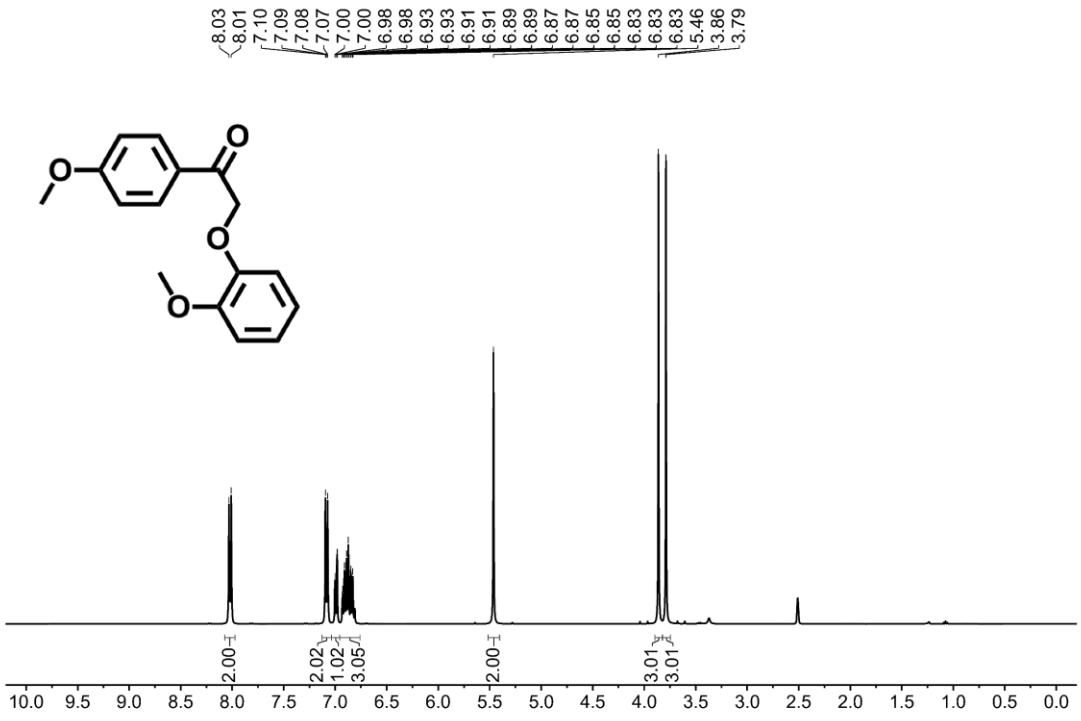
8.03
8.01
7.10
7.09
7.08
7.07
7.00
7.00
6.98
6.98
6.93
6.93
6.91
6.91
6.89
6.89
6.87
6.87
6.85
6.85
6.83
6.83
6.83
5.46
3.86
3.79
O
O
O
O
2.00
2.02
1.02
3.05
2.00
3.01
3.01
10.0 9.5 9.0 8.5 8.0 7.5 7.0 6.5 6.0 5.5 5.0 4.5 4.0 3.5 3.0 2.5 2.0 1.5 1.0 0.5 0.0

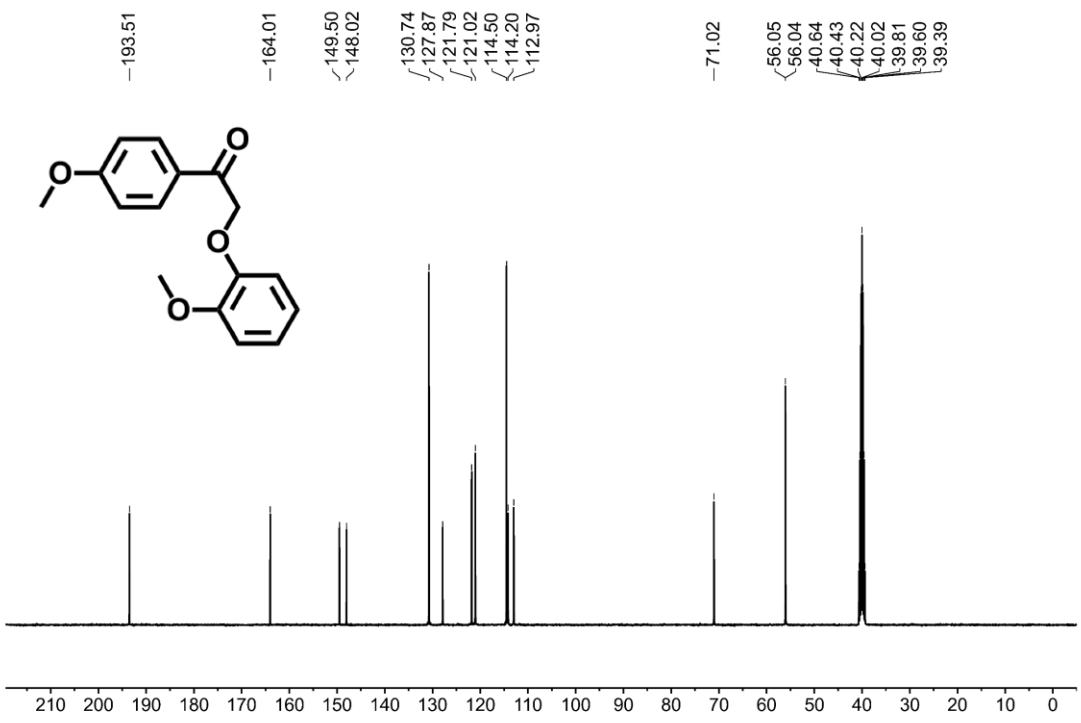
193.51
164.01
149.50
148.02
130.74
127.87
121.79
121.02
114.50
114.20
112.97
71.02
56.05
56.04
40.64
40.43
40.22
40.02
39.81
39.60
39.39
O
O
O
O
210 200 190 180 170 160 150 140 130 120 110 100 90 80 70 60 50 40 30 20 10 0

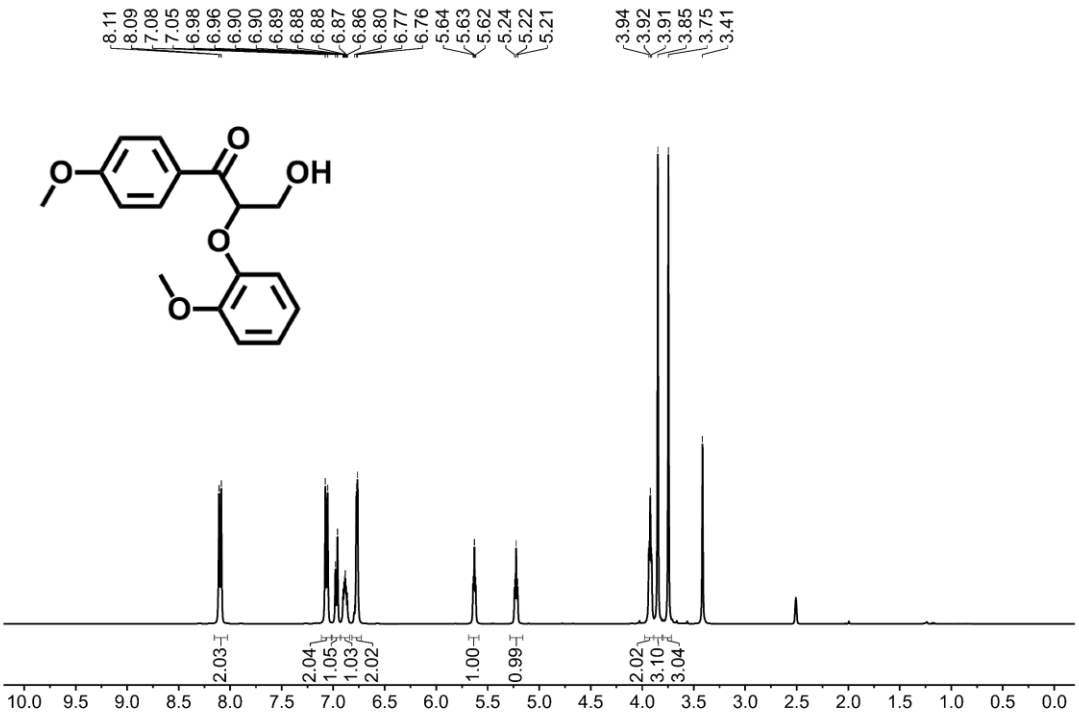
8.11
8.09
7.08
7.05
6.98
6.96
6.90
6.90
6.89
6.88
6.88
6.87
6.86
6.80
6.77
6.76
5.64
5.63
5.62
5.24
5.22
5.21
3.94
3.92
3.91
3.85
3.75
3.41
O
OH
O
O
2.03
2.04
1.05
1.03
2.02
1.00
0.99
2.02
3.10
3.04
10.0 9.5 9.0 8.5 8.0 7.5 7.0 6.5 6.0 5.5 5.0 4.5 4.0 3.5 3.0 2.5 2.0 1.5 1.0 0.5 0.0

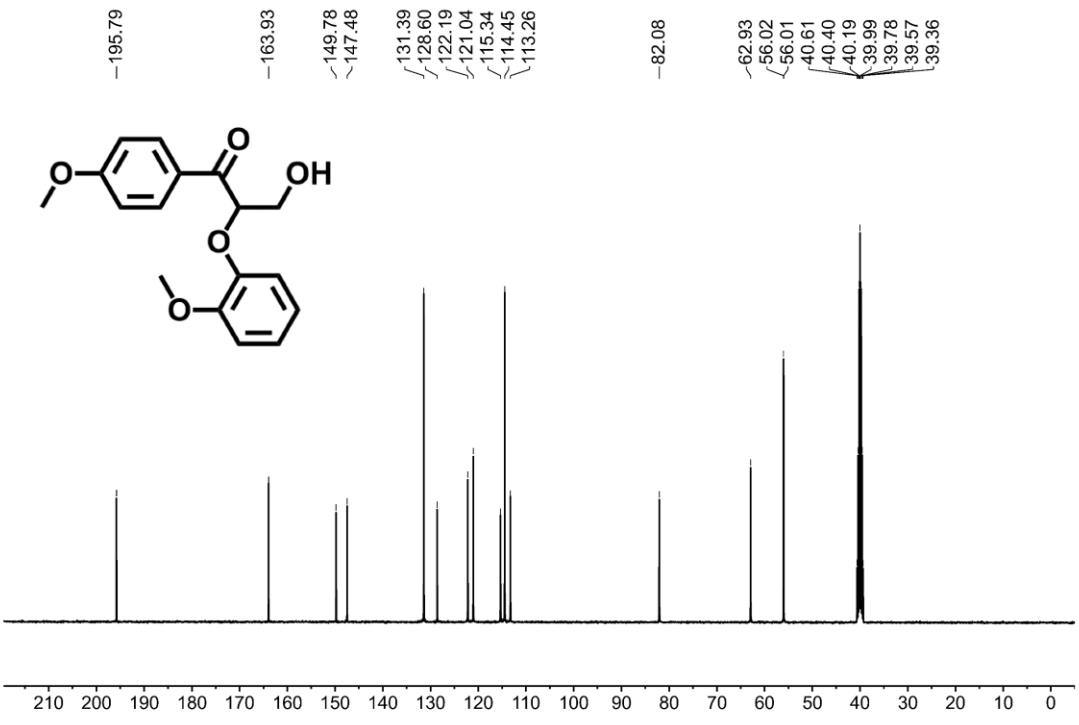
195.79
163.93
149.78
147.48
131.39
128.60
122.19
121.04
115.34
114.45
113.26
82.08
62.93
56.02
56.01
40.61
40.40
40.19
39.99
39.78
39.57
39.36
O
OH
O
O
210 200 190 180 170 160 150 140 130 120 110 100 90 80 70 60 50 40 30 20 10 0

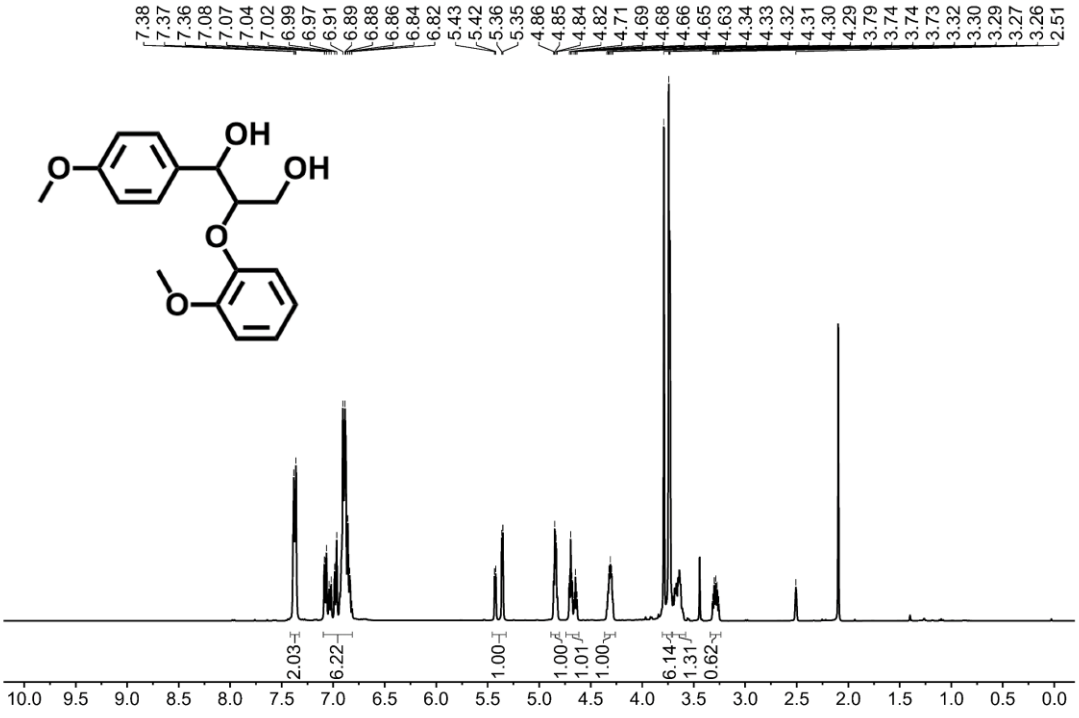
7.38
7.37
7.36
7.08
7.07
7.04
7.02
6.99
6.97
6.91
6.89
6.88
6.86
6.84
6.82
5.43
5.42
5.36
5.35
4.86
4.85
4.84
4.82
4.71
4.69
4.68
4.66
4.65
4.63
4.34
4.33
4.32
4.31
4.30
4.29
3.79
3.74
3.74
3.73
3.32
3.30
3.29
3.27
3.26
2.51
OH
OH
O
O
2.03
6.22
1.00
1.00
1.01
1.00
6.14
1.31
0.62
10.0 9.5 9.0 8.5 8.0 7.5 7.0 6.5 6.0 5.5 5.0 4.5 4.0 3.5 3.0 2.5 2.0 1.5 1.0 0.5 0.0

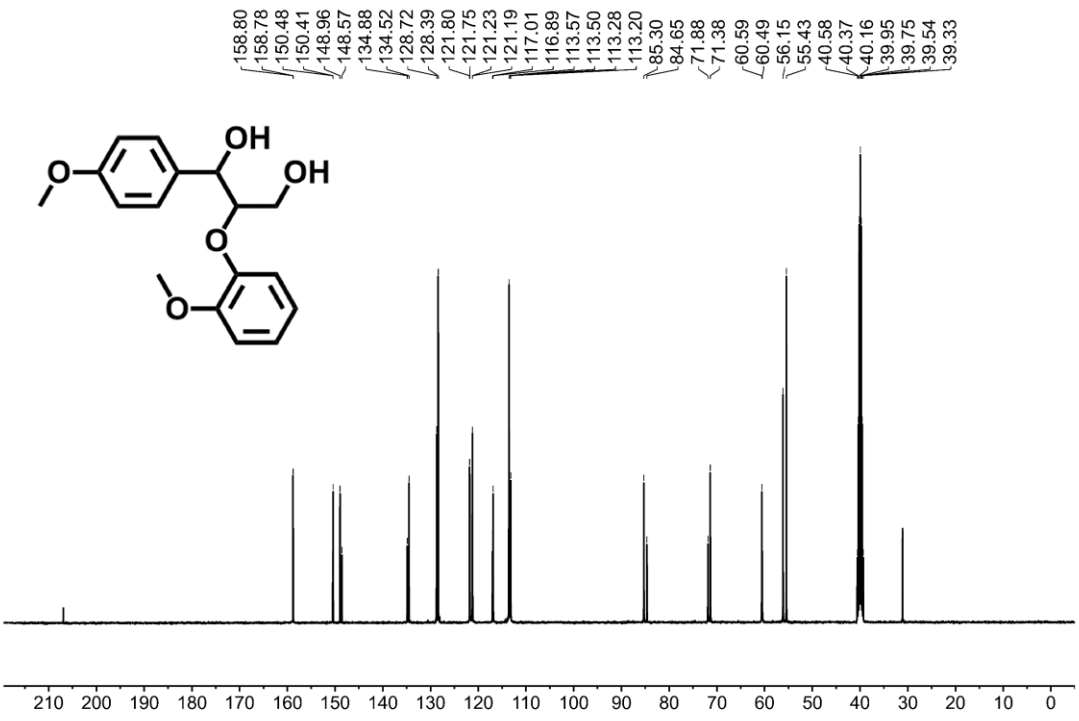
158.80
158.78
150.48
150.41
148.96
148.57
134.88
134.52
128.72
128.39
121.80
121.75
121.23
121.19
117.01
116.89
113.57
113.50
113.28
113.20
85.30
84.65
71.88
71.38
60.59
60.49
56.15
55.43
40.58
40.37
40.16
39.95
39.75
39.54
39.33
OH
OH
O
O
210 200 190 180 170 160 150 140 130 120 110 100 90 80 70 60 50 40 30 20 10 0

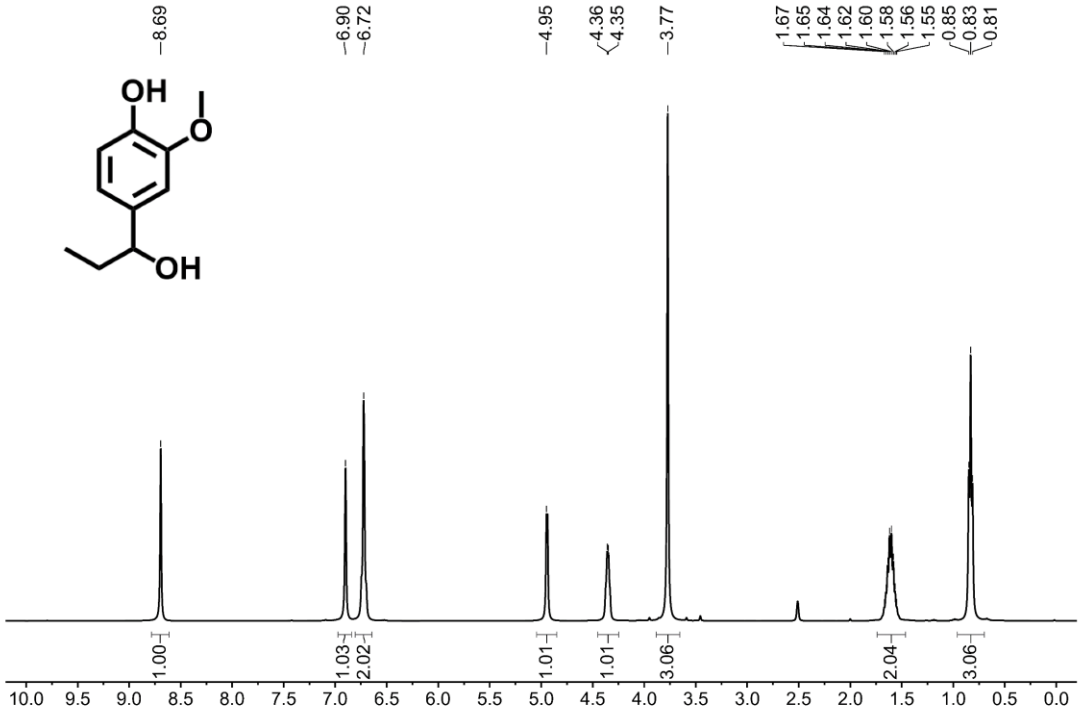
8.69
6.90
6.72
4.95
4.36
4.35
3.77
1.67
1.65
1.64
1.62
1.60
1.58
1.56
1.55
0.85
0.83
0.81
OH
O
OH
1.00
1.03
2.02
1.01
1.01
3.06
2.04
3.06
10.0 9.5 9.0 8.5 8.0 7.5 7.0 6.5 6.0 5.5 5.0 4.5 4.0 3.5 3.0 2.5 2.0 1.5 1.0 0.5 0.0

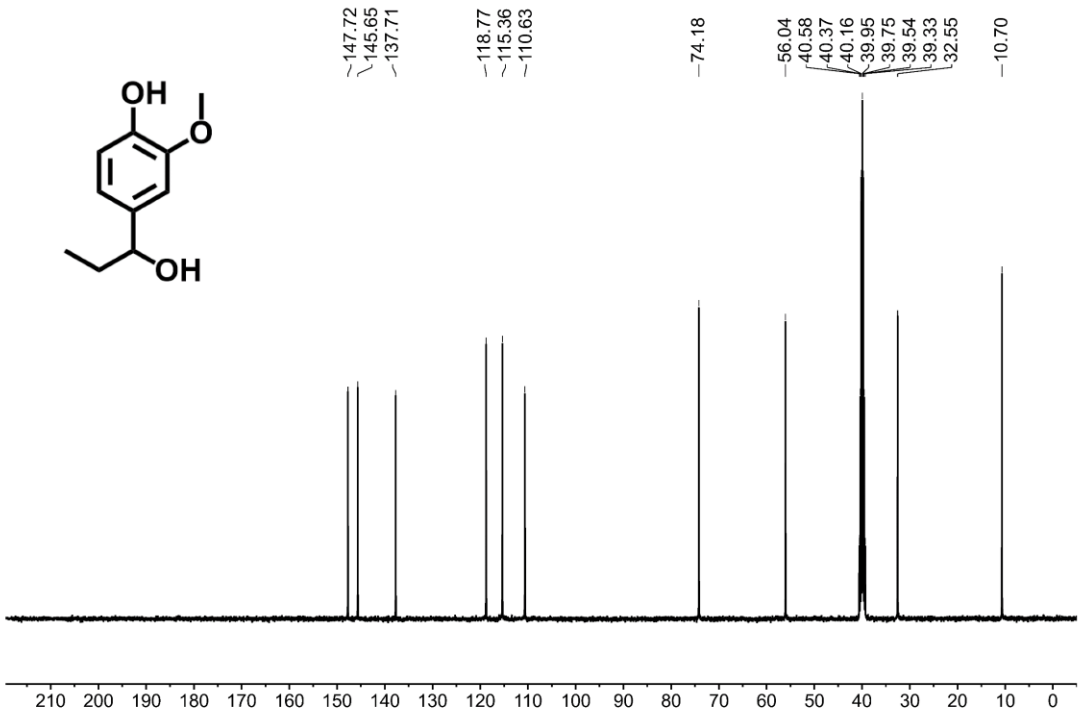
147.72
145.65
137.71
118.77
115.36
110.63
74.18
56.04
40.58
40.37
40.16
39.95
39.75
39.54
39.33
32.55
10.70
OH
O
OH
210 200 190 180 170 160 150 140 130 120 110 100 90 80 70 60 50 40 30 20 10 0

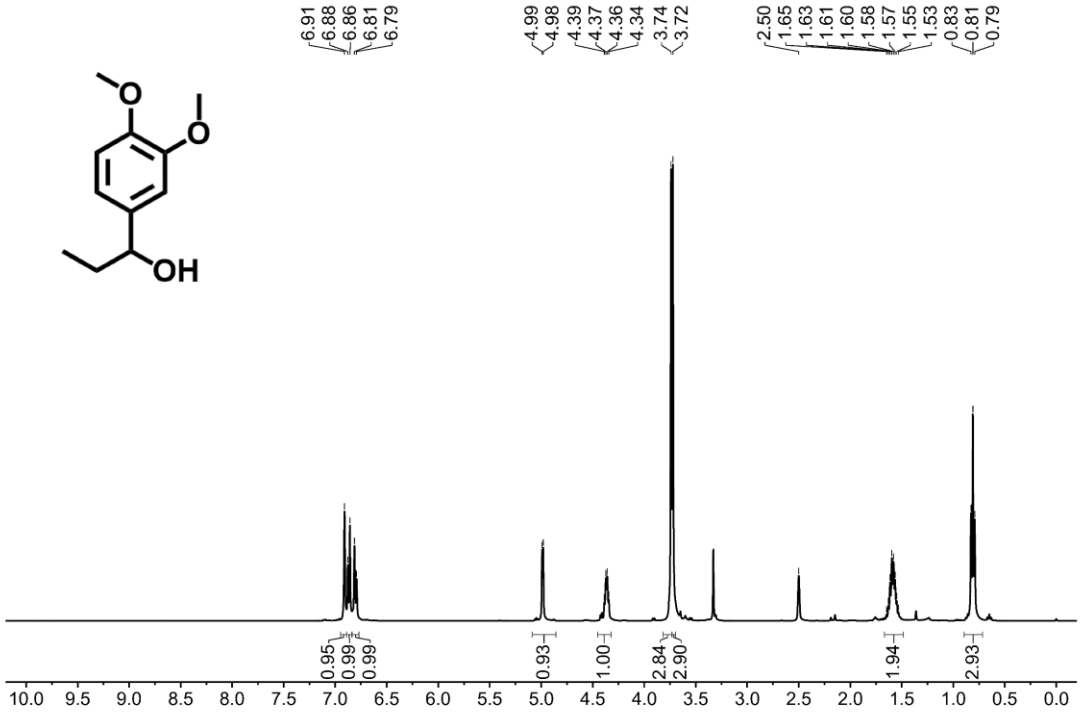
6.91
6.88
6.86
6.81
6.79
4.99
4.98
4.39
4.37
4.36
4.34
3.74
3.72
2.50
1.65
1.63
1.61
1.60
1.58
1.57
1.55
1.53
0.83
0.81
0.79
O
O
OH
0.95
0.99
0.99
0.93
1.00
2.84
2.90
1.94
2.93
10.0 9.5 9.0 8.5 8.0 7.5 7.0 6.5 6.0 5.5 5.0 4.5 4.0 3.5 3.0 2.5 2.0 1.5 1.0 0.5 0.0

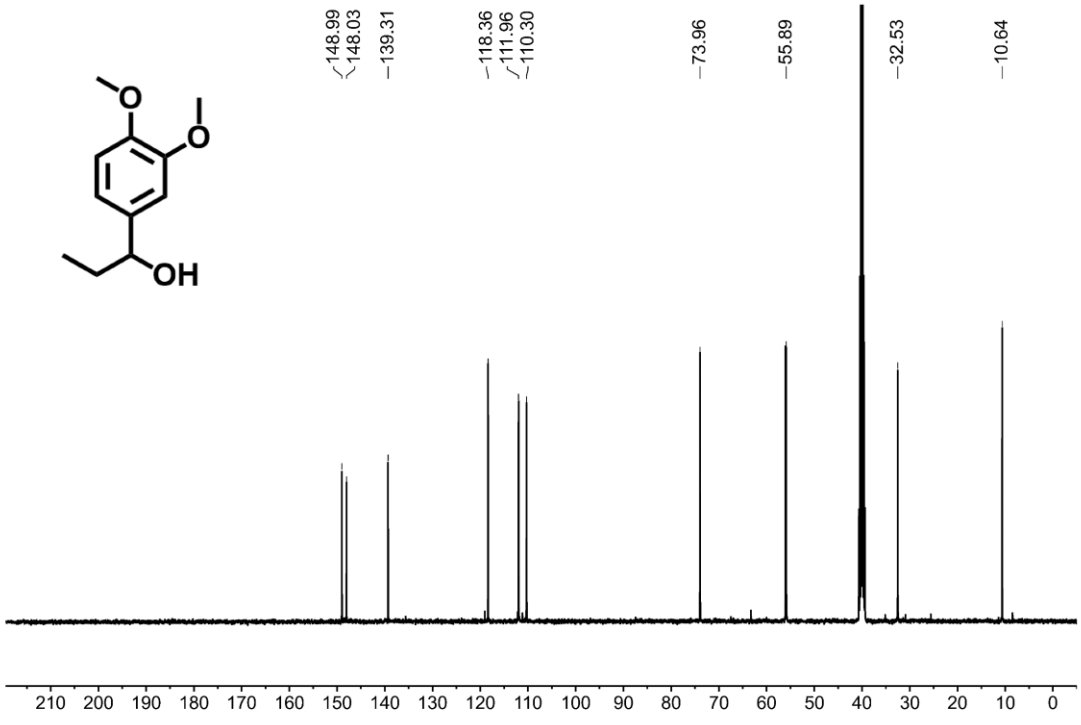
148.99
148.03
139.31
118.36
111.96
110.30
73.96
55.89
32.53
10.64
O
O
OH
210 200 190 180 170 160 150 140 130 120 110 100 90 80 70 60 50 40 30 20 10 0

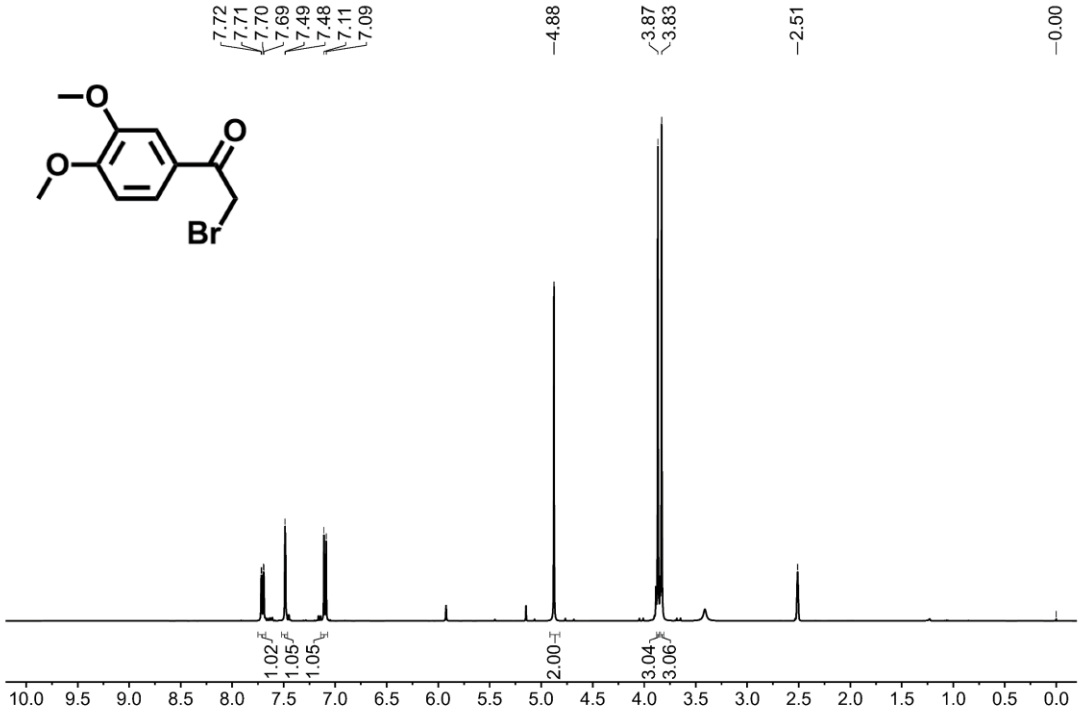
7.72
7.71
7.70
7.69
7.49
7.48
7.11
7.09
4.88
3.87
3.83
2.51
0.00
O
O
Br
1.02
1.05
1.05
2.00
3.04
3.06
10.0 9.5 9.0 8.5 8.0 7.5 7.0 6.5 6.0 5.5 5.0 4.5 4.0 3.5 3.0 2.5 2.0 1.5 1.0 0.5 0.0

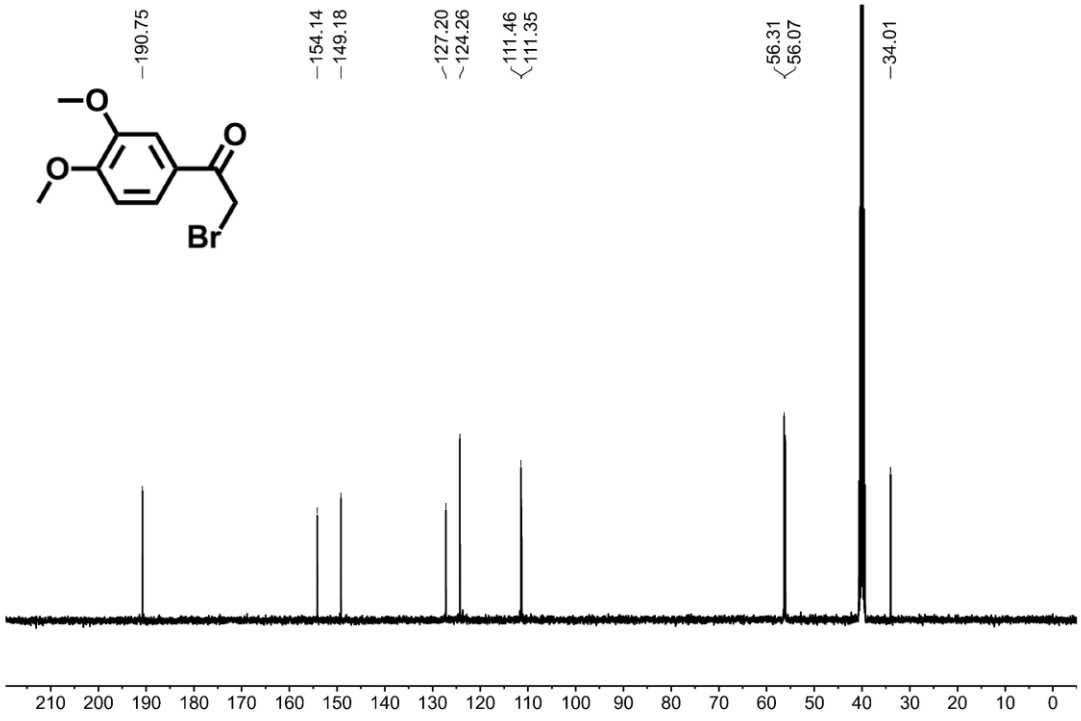
190.75
154.14
149.18
127.20
124.26
111.46
111.35
56.31
56.07
34.01
O
O
Br
210 200 190 180 170 160 150 140 130 120 110 100 90 80 70 60 50 40 30 20 10 0

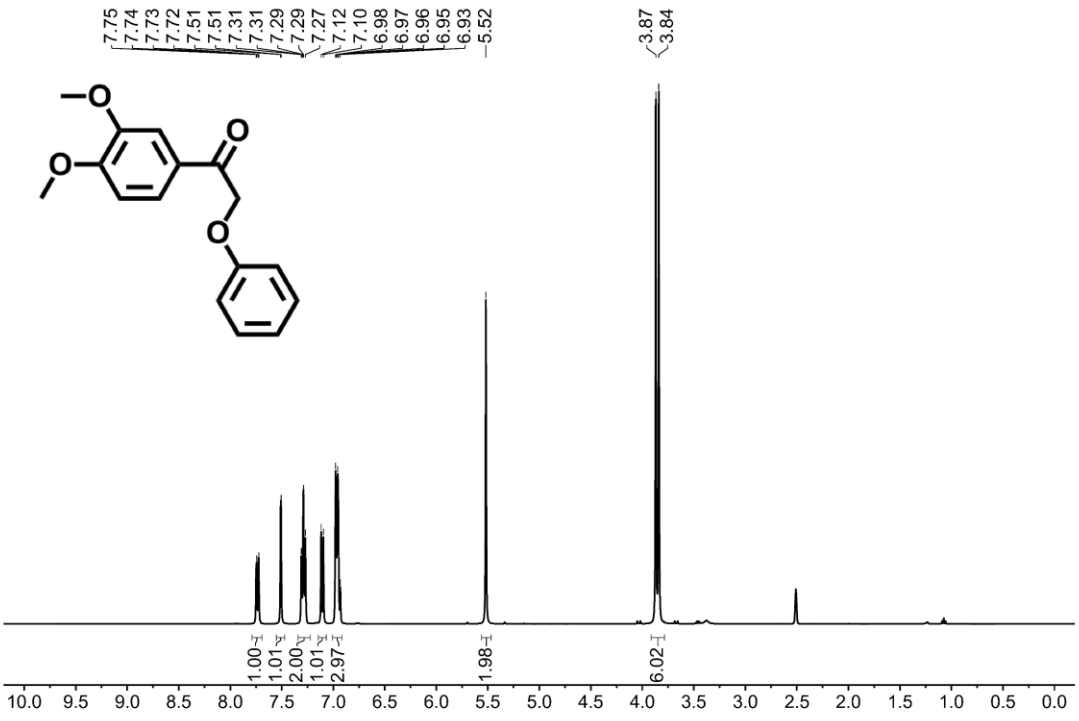
7.75
7.74
7.73
7.72
7.51
7.51
7.31
7.31
7.29
7.29
7.27
7.12
7.10
6.98
6.97
6.96
6.95
6.93
5.52
3.87
3.84
1.00
1.01
2.00
1.01
2.97
1.98
6.02
10.0 9.5 9.0 8.5 8.0 7.5 7.0 6.5 6.0 5.5 5.0 4.5 4.0 3.5 3.0 2.5 2.0 1.5 1.0 0.5 0.0

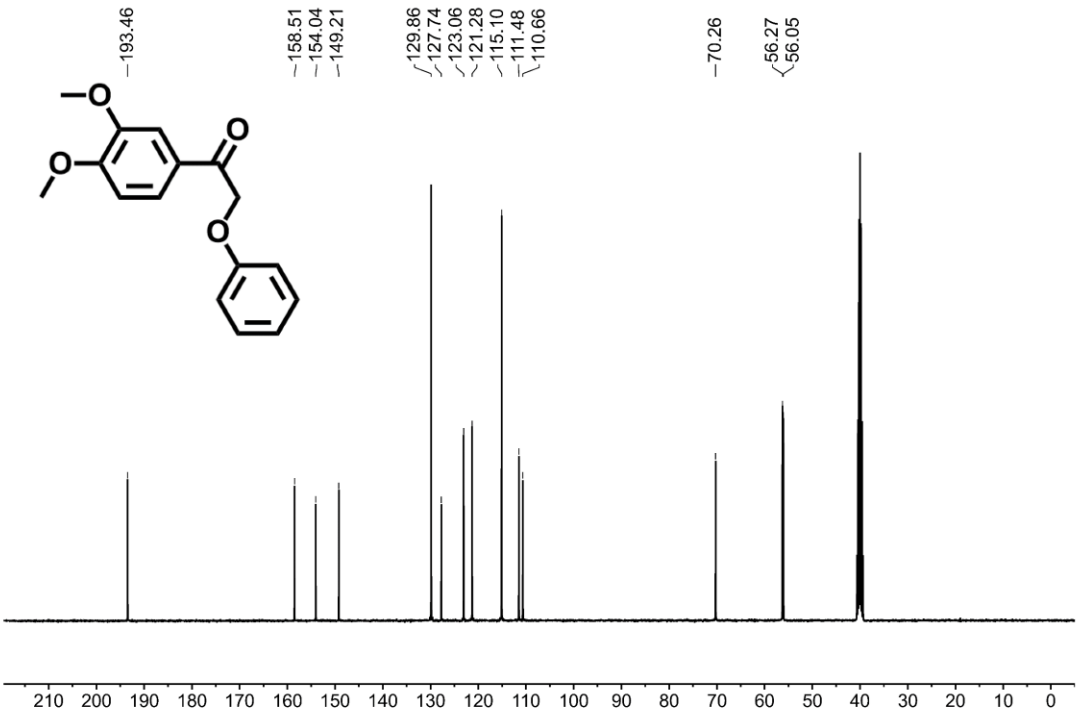
193.46
158.51
154.04
149.21
129.86
127.74
123.06
121.28
115.10
111.48
110.66
70.26
56.27
56.05
210 200 190 180 170 160 150 140 130 120 110 100 90 80 70 60 50 40 30 20 10 0

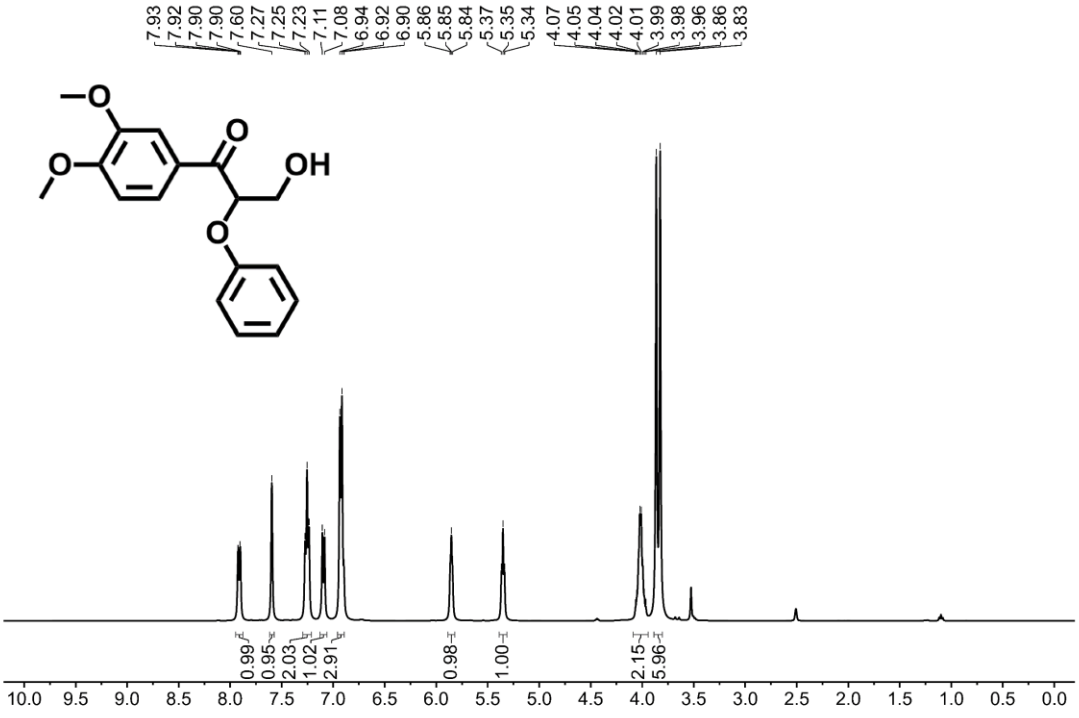
7.93
7.92
7.90
7.90
7.60
7.27
7.25
7.23
7.11
7.08
6.94
6.92
6.90
5.86
5.85
5.84
5.37
5.35
5.34
4.07
4.05
4.04
4.02
4.01
3.99
3.98
3.96
3.86
3.83
O
O
OH
O
0.99
0.95
2.03
1.02
2.91
0.98
1.00
2.15
5.96
10.0 9.5 9.0 8.5 8.0 7.5 7.0 6.5 6.0 5.5 5.0 4.5 4.0 3.5 3.0 2.5 2.0 1.5 1.0 0.5 0.0

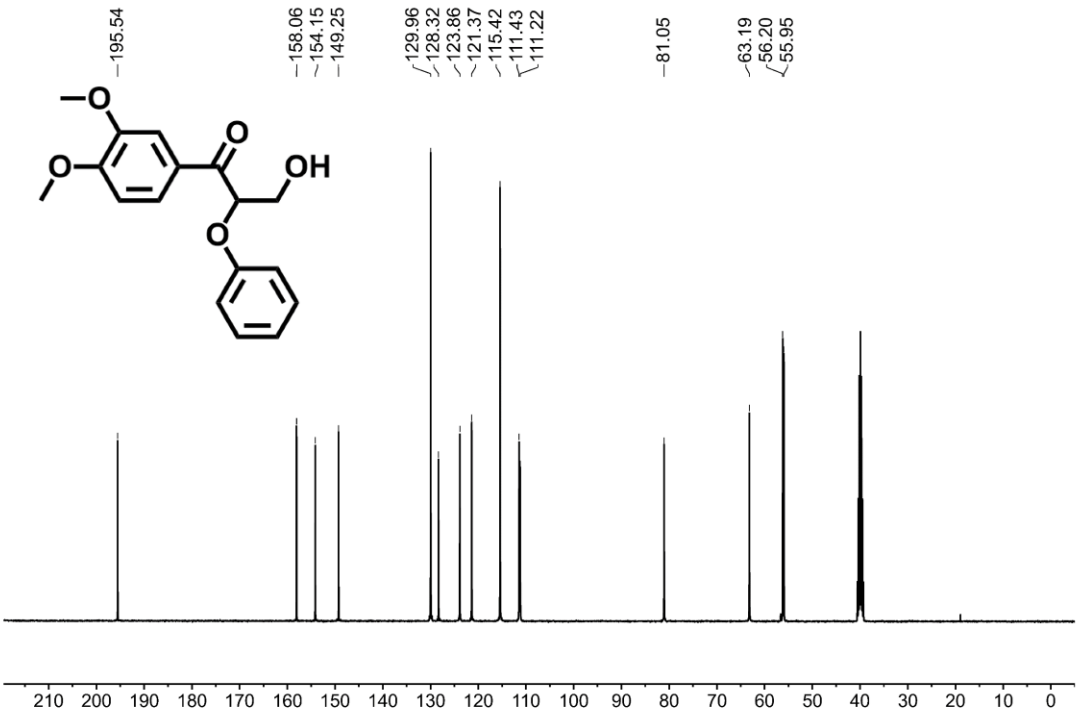
195.54
158.06
154.15
149.25
129.96
128.32
123.86
121.37
115.42
111.43
111.22
81.05
63.19
56.20
55.95
O
O
OH
O
210 200 190 180 170 160 150 140 130 120 110 100 90 80 70 60 50 40 30 20 10 0

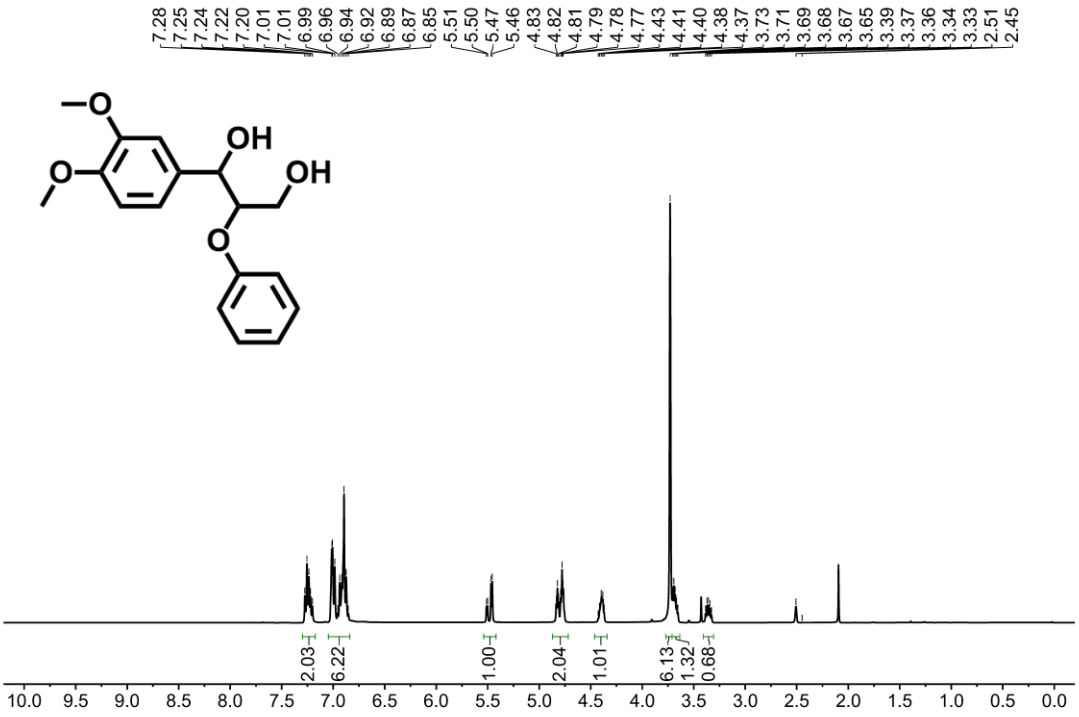
7.28
7.25
7.24
7.22
7.20
7.01
7.01
6.99
6.96
6.94
6.92
6.89
6.87
6.85
5.51
5.50
5.47
5.46
4.83
4.82
4.81
4.79
4.78
4.77
4.43
4.41
4.40
4.38
4.37
3.73
3.71
3.69
3.68
3.67
3.65
3.39
3.37
3.36
3.34
3.33
2.51
2.45
OH
OH
2.03
6.22
1.00
2.04
1.01
6.13
1.32
0.68
10.0 9.5 9.0 8.5 8.0 7.5 7.0 6.5 6.0 5.5 5.0 4.5 4.0 3.5 3.0 2.5 2.0 1.5 1.0 0.5 0.0

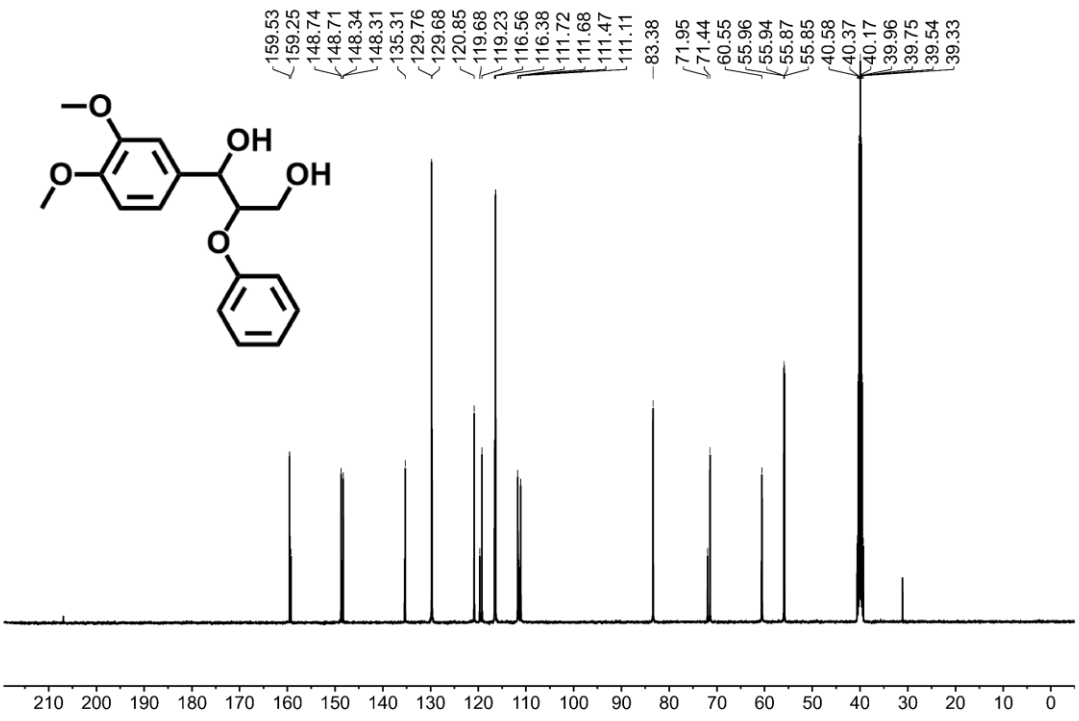
159.53
159.25
148.74
148.71
148.34
148.31
135.31
129.76
129.68
120.85
119.68
119.23
116.56
116.38
111.72
111.68
111.47
111.11
83.38
71.95
71.44
60.55
55.96
55.94
55.87
55.85
40.58
40.37
40.17
39.96
39.75
39.54
39.33
OH
OH
210 200 190 180 170 160 150 140 130 120 110 100 90 80 70 60 50 40 30 20 10 0

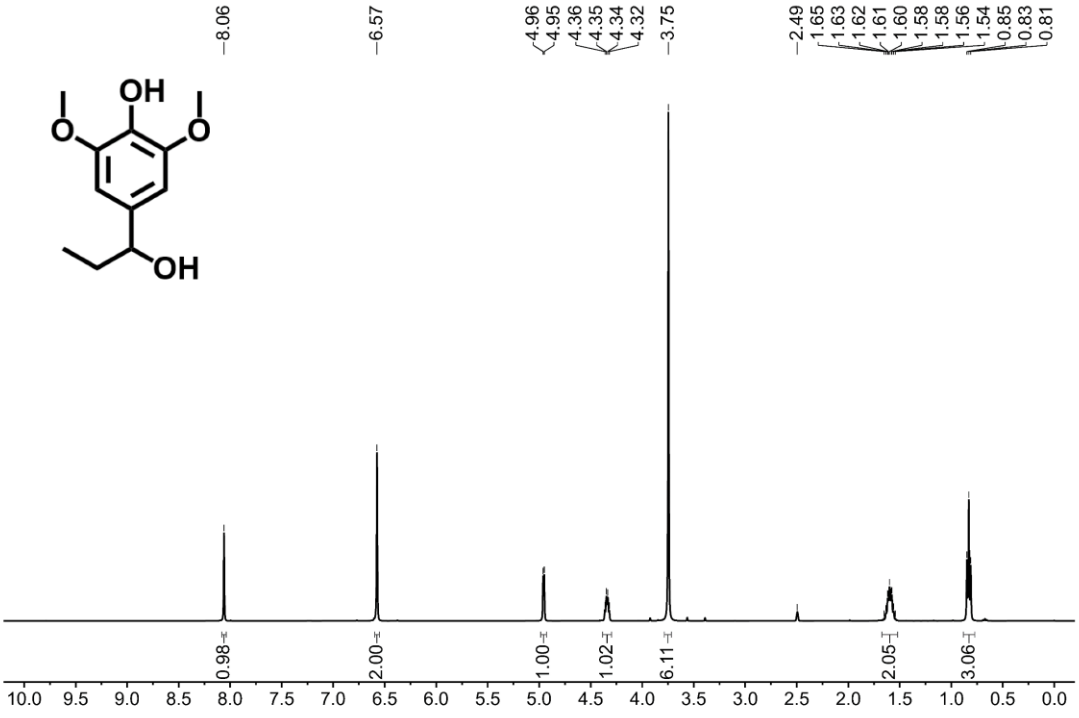
8.06
6.57
4.96
4.95
4.36
4.35
4.34
4.32
3.75
2.49
1.65
1.63
1.62
1.61
1.60
1.58
1.58
1.56
1.54
0.85
0.83
0.81
OH
O
O
OH
0.98
2.00
1.00
1.02
6.11
2.05
3.06
10.0 9.5 9.0 8.5 8.0 7.5 7.0 6.5 6.0 5.5 5.0 4.5 4.0 3.5 3.0 2.5 2.0 1.5 1.0 0.5 0.0

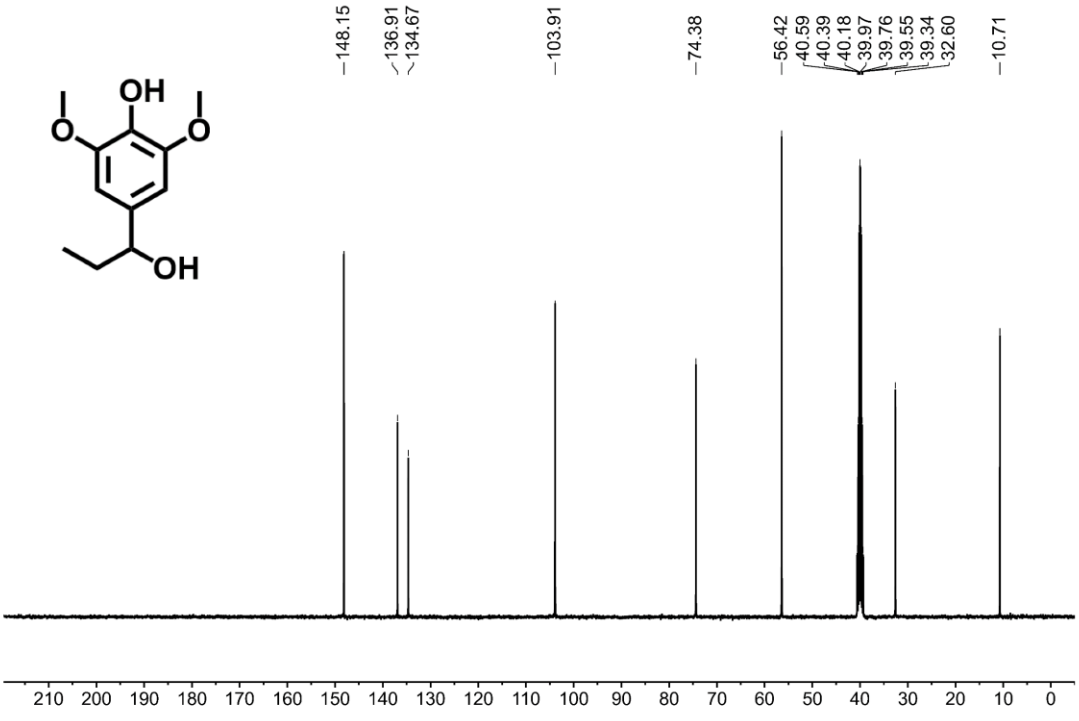
148.15
136.91
134.67
103.91
74.38
56.42
40.59
40.39
40.18
39.97
39.76
39.55
39.34
32.60
10.71
OH
O
O
OH
210 200 190 180 170 160 150 140 130 120 110 100 90 80 70 60 50 40 30 20 10 0

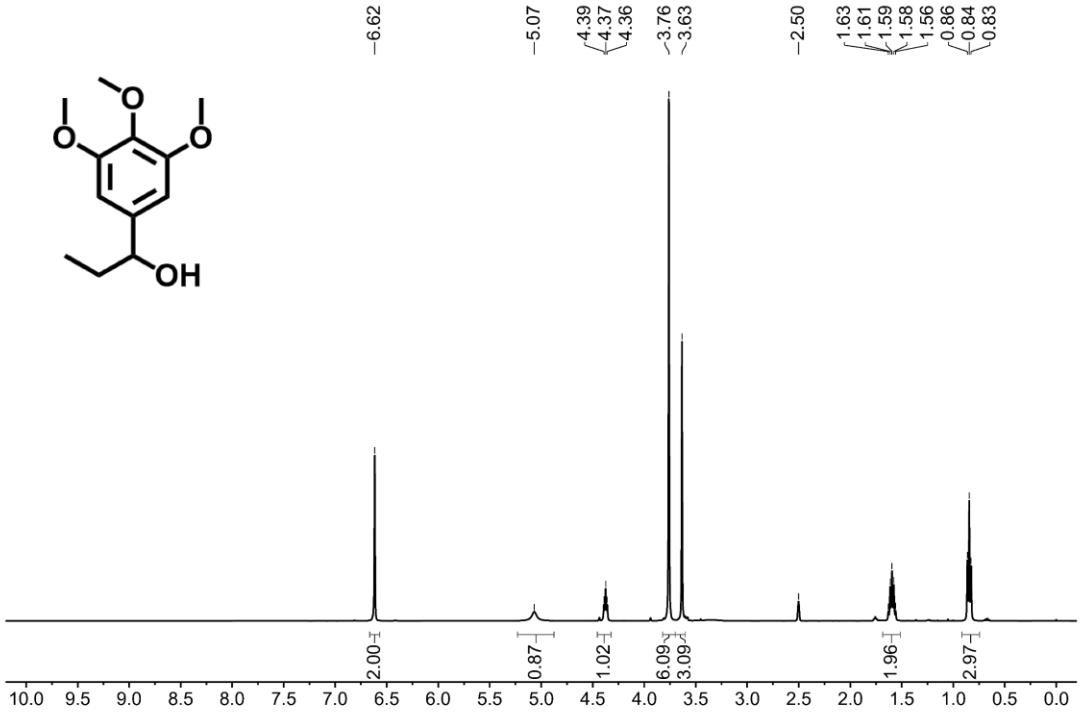
6.62
5.07
4.39
4.37
4.36
3.76
3.63
2.50
1.63
1.61
1.59
1.58
1.56
0.86
0.84
0.83
O
O
O
OH
2.00
0.87
1.02
6.09
3.09
1.96
2.97
10.0 9.5 9.0 8.5 8.0 7.5 7.0 6.5 6.0 5.5 5.0 4.5 4.0 3.5 3.0 2.5 2.0 1.5 1.0 0.5 0.0

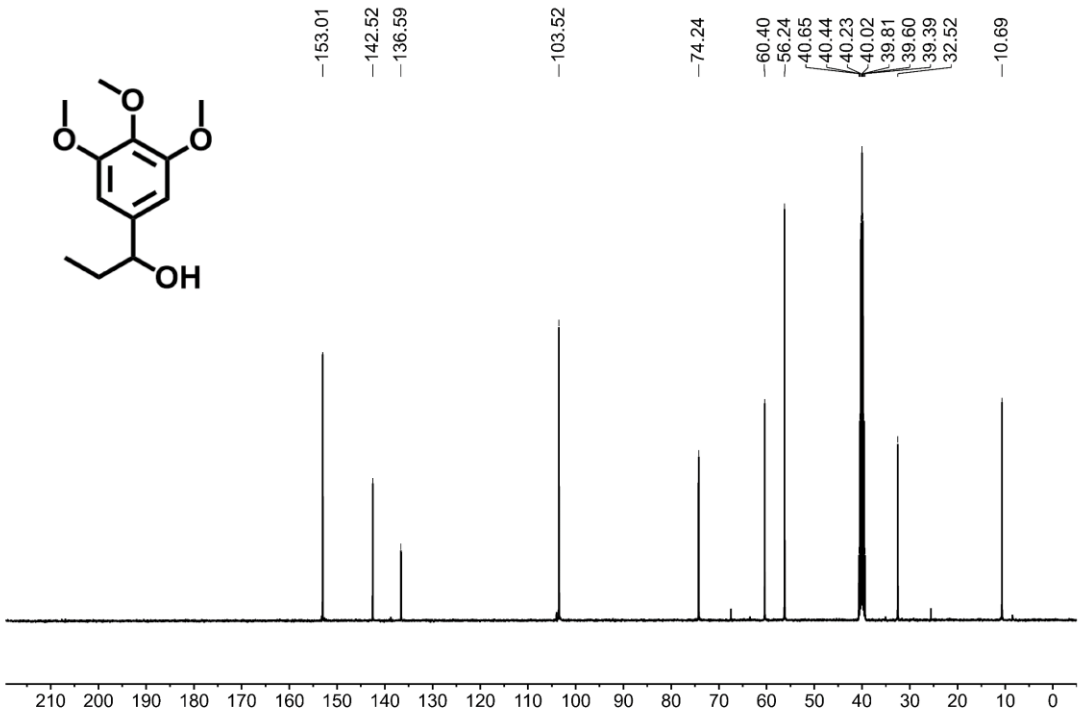
153.01
142.52
136.59
103.52
74.24
60.40
56.24
40.65
40.44
40.23
40.02
39.81
39.60
39.39
32.52
10.69
O
O
O
OH
210 200 190 180 170 160 150 140 130 120 110 100 90 80 70 60 50 40 30 20 10 0

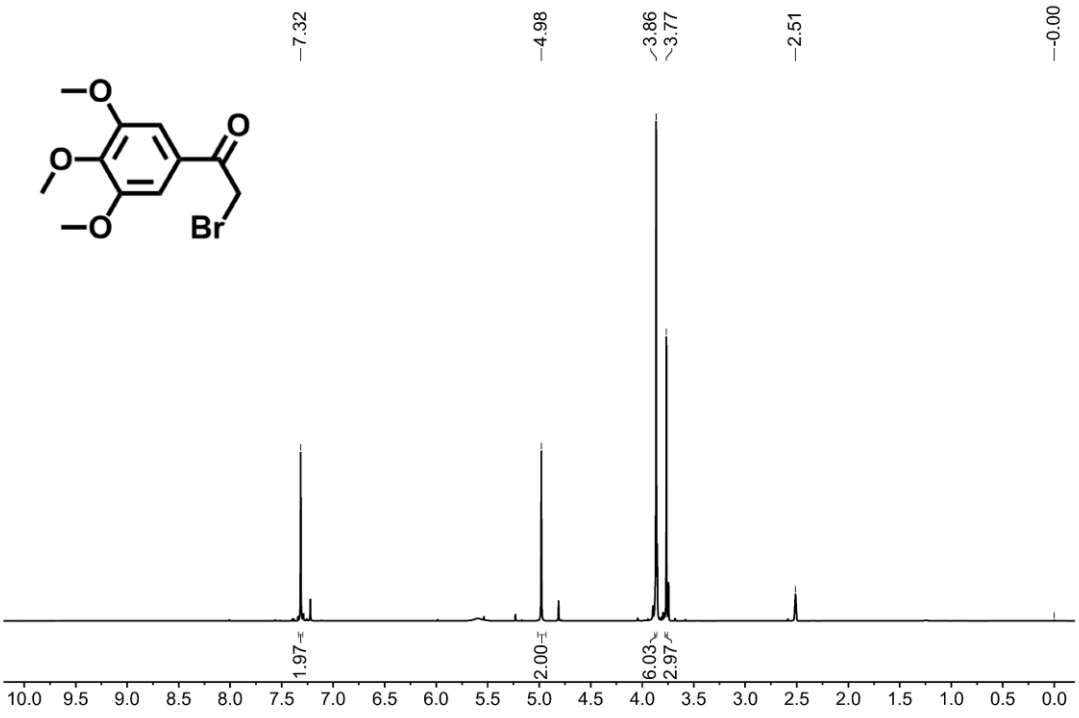
7.32
4.98
3.86
3.77
2.51
0.00
1.97
2.00
6.03
2.97
10.0 9.5 9.0 8.5 8.0 7.5 7.0 6.5 6.0 5.5 5.0 4.5 4.0 3.5 3.0 2.5 2.0 1.5 1.0 0.5 0.0
O
O
O
O
Br

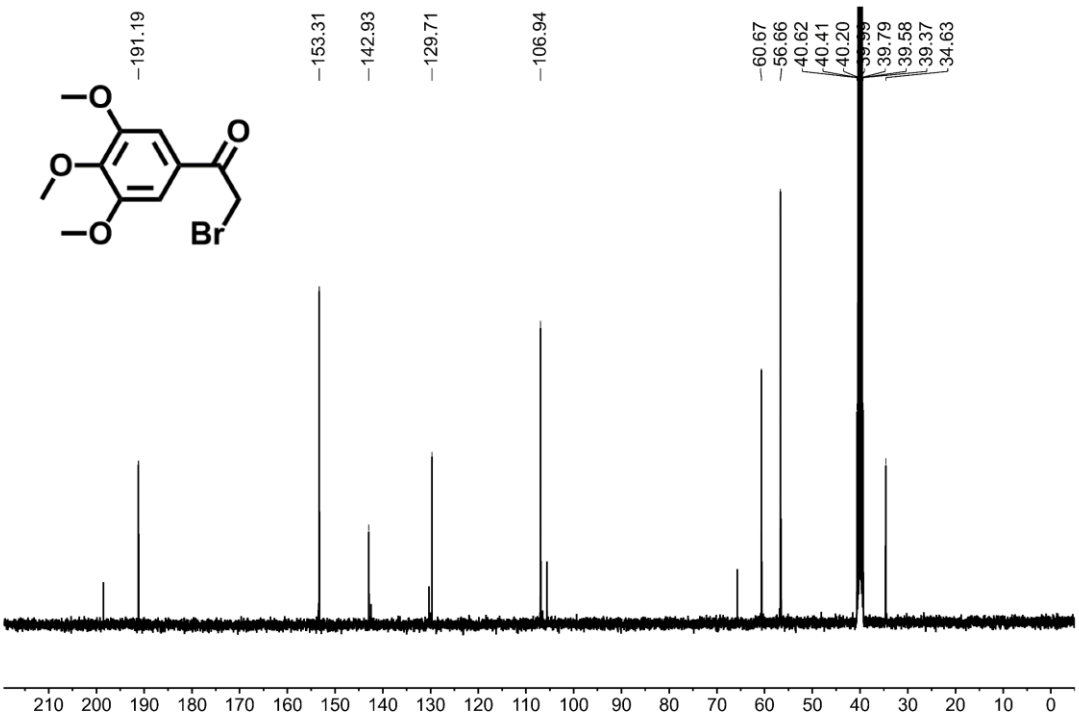
191.19
153.31
142.93
129.71
106.94
60.67
56.66
40.62
40.41
40.20
39.79
39.58
39.37
34.63
210 200 190 180 170 160 150 140 130 120 110 100 90 80 70 60 50 40 30 20 10 0
O
O
O
O
Br

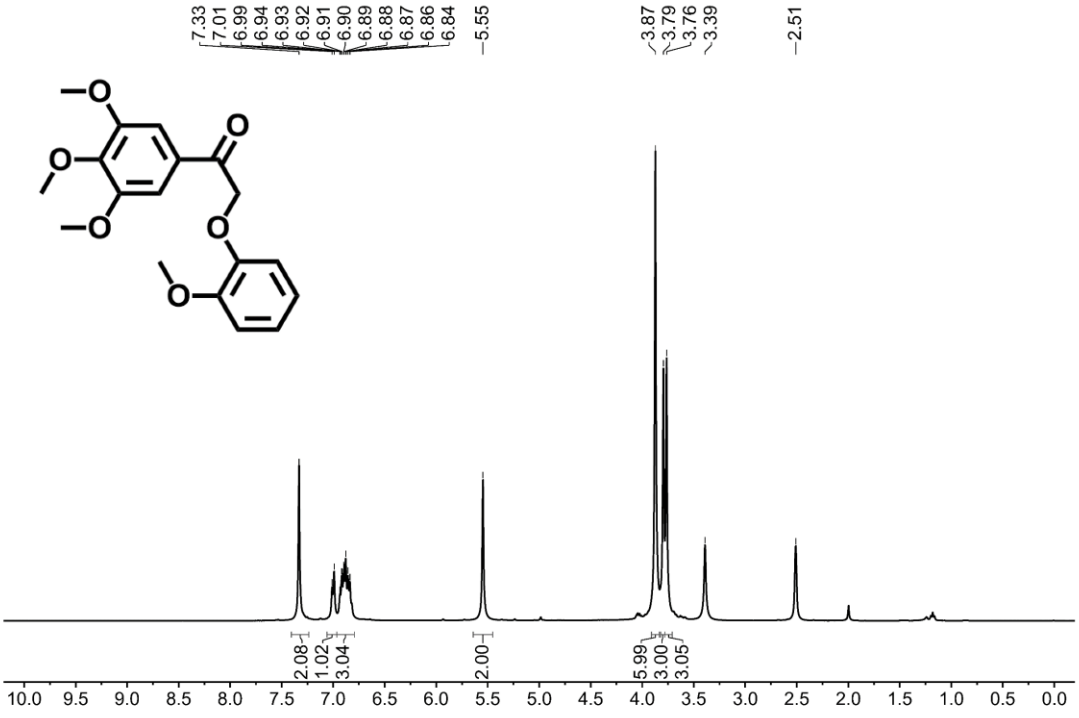
7.33
7.01
6.99
6.94
6.93
6.92
6.91
6.90
6.89
6.88
6.87
6.86
6.84
5.55
3.87
3.79
3.76
3.39
2.51
2.08
1.02
3.04
2.00
5.99
3.00
3.05
10.0 9.5 9.0 8.5 8.0 7.5 7.0 6.5 6.0 5.5 5.0 4.5 4.0 3.5 3.0 2.5 2.0 1.5 1.0 0.5 0.0

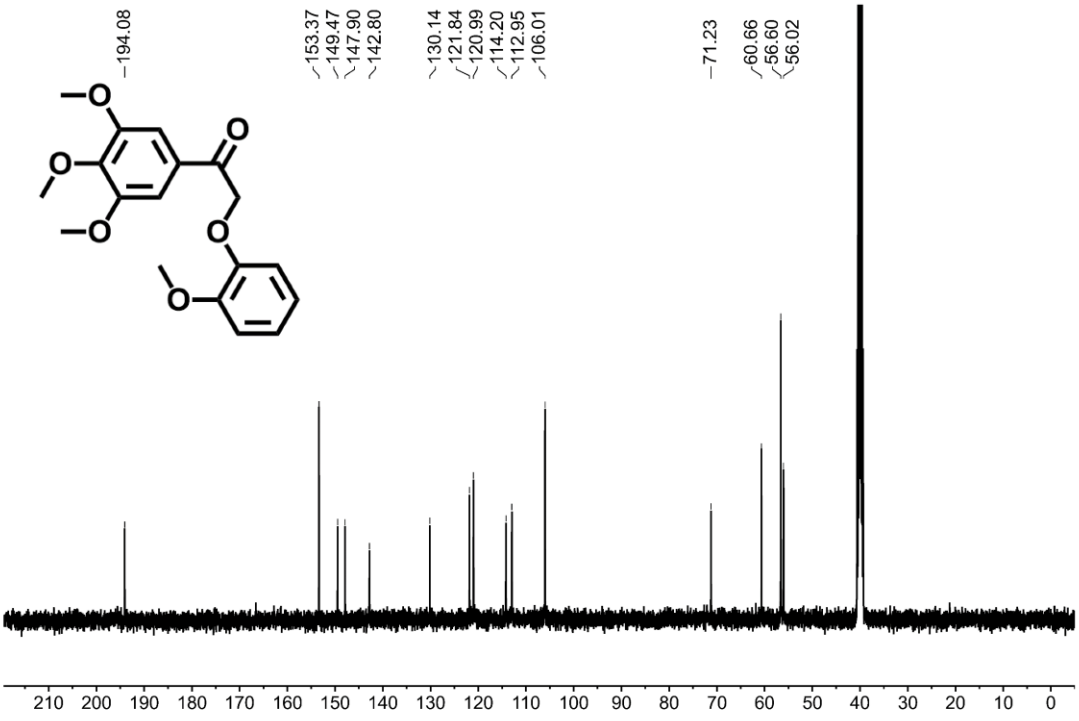
194.08
153.37
149.47
147.90
142.80
130.14
121.84
120.99
114.20
112.95
106.01
71.23
60.66
56.60
56.02
210 200 190 180 170 160 150 140 130 120 110 100 90 80 70 60 50 40 30 20 10 0

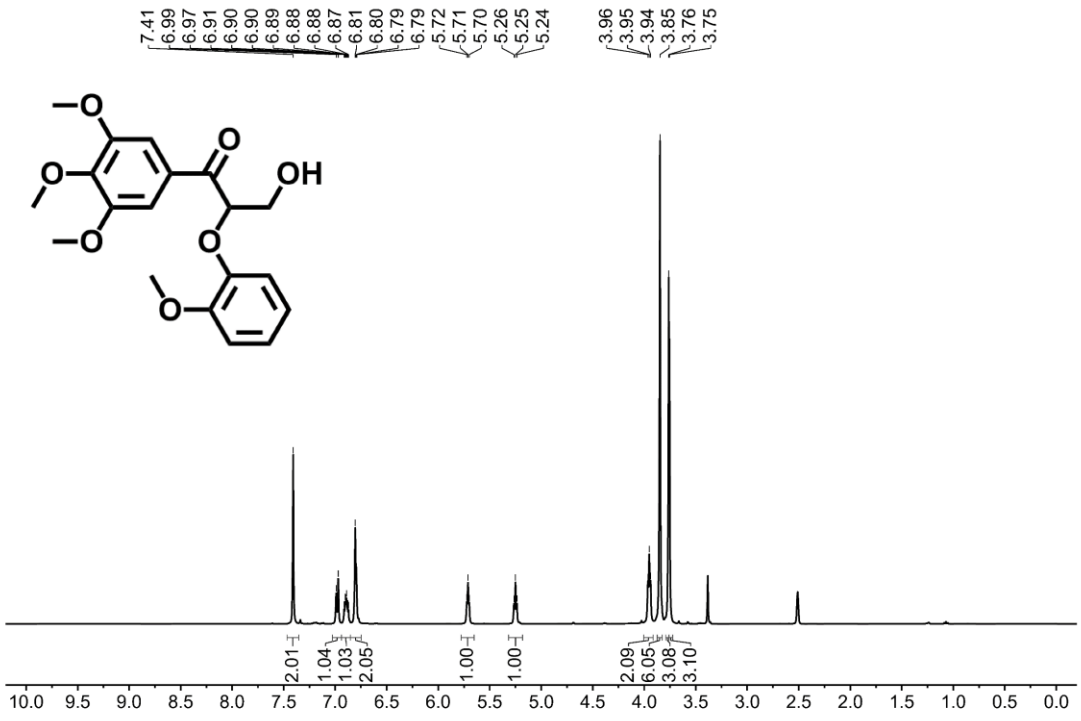
7.41
6.99
6.97
6.91
6.90
6.90
6.89
6.88
6.88
6.87
6.81
6.80
6.79
6.79
5.72
5.71
5.70
5.26
5.25
5.24
3.96
3.95
3.94
3.85
3.76
3.75
OH
2.01
1.04
1.03
2.05
1.00
1.00
2.09
6.05
3.08
3.10
10.0 9.5 9.0 8.5 8.0 7.5 7.0 6.5 6.0 5.5 5.0 4.5 4.0 3.5 3.0 2.5 2.0 1.5 1.0 0.5 0.0

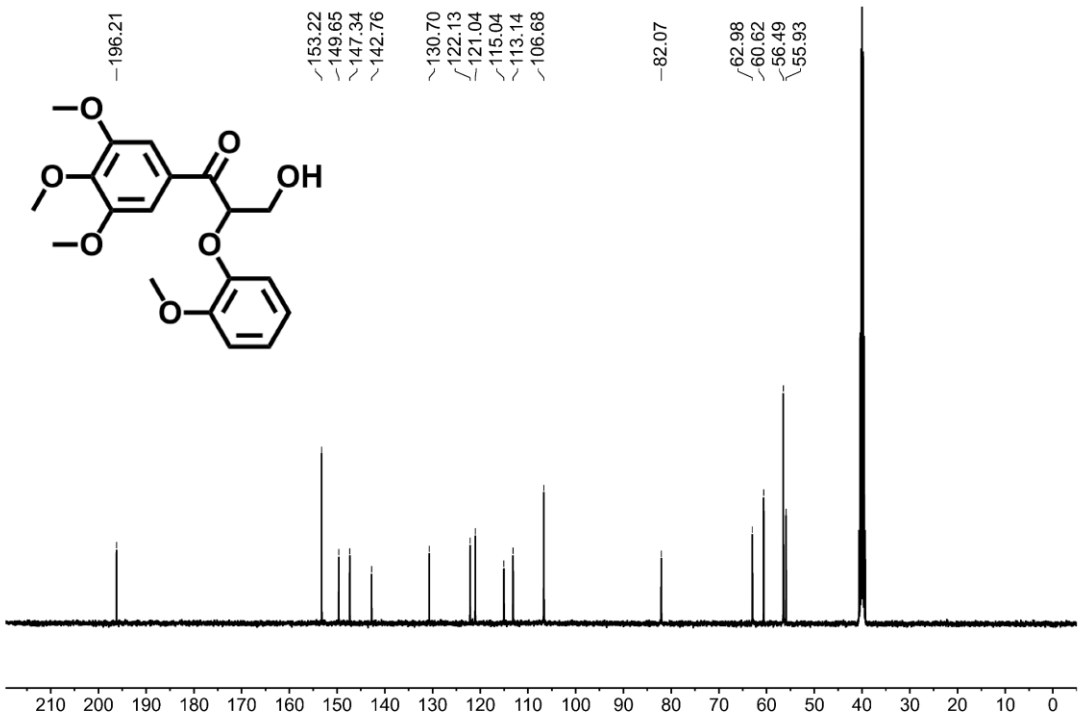
196.21
153.22
149.65
147.34
142.76
130.70
122.13
121.04
115.04
113.14
106.68
82.07
62.98
60.62
56.49
55.93
OH
210 200 190 180 170 160 150 140 130 120 110 100 90 80 70 60 50 40 30 20 10 0

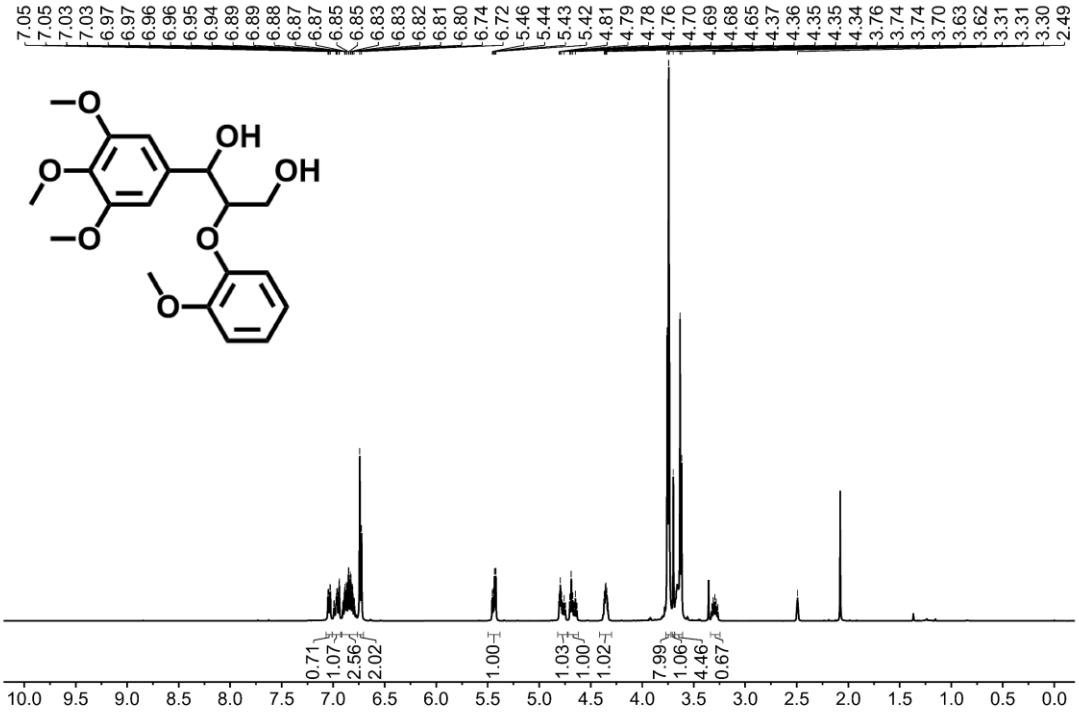
7.05
7.05
7.03
7.03
6.97
6.97
6.96
6.96
6.95
6.94
6.89
6.89
6.88
6.87
6.85
6.85
6.83
6.82
6.81
6.80
6.74
6.72
5.46
5.44
5.43
5.42
4.81
4.79
4.78
4.76
4.70
4.69
4.68
4.65
4.37
4.36
4.35
4.35
4.34
3.76
3.74
3.74
3.70
3.63
3.62
3.31
3.31
3.30
2.49
OH
OH
O
O
O
O
O
0.71
1.07
2.56
2.02
1.00
1.03
1.00
1.02
7.99
1.06
4.46
0.67
10.0 9.5 9.0 8.5 8.0 7.5 7.0 6.5 6.0 5.5 5.0 4.5 4.0 3.5 3.0 2.5 2.0 1.5 1.0 0.5 0.0

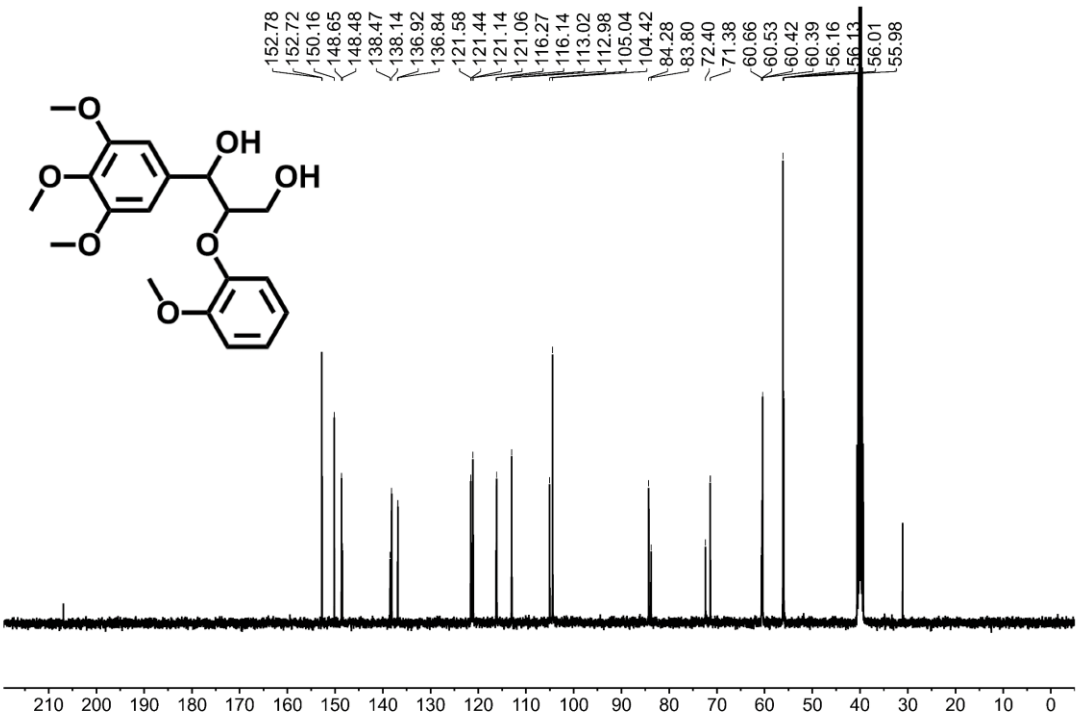
152.78
152.72
150.16
148.65
148.48
138.47
138.14
136.92
136.84
121.58
121.44
121.14
121.06
116.27
116.14
113.02
112.98
105.04
104.42
84.28
83.80
72.40
71.38
60.66
60.53
60.42
60.39
56.16
56.13
56.01
55.98
OH
OH
O
O
O
O
O
210 200 190 180 170 160 150 140 130 120 110 100 90 80 70 60 50 40 30 20 10 0

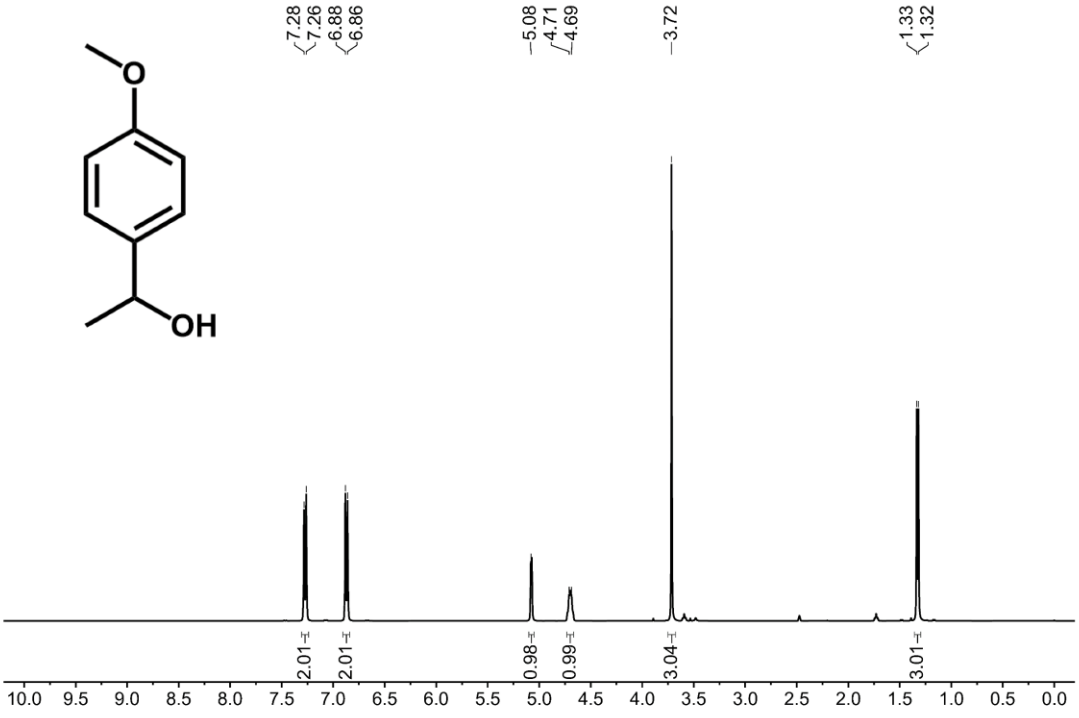
7.28
7.26
6.88
6.86
5.08
4.71
4.69
3.72
1.33
1.32
O
OH
2.01
2.01
0.98
0.99
3.04
3.01
10.0 9.5 9.0 8.5 8.0 7.5 7.0 6.5 6.0 5.5 5.0 4.5 4.0 3.5 3.0 2.5 2.0 1.5 1.0 0.5 0.0

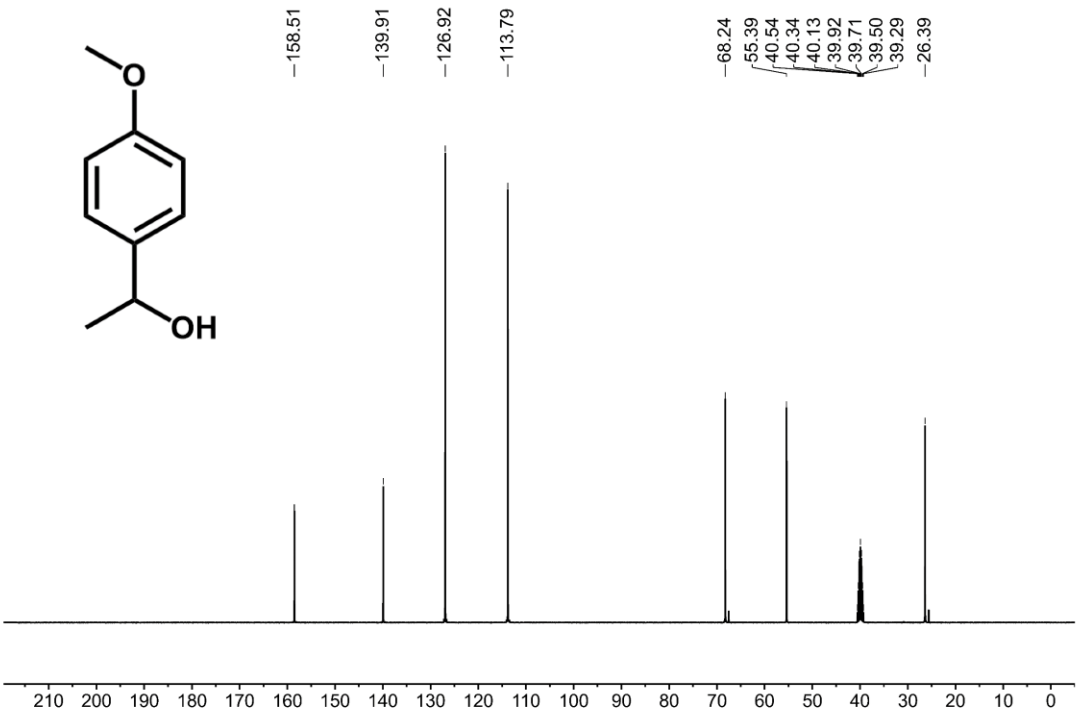
158.51
139.91
126.92
113.79
68.24
55.39
40.54
40.34
40.13
39.92
39.71
39.50
39.29
26.39
O
OH
210 200 190 180 170 160 150 140 130 120 110 100 90 80 70 60 50 40 30 20 10 0

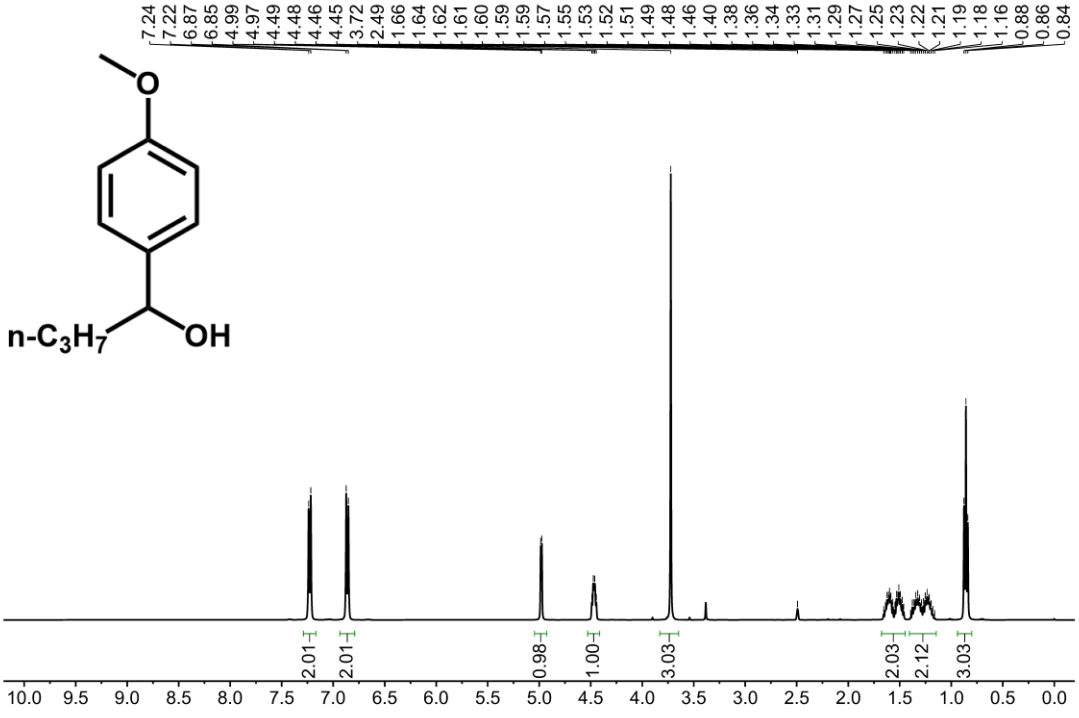
7.24
7.22
6.87
6.85
4.99
4.97
4.49
4.48
4.46
4.45
3.72
2.49
1.66
1.64
1.62
1.61
1.60
1.59
1.59
1.57
1.55
1.53
1.52
1.51
1.49
1.48
1.46
1.40
1.38
1.36
1.34
1.33
1.31
1.29
1.27
1.25
1.23
1.22
1.21
1.19
1.18
1.16
0.88
0.86
0.84
O
n-C3H7
OH
2.01
2.01
0.98
1.00
3.03
2.03
2.12
3.03
10.0 9.5 9.0 8.5 8.0 7.5 7.0 6.5 6.0 5.5 5.0 4.5 4.0 3.5 3.0 2.5 2.0 1.5 1.0 0.5 0.0

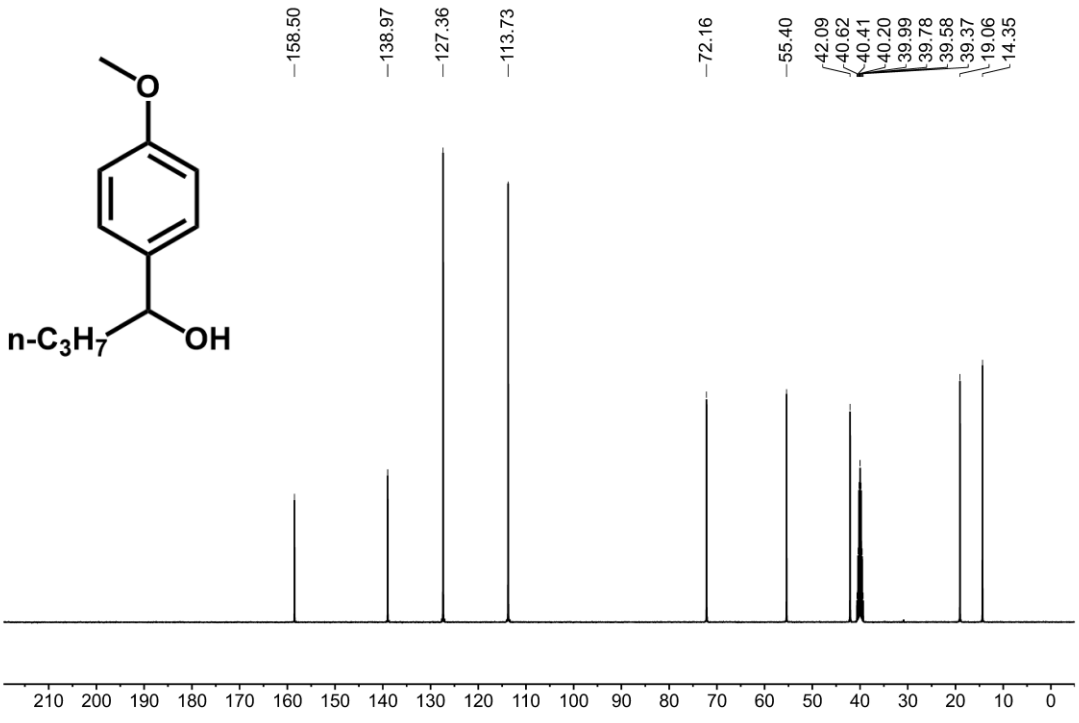
158.50
138.97
127.36
113.73
72.16
55.40
42.09
40.62
40.41
40.20
39.99
39.78
39.58
39.37
19.06
14.35
O
n-C3H7
OH
210 200 190 180 170 160 150 140 130 120 110 100 90 80 70 60 50 40 30 20 10 0

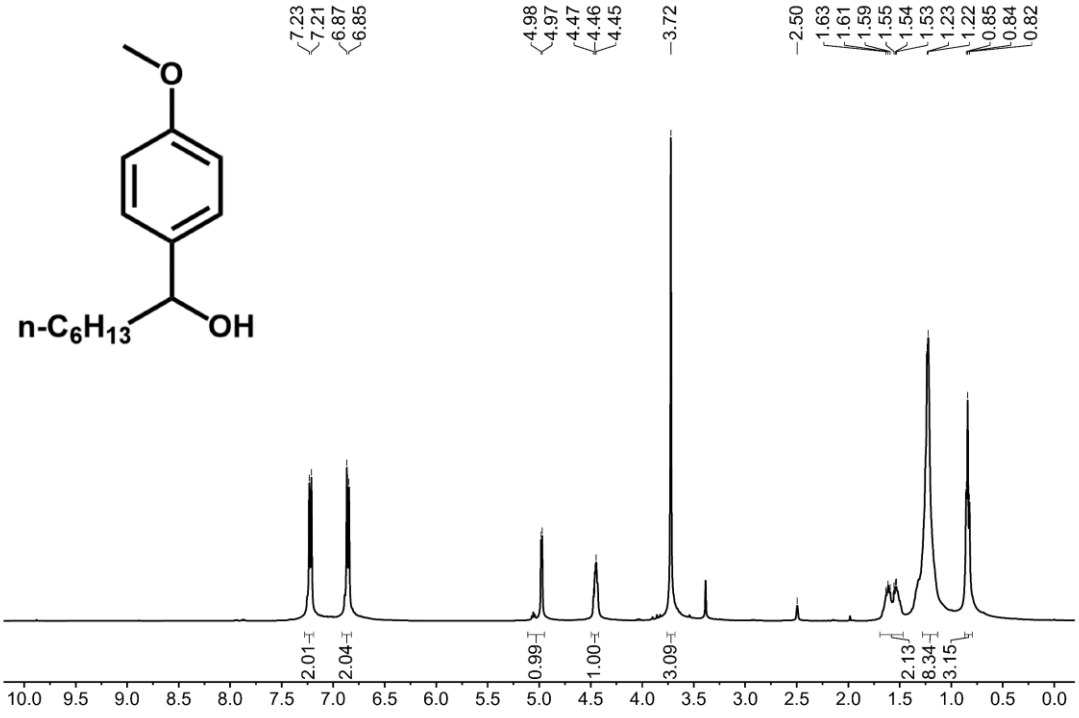
7.23
7.21
6.87
6.85
4.98
4.97
4.47
4.46
4.45
3.72
2.50
1.63
1.61
1.59
1.55
1.54
1.53
1.23
1.22
0.85
0.84
0.82
O
n-C6H13
OH
2.01
2.04
0.99
1.00
3.09
2.13
8.34
3.15
10.0 9.5 9.0 8.5 8.0 7.5 7.0 6.5 6.0 5.5 5.0 4.5 4.0 3.5 3.0 2.5 2.0 1.5 1.0 0.5 0.0

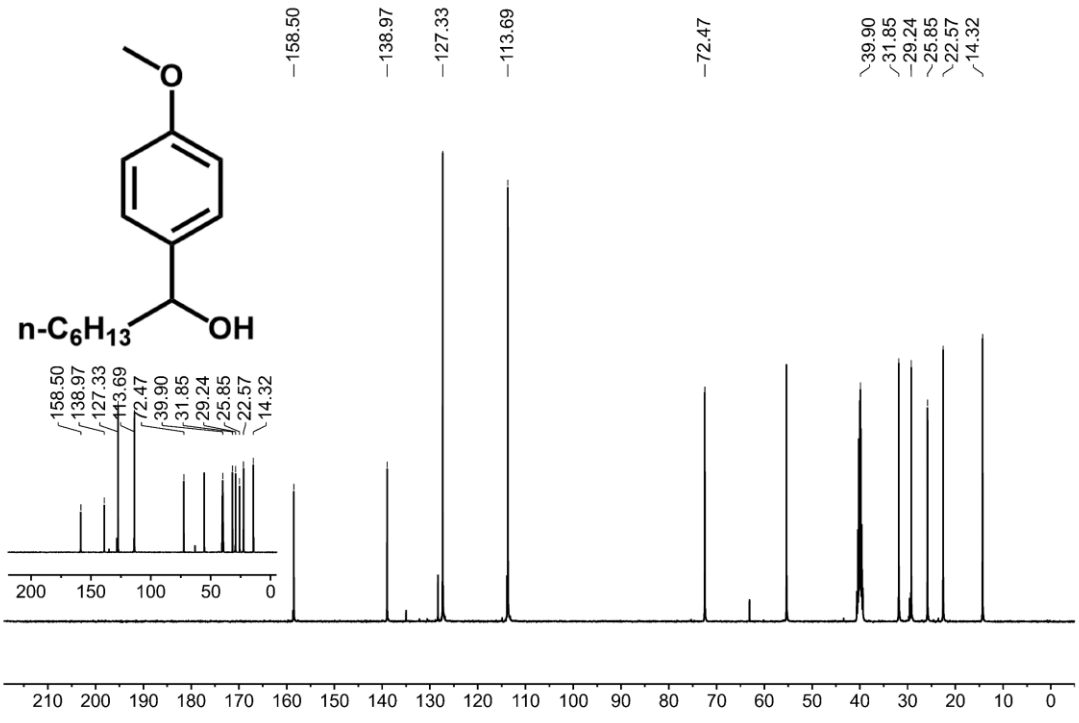
158.50
138.97
127.33
113.69
72.47
39.90
31.85
29.24
25.85
22.57
14.32
O
n-C6H13
OH
200 150 100 50 0
210 200 190 180 170 160 150 140 130 120 110 100 90 80 70 60 50 40 30 20 10 0

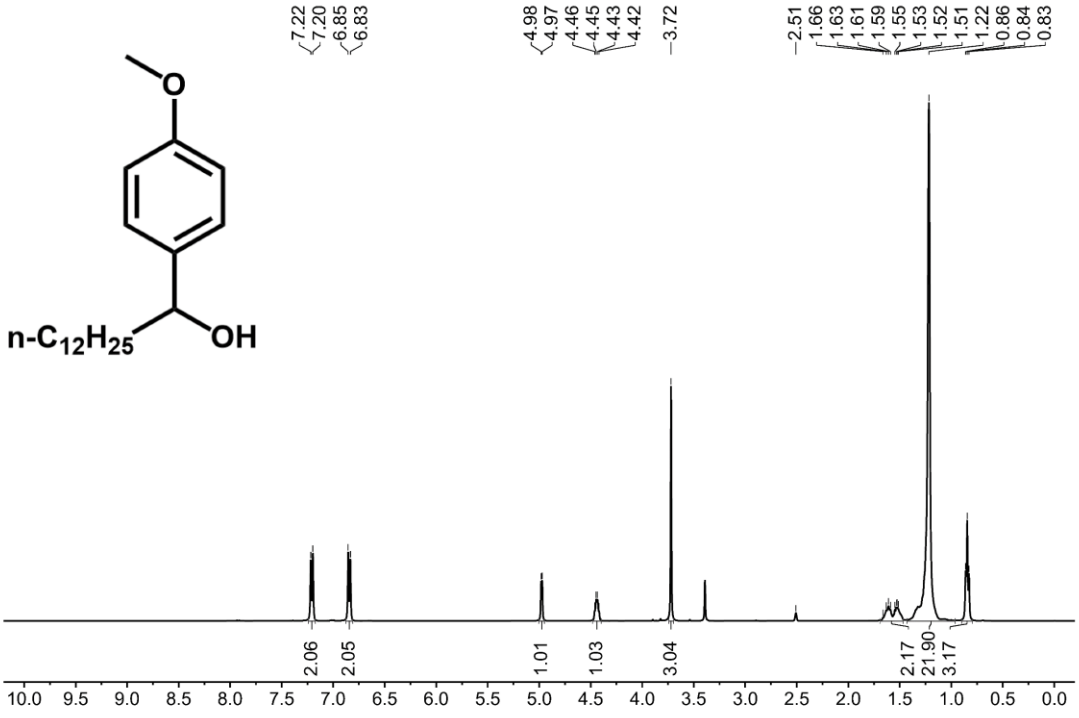
7.22
7.20
6.85
6.83
4.98
4.97
4.46
4.45
4.43
4.42
3.72
2.51
1.66
1.63
1.61
1.59
1.55
1.53
1.52
1.51
1.22
0.86
0.84
0.83
O
n-C12H25
OH
2.06
2.05
1.01
1.03
3.04
2.17
21.90
3.17
10.0 9.5 9.0 8.5 8.0 7.5 7.0 6.5 6.0 5.5 5.0 4.5 4.0 3.5 3.0 2.5 2.0 1.5 1.0 0.5 0.0

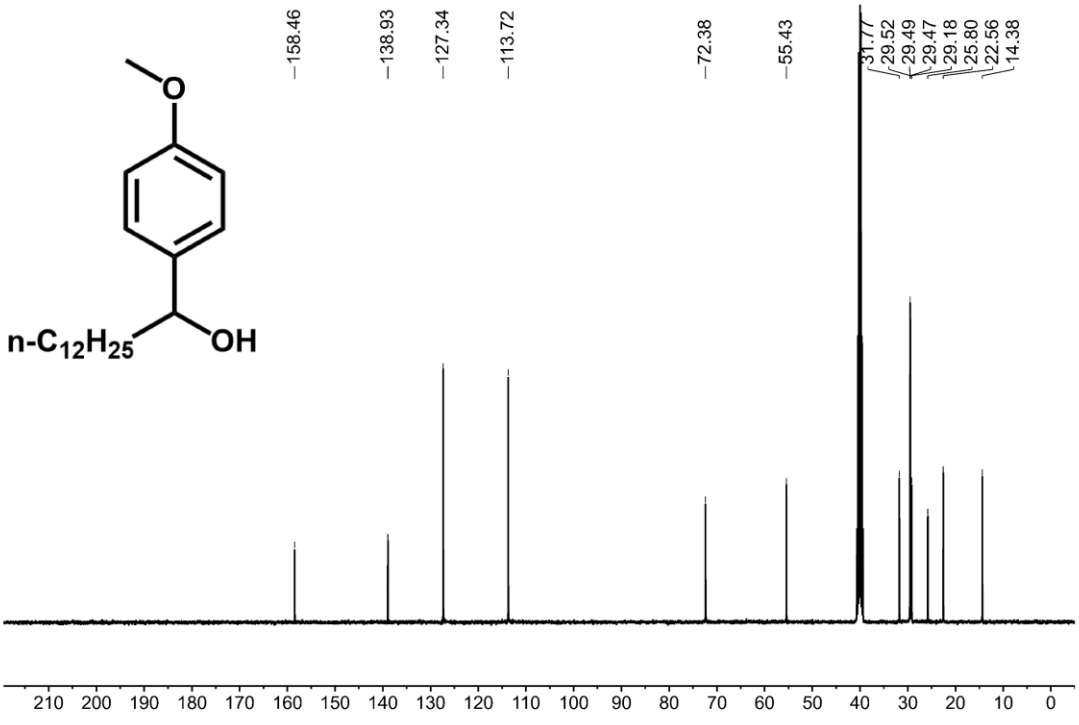
158.46
138.93
127.34
113.72
72.38
55.43
31.77
29.52
29.49
29.47
29.18
25.80
22.56
14.38
O
n-C12H25
OH
210 200 190 180 170 160 150 140 130 120 110 100 90 80 70 60 50 40 30 20 10 0

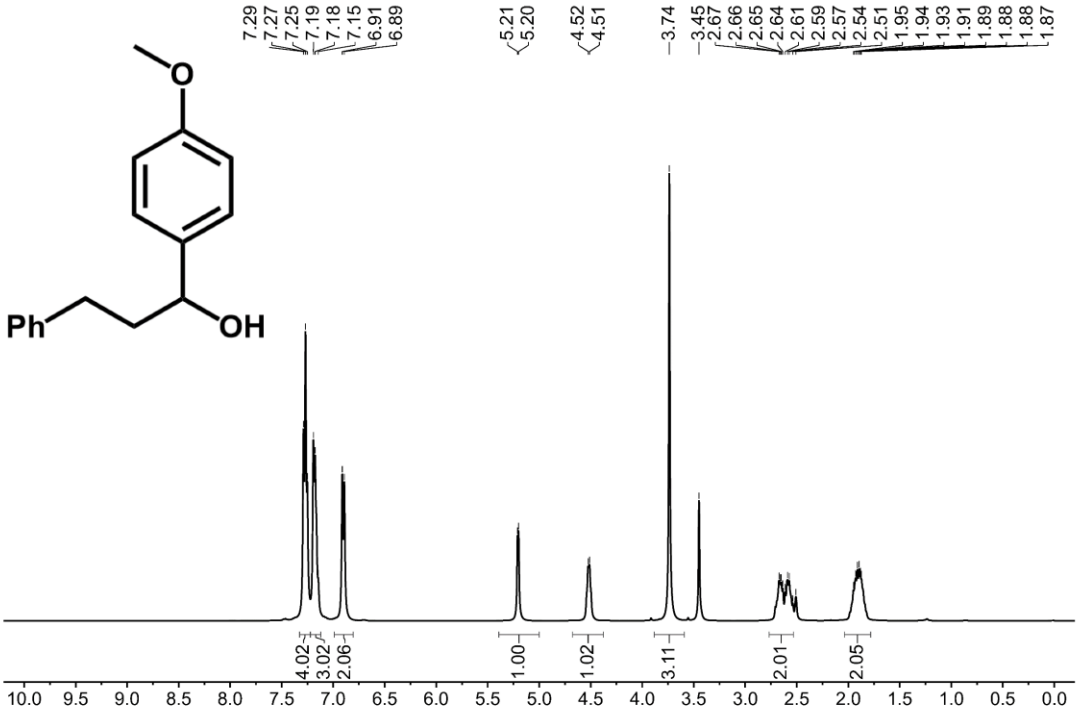
7.29
7.27
7.25
7.19
7.18
7.15
6.91
6.89
5.21
5.20
4.52
4.51
3.74
3.45
2.67
2.66
2.65
2.64
2.61
2.59
2.57
2.54
2.51
1.95
1.94
1.93
1.91
1.89
1.88
1.88
1.87
O
Ph
OH
4.02
3.02
2.06
1.00
1.02
3.11
2.01
2.05
10.0 9.5 9.0 8.5 8.0 7.5 7.0 6.5 6.0 5.5 5.0 4.5 4.0 3.5 3.0 2.5 2.0 1.5 1.0 0.5 0.0

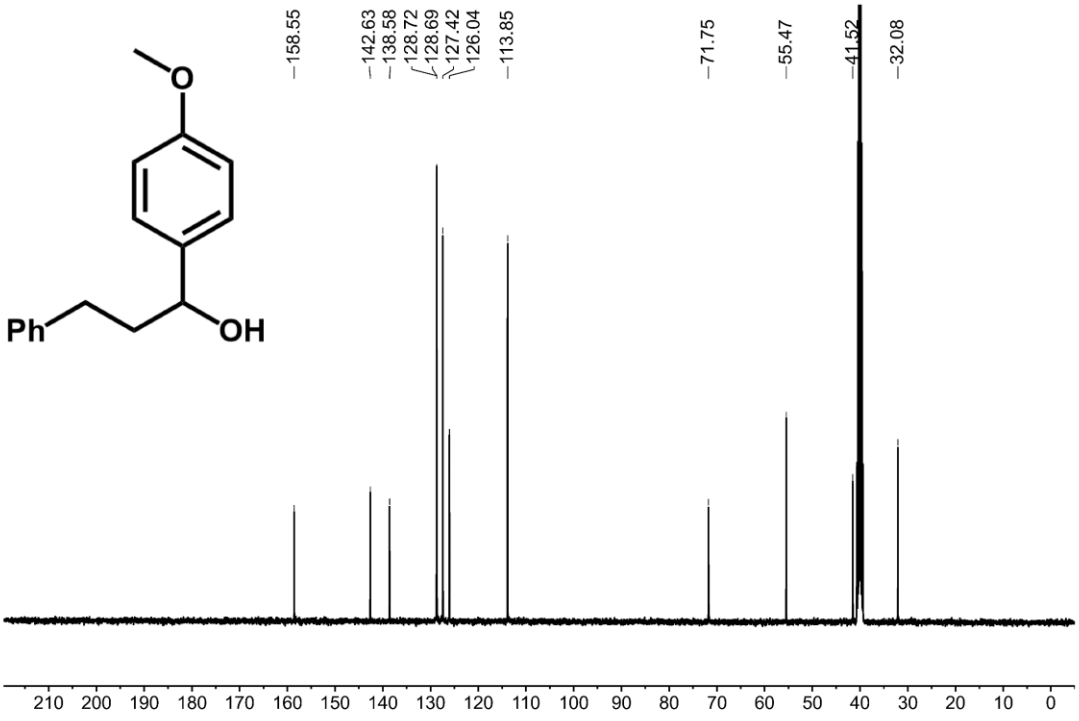
158.55
142.63
138.58
128.72
128.69
127.42
126.04
113.85
71.75
55.47
41.52
32.08
O
Ph
OH
210 200 190 180 170 160 150 140 130 120 110 100 90 80 70 60 50 40 30 20 10 0

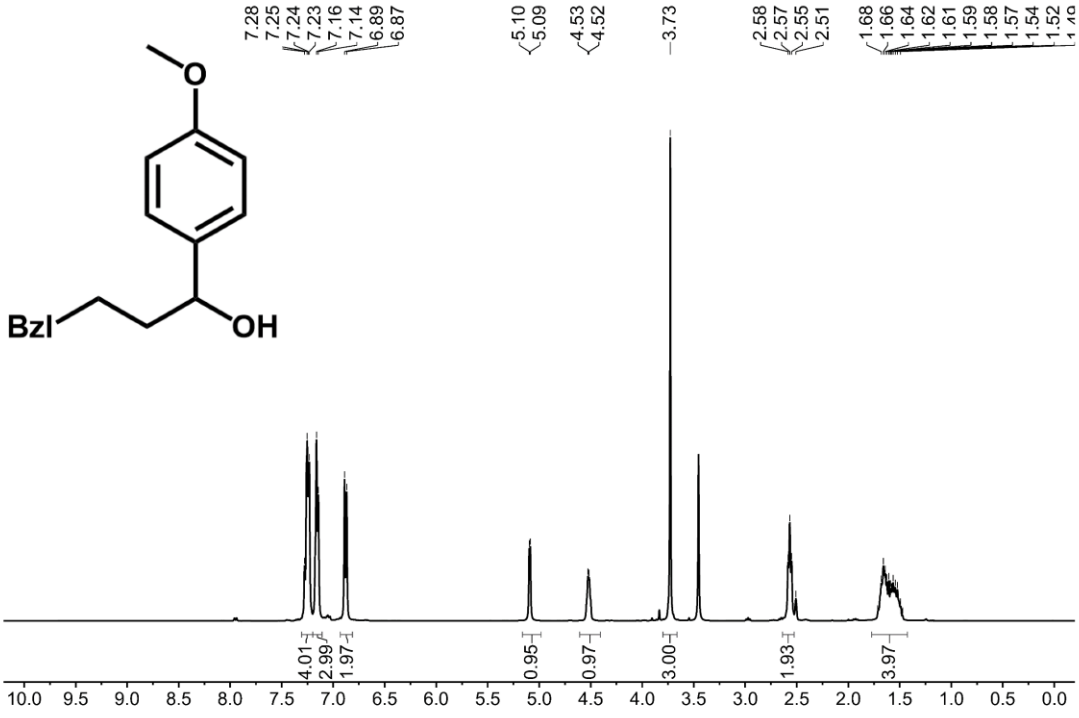
7.28
7.25
7.24
7.23
7.16
7.14
6.89
6.87
5.10
5.09
4.53
4.52
3.73
2.58
2.57
2.55
2.51
1.68
1.66
1.64
1.62
1.61
1.59
1.58
1.57
1.54
1.52
O
Bzl
OH
4.01
2.99
1.97
0.95
0.97
3.00
1.93
3.97
10.0 9.5 9.0 8.5 8.0 7.5 7.0 6.5 6.0 5.5 5.0 4.5 4.0 3.5 3.0 2.5 2.0 1.5 1.0 0.5 0.0

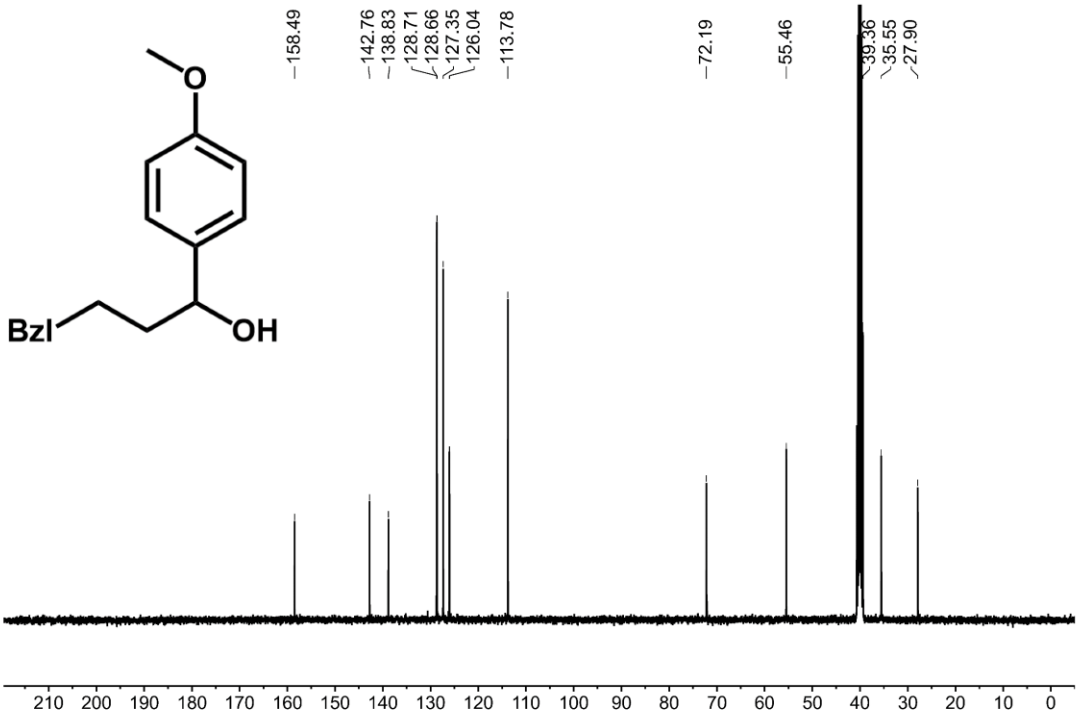
158.49
142.76
138.83
128.71
128.66
127.35
126.04
113.78
72.19
55.46
39.36
35.55
27.90
O
Bzl
OH
210 200 190 180 170 160 150 140 130 120 110 100 90 80 70 60 50 40 30 20 10 0

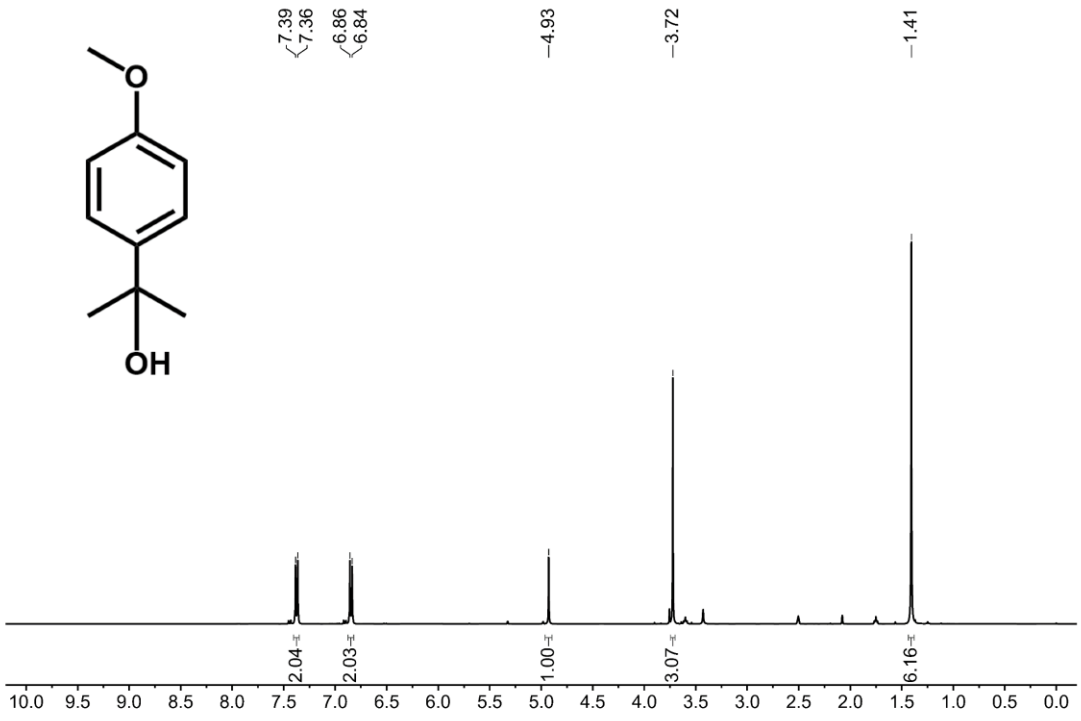
7.39
7.36
6.86
6.84
4.93
3.72
1.41
O
OH
2.04
2.03
1.00
3.07
6.16
10.0 9.5 9.0 8.5 8.0 7.5 7.0 6.5 6.0 5.5 5.0 4.5 4.0 3.5 3.0 2.5 2.0 1.5 1.0 0.5 0.0

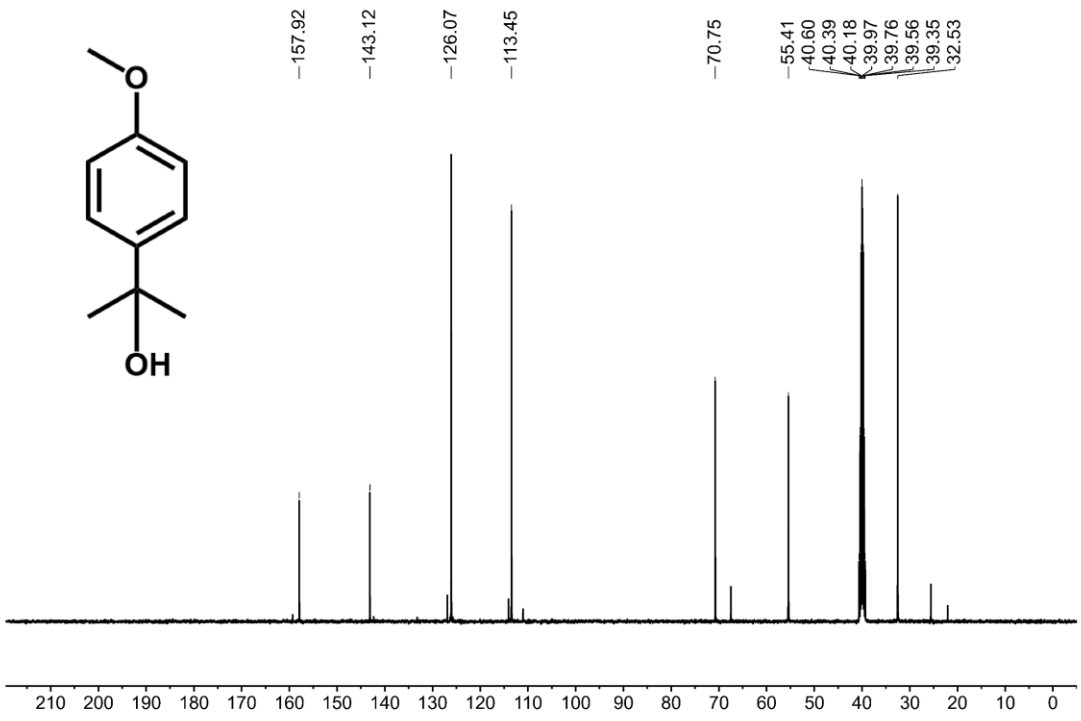
157.92
143.12
126.07
113.45
70.75
55.41
40.60
40.39
40.18
39.97
39.76
39.56
39.35
32.53
O
OH
210 200 190 180 170 160 150 140 130 120 110 100 90 80 70 60 50 40 30 20 10 0

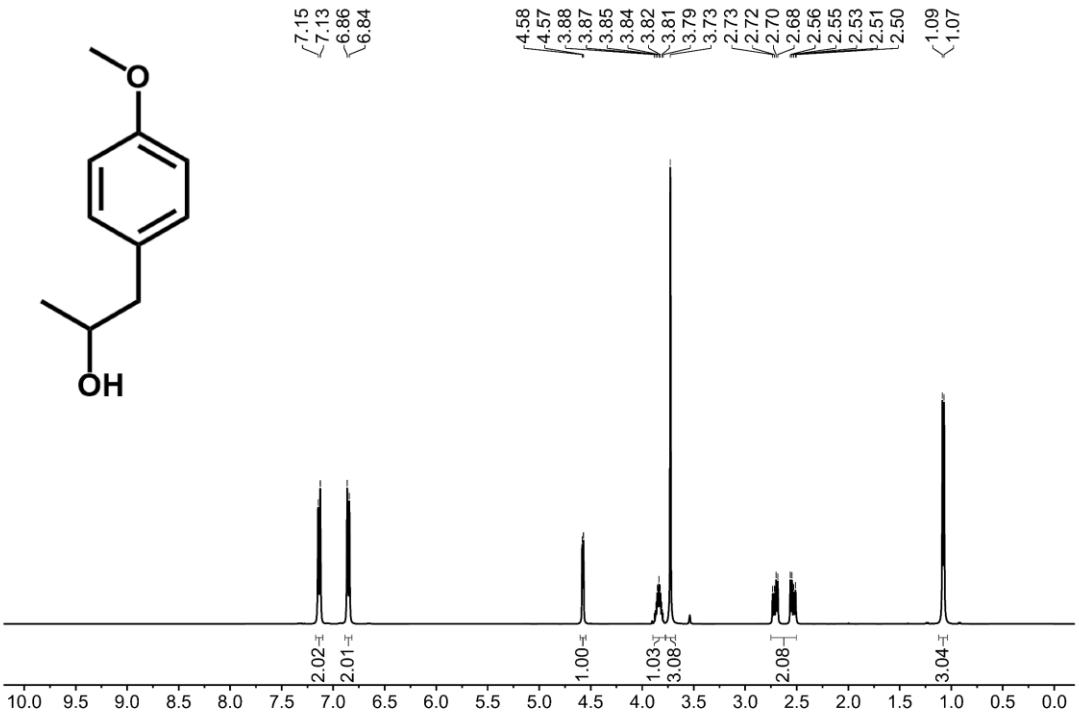
O
OH
7.15
7.13
6.86
6.84
4.58
4.57
3.88
3.87
3.85
3.84
3.82
3.81
3.79
3.73
2.73
2.72
2.70
2.68
2.56
2.55
2.53
2.51
2.50
1.09
1.07
2.02
2.01
1.00
1.03
3.08
2.08
3.04
10.0 9.5 9.0 8.5 8.0 7.5 7.0 6.5 6.0 5.5 5.0 4.5 4.0 3.5 3.0 2.5 2.0 1.5 1.0 0.5 0.0

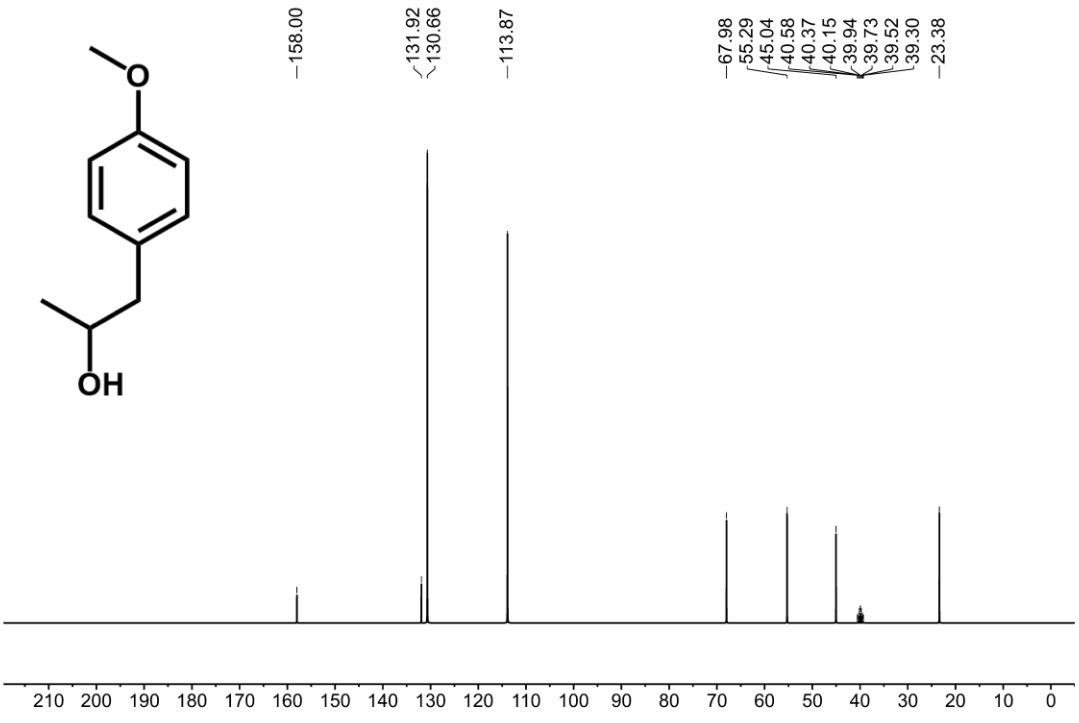
O
OH
158.00
131.92
130.66
113.87
67.98
55.29
45.04
40.58
40.37
40.15
39.94
39.73
39.52
39.30
23.38
210 200 190 180 170 160 150 140 130 120 110 100 90 80 70 60 50 40 30 20 10 0

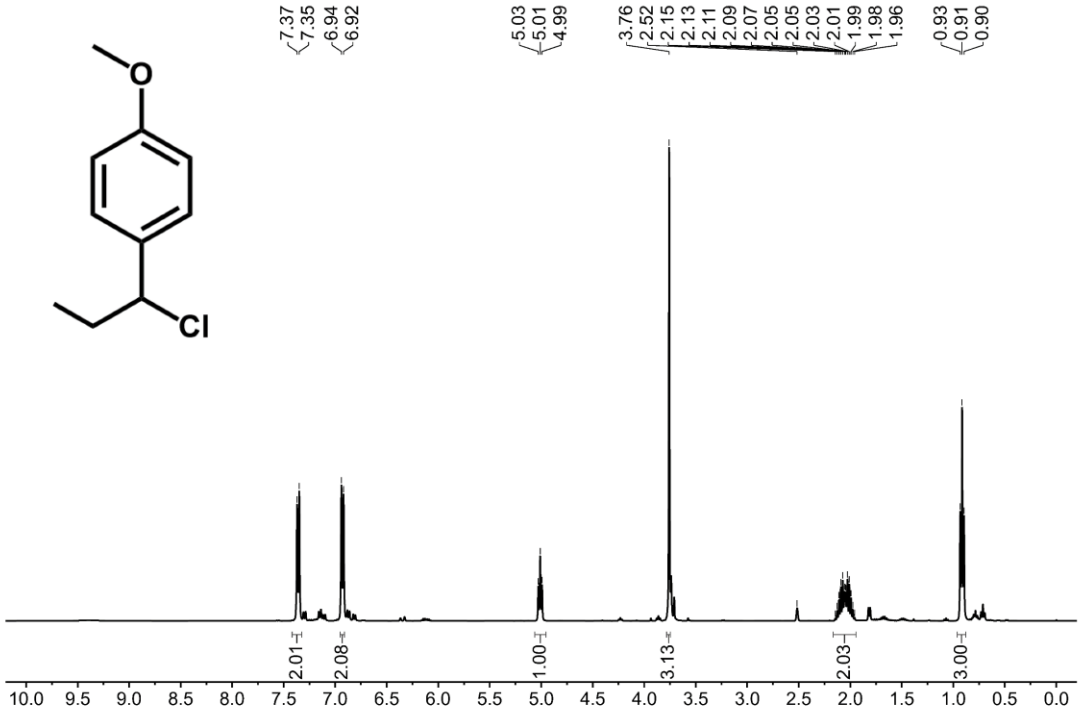
O
Cl
7.37
7.35
6.94
6.92
5.03
5.01
4.99
3.76
2.52
2.15
2.13
2.11
2.09
2.07
2.05
2.05
2.03
2.01
1.99
1.98
1.96
0.93
0.91
0.90
2.01
2.08
1.00
3.13
2.03
3.00
10.0 9.5 9.0 8.5 8.0 7.5 7.0 6.5 6.0 5.5 5.0 4.5 4.0 3.5 3.0 2.5 2.0 1.5 1.0 0.5 0.0

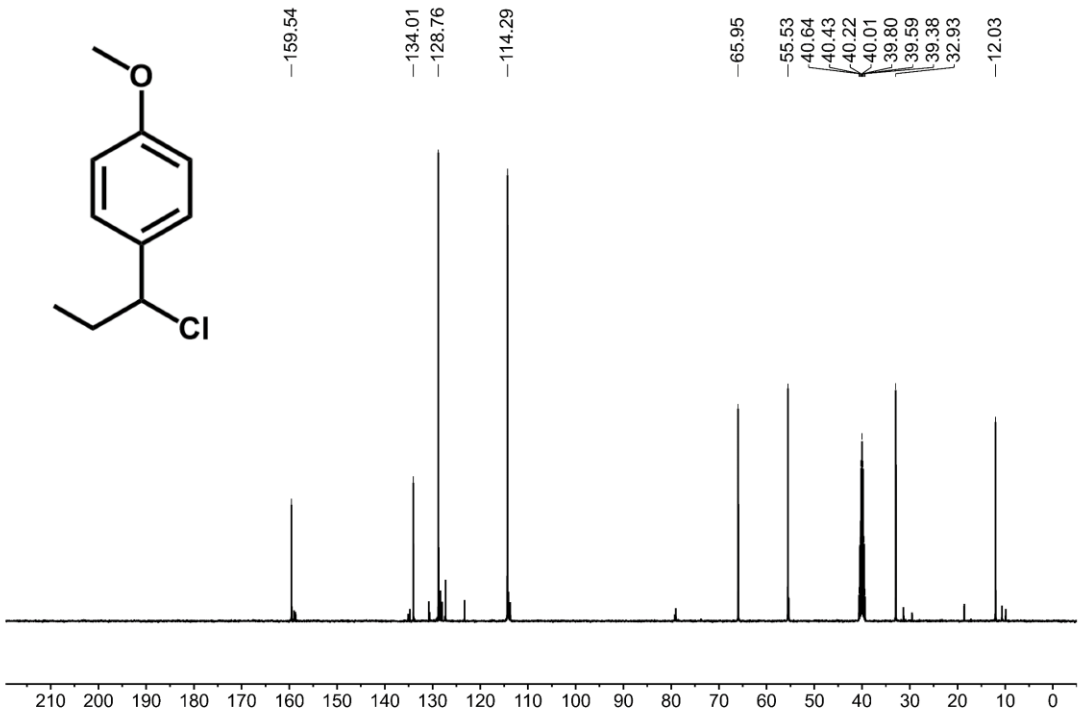
O
Cl
159.54
134.01
128.76
114.29
65.95
55.53
40.64
40.43
40.22
40.01
39.80
39.59
39.38
32.93
12.03
210 200 190 180 170 160 150 140 130 120 110 100 90 80 70 60 50 40 30 20 10 0

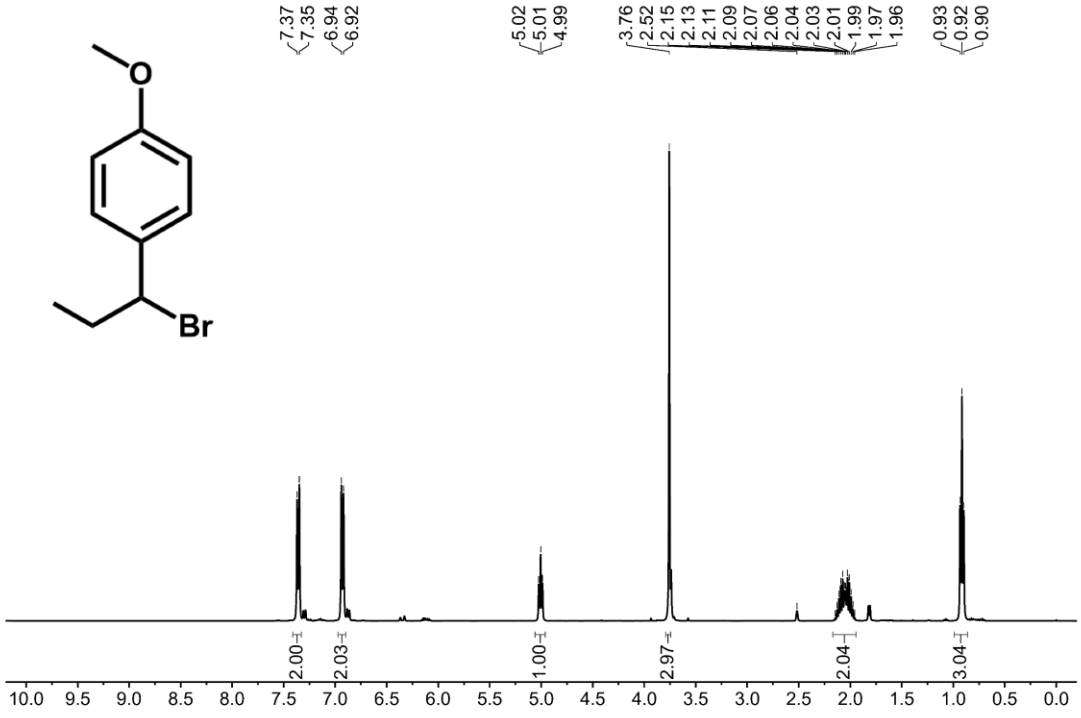
7.37
7.35
6.94
6.92
5.02
5.01
4.99
3.76
2.52
2.15
2.13
2.11
2.09
2.07
2.06
2.04
2.03
2.01
1.99
1.97
1.96
0.93
0.92
0.90
O
Br
2.00
2.03
1.00
2.97
2.04
3.04
10.0 9.5 9.0 8.5 8.0 7.5 7.0 6.5 6.0 5.5 5.0 4.5 4.0 3.5 3.0 2.5 2.0 1.5 1.0 0.5 0.0

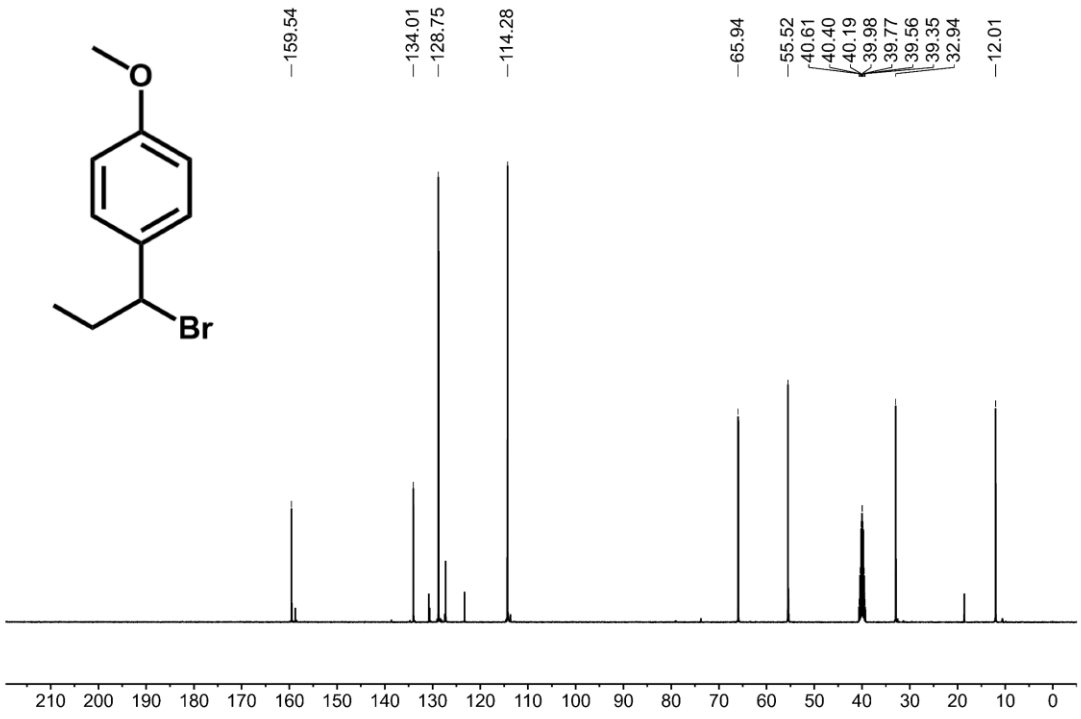
159.54
134.01
128.75
114.28
65.94
55.52
40.61
40.40
40.19
39.98
39.77
39.56
39.35
32.94
12.01
O
Br
210 200 190 180 170 160 150 140 130 120 110 100 90 80 70 60 50 40 30 20 10 0

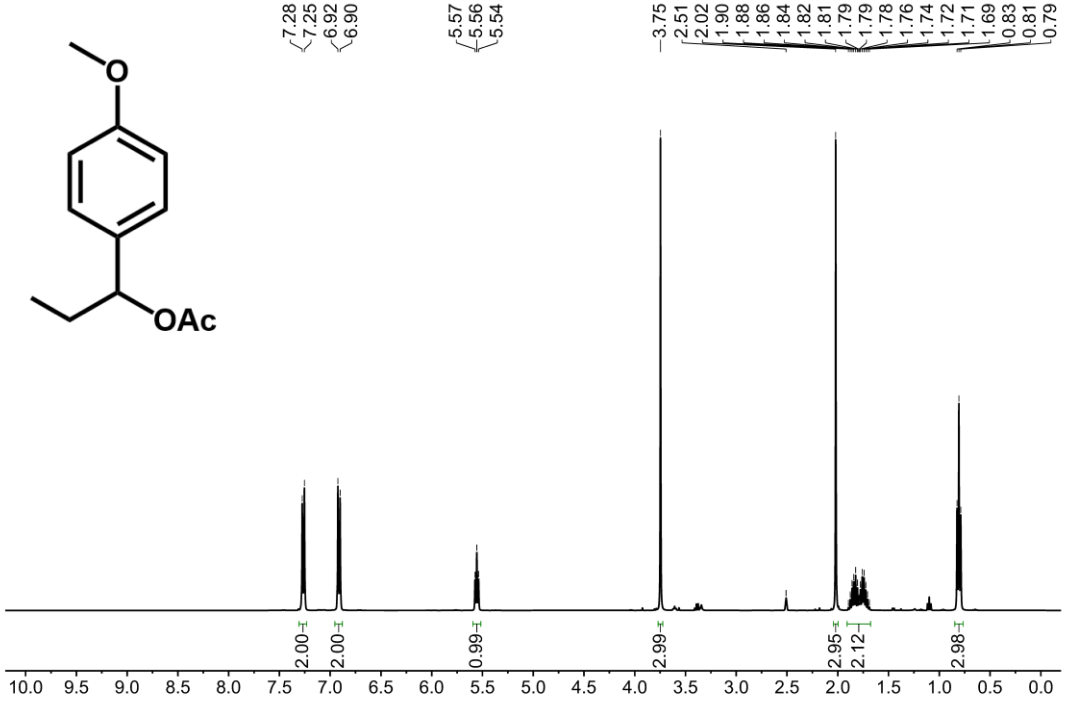
7.28
7.25
6.92
6.90
5.57
5.56
5.54
3.75
2.51
2.02
1.90
1.88
1.86
1.84
1.82
1.81
1.79
1.79
1.78
1.76
1.74
1.72
1.71
1.69
0.83
0.81
0.79
O
OAc
2.00
2.00
0.99
2.99
2.95
2.12
2.98
10.0 9.5 9.0 8.5 8.0 7.5 7.0 6.5 6.0 5.5 5.0 4.5 4.0 3.5 3.0 2.5 2.0 1.5 1.0 0.5 0.0

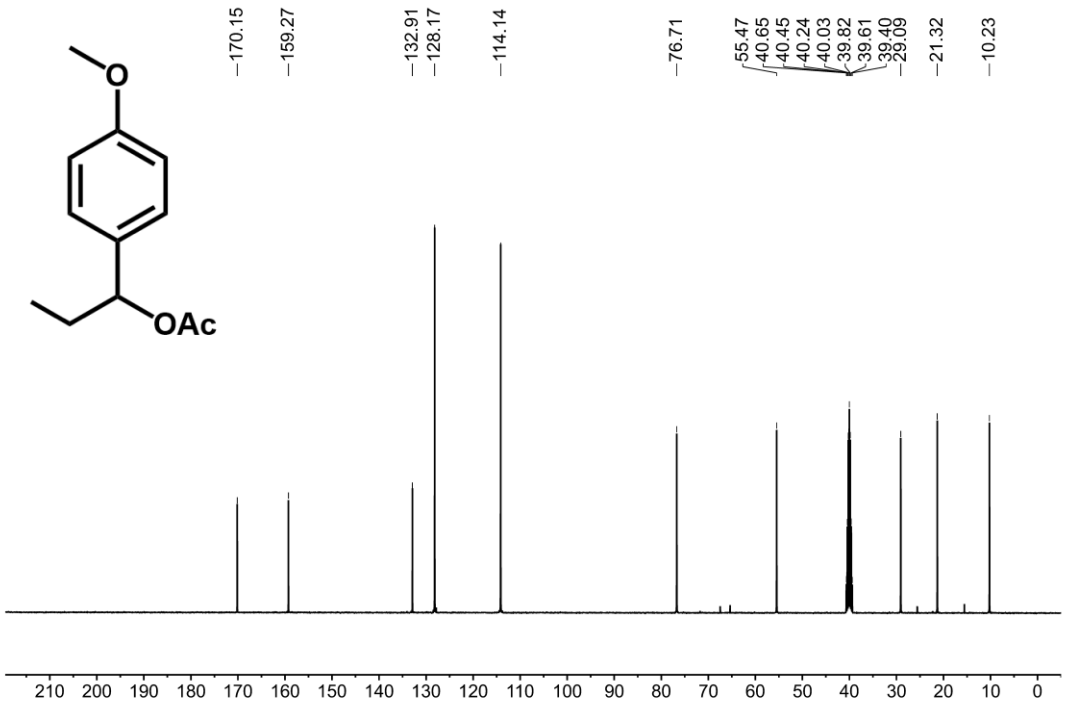
170.15
159.27
132.91
128.17
114.14
76.71
55.47
40.65
40.45
40.24
40.03
39.82
39.61
39.40
29.09
21.32
10.23
O
OAc
210 200 190 180 170 160 150 140 130 120 110 100 90 80 70 60 50 40 30 20 10 0

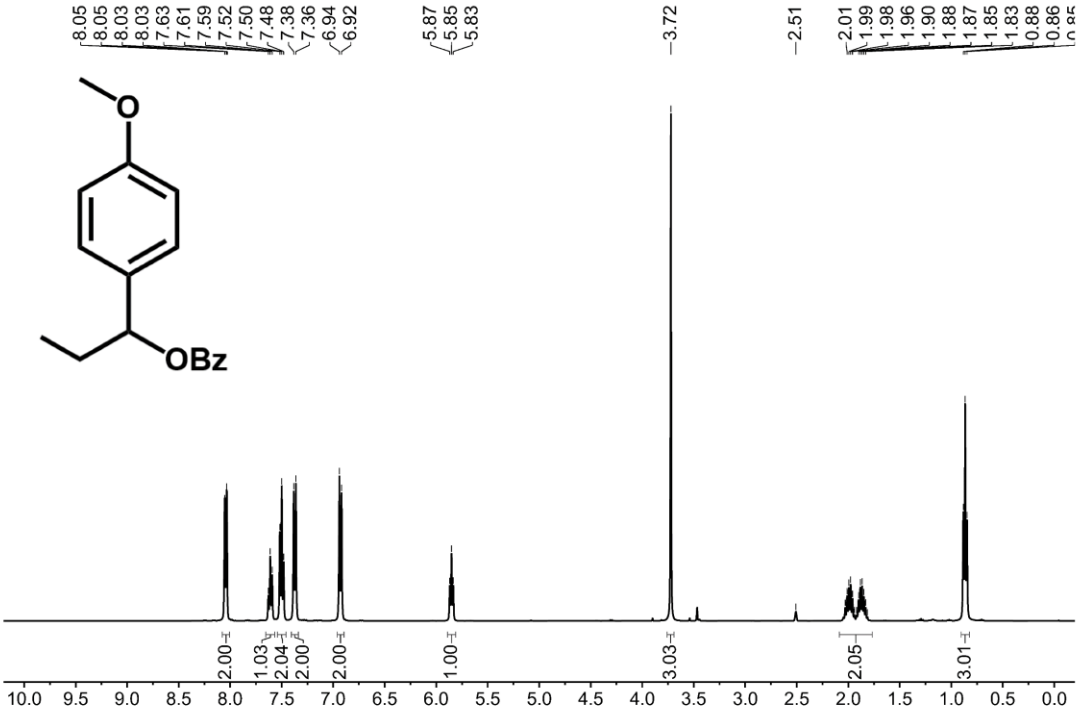
8.05
8.05
8.03
8.03
7.63
7.61
7.59
7.52
7.50
7.48
7.38
7.36
6.94
6.92
5.87
5.85
5.83
3.72
2.51
2.01
1.99
1.98
1.96
1.90
1.88
1.87
1.85
1.83
0.88
0.86
O
OBz
2.00
1.03
2.04
2.00
2.00
1.00
3.03
2.05
3.01
10.0 9.5 9.0 8.5 8.0 7.5 7.0 6.5 6.0 5.5 5.0 4.5 4.0 3.5 3.0 2.5 2.0 1.5 1.0 0.5 0.0

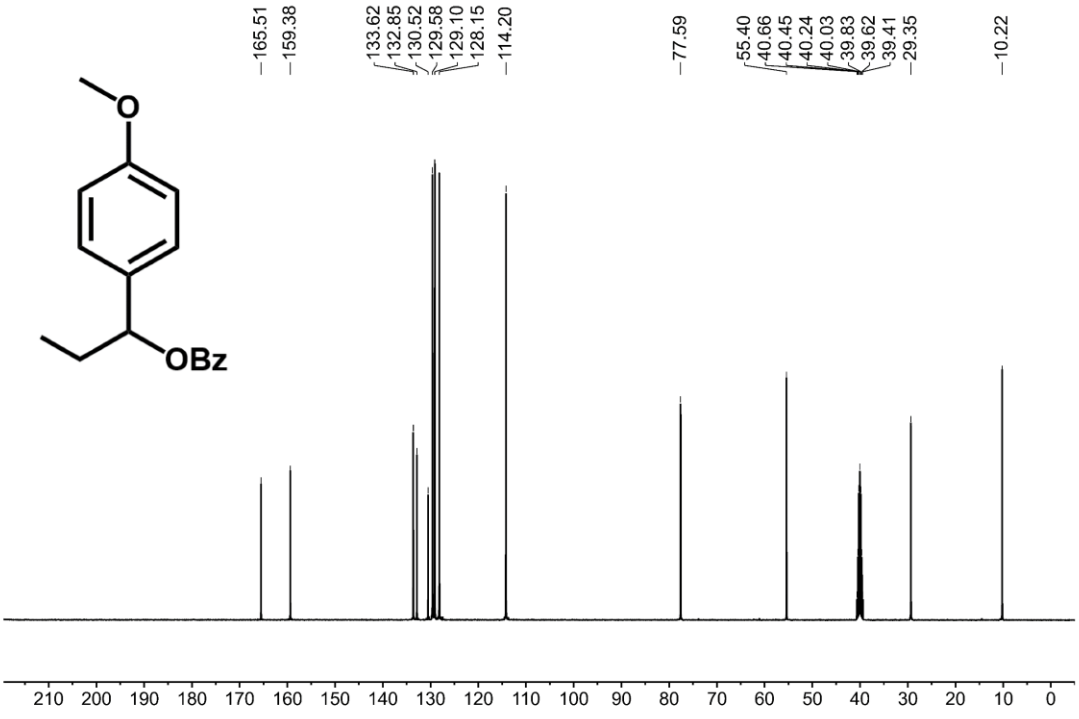
165.51
159.38
133.62
132.85
130.52
129.58
129.10
128.15
114.20
77.59
55.40
40.66
40.45
40.24
40.03
39.83
39.62
39.41
29.35
10.22
O
OBz
210 200 190 180 170 160 150 140 130 120 110 100 90 80 70 60 50 40 30 20 10 0

REFERENCES AND NOTES

1. S.-i. Niwa, M. Eswaramoorthy, J. Nair, A. Raj, N. Itoh, H. Shoji, T. Namba, F. Mizukami, A one-step conversion of benzene to phenol with a palladium membrane. *Science* **295**, 105–107 (2002).

2. F. Zhu, J. A. Johnson, D. W. Ablin, G. A. Ernst, Market and technology overview, in *Efficient Petrochemical Processes: Technology, Design and Operation* (Wiley, ed. 1, 2020), pp. 21–22.

3. H. Liu, T. Jiang, B. Han, S. Liang, Y. Zhou, Selective phenol hydrogenation to cyclohexanone over a dual supported Pd-Lewis acid catalyst. *Science* **326**, 1250–1252 (2009).

4. Y. Morimoto, S. Bunno, N. Fujieda, H. Sugimoto, S. Itoh, Direct hydroxylation of benzene to phenol using hydrogen peroxide catalyzed by nickel complexes supported by pyridylalkylamine ligands. *J. Am. Chem. Soc.* **137**, 5867–5870 (2015).

5. P. T. Tanev, M. Chibwe, T. J. Pinnavaia, Titanium-containing mesoporous molecular sieves for catalytic oxidation of aromatic compounds. *Nature* **368**, 321–323 (1994).

6. T. Zhang, D. Zhang, X. Han, T. Dong, X. Guo, C. Song, R. Si, W. Liu, Y. Liu, Z. Zhao, Preassembly strategy to fabricate porous hollow carbonitride spheres inlaid with single Cu-N_3 sites for selective oxidation of benzene to phenol. *J. Am. Chem. Soc.* **140**, 16936–16940 (2018).

7. W. P. Deng, Y. Z. Wang, S. Zhang, K. M. Gupta, M. J. Hulsey, H. Asakura, L. M. Liu, Y. Han, E. M. Karp, G. T. Beckham, P. J. Dyson, J. W. Jiang, T. Tanaka, Y. Wang, N. Yan, Catalytic amino acid production from biomass-derived intermediates. *Proc. Natl. Acad. Sci. U.S.A.* **115**, 5093–5098 (2018).

8. A. J. Ragauskas, G. T. Beckham, M. J. Biddy, R. Chandra, F. Chen, M. F. Davis, B. H. Davison, R. A. Dixon, P. Gilna, M. Keller, P. Langan, A. K. Naskar, J. N. Saddler, T. J. Tschaplinski, G. A. Tuskan, C. E. Wyman, Lignin valorization: Improving lignin processing in the biorefinery. *Science* **344**, 709–719 (2014).

9. Y. Shao, Q. N. Xia, L. Dong, X. H. Liu, X. Han, S. F. Parker, Y. Q. Cheng, L. L. Daemen, A. J. Ramirez-Cuesta, S. H. Yang, Y. Q. Wang, Selective production of arenes via direct lignin upgrading over a niobium-based catalyst. *Nat. Commun.* **8**, 16104 (2017).

10. X. J. Wu, X. T. Fan, S. J. Xie, J. C. Lin, J. Cheng, Q. H. Zhang, L. Y. Chen, Y. Wang, Solar energy-driven lignin-first approach to full utilization of lignocellulosic biomass under mild conditions. *Nat. Catal.* **1**, 772–780 (2018).

11. H. Q. Zeng, D. W. Cao, Z. H. Qiu, C. J. Li, Palladium-catalyzed formal cross-coupling of diaryl ethers with amines: Slicing the 4-O-5 linkage in lignin models. *Angew. Chem. Int. Ed.* **57**, 3752–3757 (2018).

12. Y. H. Liao, S. F. Koelewijn, G. V. den Bossche, J. V. Aelst, S. V. den Bosch, T. Renders, K. Navare, T. NicolaI, K. V. Aelst, M. Maesen, H. Matsushima, J. Thevelein, K. V. Acker, B. Lagrain, D. Verboekend, B. F. Sels, A sustainable wood biorefinery for low-carbon footprint chemicals production. *Science* **367**, 1385–1390 (2020).

13. M. Wang, M. J. Liu, H. J. Li, Z. T. Zhao, X. C. Zhang, F. Wang, Dealkylation of lignin to phenol via oxidation-hydrogenation strategy. *ACS Catal.* **8**, 6837–6843 (2018).

14. P. Sudarsanam, E. Peeters, E. V. Makshina, V. I. Parvulescu, B. F. Sels, Advances in porous and nanoscale catalysts for viable biomass conversion. *Chem. Soc. Rev.* **48**, 2366–2421 (2019).

15. A. Rahimi, A. Ulbrich, J. J. Coon, S. S. Stahl, Formic-acid-induced depolymerization of oxidized lignin to aromatics. *Nature* **515**, 249–252 (2014).

16. W. Lan, J. B. de Bueren, J. S. Luterbacher, Highly selective oxidation and depolymerization of α, γ-diol-protected lignin. *Angew. Chem. Int. Ed.* **58**, 2649–2654 (2019).

17. L. Shuai, M. T. Amiri, Y. M. Questell-Santiago, F. Héroguel, Y. D. Li, H. Kim, R. Meilan, C. Chapple, J. Ralph, J. S. Luterbacher, Formaldehyde stabilization facilitates lignin monomer production during biomass depolymerization. *Science* **354**, 329–333 (2016).

18. Z. Sun, B. Fridrich, A. de Santi, S. Elangovan, K. Barta, Bright side of lignin depolymerization: Toward new platform chemicals. *Chem. Rev.* **118**, 614–678 (2018).

19. T. Renders, W. Schutyser, S. V. den Bosch, S. F. Koelewijn, T. Vangeel, C. M. Courtin, B. F. Sels, Influence of acidic (H_3PO_4) and alkaline (NaOH) additives on the catalytic reductive fractionation of lignocellulose. *ACS Catal.* **6**, 2055–2066 (2016)

20. D. J. McClelland, P. H. Galebach, A. H. Motagamwala, A. M. Wittrig, S. D. Karlen, J. S. Buchanan, J. A. Dumesic, G. W. Huber, Supercritical methanol depolymerization and hydrodeoxygenation of lignin and biomass over reduced copper porous metal oxides. *Green Chem.* **21**, 2988–3005 (2019)

21. S. Toppi, C. Thomas, C. Sayag, D. Brodzki, K. Fajerwerg, F. L. Peltier, C. Travers, G. D. Mariadassoua, On the radical cracking of n-propylbenzene to ethylbenzene or toluene over Sn/Al_2O_3-Cl catalysts under reforming conditions. *J. Catal.* **230**, 255–268 (2005).

22. A. J. Smaligo, M. Swain, J. C. Quintana, M. F. Tan, D. A. Kim, O. Kwon, Hydrodealkenylative $C(sp^3)$-$C(sp^2)$ bond fragmentation. *Science* **364**, 681–685 (2019).

23. S. K. Murphy, J. W. Park, F. A. Cruz, V. M. Dong, Rh-catalyzed C-C bond cleavage by transfer hydroformylation. *Science* **347**, 56–60 (2015).

24. A. Corma, From microporous to mesoporous molecular sieve materials and their use in catalysis. *Chem. Rev.* **97**, 2373–2419 (1997).

25. C. Fan, X. Y. Lv, L. J. Xiao, J. H. Xie, Q. L. Zhou, Alkenyl exchange of allylamines via nickel(0)-catalyzed C-C bond cleavage. *J. Am. Chem. Soc.* **141**, 2889–2893 (2019).

26. S. Hu, T. Shima, Z. Hou, Carbon–carbon bond cleavage and rearrangement of benzene by a trinuclear titanium hydride. *Nature* **512**, 413–415 (2014)

27. Y. Liu, X. Yuan, X. Guo, X. Zhang, B. Chen, Efficient 2-aryl benzothiazole formation from acetophenones, anilines, and elemental sulfur by iodine-catalyzed oxidative C(CO)-C(alkyl) bond cleavage. *Tetrahedron* **74**, 6057–6062 (2018).

28. M. Wang, J. M. Lu, L. H. Li, H. F. Liu, F. Wang, Oxidative C(OH)-C bond cleavage of secondary alcohols to acids over a copper catalyst with molecular oxygen as the oxidant. *J. Catal.* **348**, 160–167 (2017).

29. H. Sun, C. Yang, F. Gao, Z. Li, W. Xia, Oxidative C-C bond cleavage of aldehydes via visible-light photoredox catalysis. *Org. Lett.* **15**, 624–627 (2013).

30. J. B. Roque, Y. Kuroda, L. T. Gottemann, R. Sarpong, Deconstructive fluorination of cyclic amines by carbon-carbon cleavage. *Science* **361**, 171–174 (2018).

31. D. L. Zhu, L. Y. Wang, D. Fan, N. N. Yan, S. J. Huang, S. T. Xu, P. Guo, M. Yang, J. M. Zhang, P. Tian, Z. M. Liu, A bottom-up strategy for the synthesis of highly siliceous faujasite-type zeolite. *Adv. Mater.* **32**, 2000272 (2020).

32. Q. L. Meng, H. L. Fan, H. Z. Liu, H. C. Zhou, Z. H. He, Z. W. Jiang, T. B. Wu, B. X. Han, Efficient transformation of anisole into methylated phenols over high silica HY zeolites under mild conditions. *ChemCatChem* **7**, 2831–2835 (2015).

33. T.-Q. Yuan, S.-N. Sun, F. Xu, R.-C. Sun, Characterization of lignin structures and lignin-carbohydrate complex (LCC) linkages by quantitative ^{13}C and 2D HSQC NMR spectroscopy. *J. Agric. Food Chem.* **59**, 10604–10614 (2011).

34. H. J. Li, A. Bunrit, J. M. Lu, Z. Y. Gao, N. C. Luo, H. F. Liu, F. Wang, Photocatalytic cleavage of aryl ether in modified lignin to nonphenolic aromatics. *ACS Catal.* **9**, 8843–8851 (2019).

35. A. K. Deepa, P. L. Dhepe, Lignin depolymerization into aromatic monomers over solid acid catalysts. *ACS Catal.* **5**, 365–379 (2015).

36. E. Blomsma, J. A. Martens, P. A. Jacobs, Reaction mechanisms of isomerization and cracking of heptane on Pd/H-beta zeolite. *J. Catal.* **155**, 141–147 (1995).

37. X. Zhou, C. Wang, Y. Y. Chu, J. Xu, Q. Wang, G. D. Qi, X. L. Zhao, N. D. Feng, F. Deng, Observation of an oxonium ion intermediate in ethanol dehydration to ethene on zeolite. *Nat. Commun.* **10**, 1961 (2019).

38. A. A. Gabrienko, S. S. Arzumanov, A. V. Toktarev, A. G. Stepanov, Solid-state NMR characterization of the structure of intermediates formed from olefins on metal oxides (Al_2O_3 and Ga_2O_3). *J. Phys. Chem. C* **116**, 21430–21438 (2012).

39. M. Zardkoohi, J. F. Haw, J. H. Lunsford, Solid-state NMR evidence for the formation of carbocations from propene in acidic zeolite-Y. *J. Am. Chem. Soc.* **109**, 5278–5280 (1987).

40. M. Haouas, S. Walspurger, F. Taulelle, J. Sommer, The initial stages of solid acid-catalyzed reactions of adsorbed propane. A mechanistic study by in situ MAS NMR. *J. Am. Chem. Soc.* **126**, 599–606 (2004).

41. X. Y. Zhang, D. X. Liu, D. D. Xu, S. S. Asahina, K. A. Cychosz, K. V. Agrawal, Y. A. Wahedi, A. Bhan, S. A. Hashimi, O. Terasaki, M. Thommes, M. Tsapatsis, Synthesis of self-pillared zeolite nanosheets by repetitive branching. *Science* **336**, 1684–1687 (2012).

42. E. Lippmaa, A. Samoson, M. Magi, High-resolution ^{27}Al NMR of aluminosilicates. *J. Am. Chem. Soc.* **108**, 1730–1735 (1986).

43. J. A. van Bokhoven, D. C. Koningsberger, P. Kunkeler, H. van Bekkum, A. P. M. Kentgens, Stepwise dealumination of zeolite beta at specific T-sites observed with ^{27}Al MAS and ^{27}Al MQ MAS NMR. *J. Am. Chem. Soc.* **122**, 12842–12847 (2000).

44. J. O. Ehresmann, W. Wang, B. Herreros, D. P. Luigi, T. N. Venkatraman, W. G. Song, J. B. Nicholas, J. F. Haw, Theoretical and experimental investigation of the effect of proton transfer on the ^{27}Al MAS NMR line shapes of zeolite-adsorbate complexes: An independent measure of solid acid strength. *J. Am. Chem. Soc.* **124**, 10868–10874 (2002).

45. G. Busca, Acid catalysts in industrial hydrocarbon chemistry. *Chem. Rev.* **107**, 5366–5410 (2007).

46. I. Kiricsi, H. Forster, G. Tasi, J. B. Nagy, Generation, characterization, and transformations of unsaturated carbenium ions in zeolites. *Chem. Rev.* **99**, 2085–2114 (1999).

47. Y. D. Li, L. Shuai, H. Kim, A. H. Motagamwala, J. K. Mobley, F. X. Yue, Y. Tobimatsu, D. Havkin-Frenkel, F. Chen, R. A. Dixon, J. S. Luterbacher, J. A. Dumesic, J. Ralph, An "ideal lignin" facilitates full biomass utilization. *Sci. Adv.* **4**, eaau2968 (2018).

48. C. A. Emeis, Determination of integrated molar extinction coefficients for infrared absorption bands of pyridine adsorbed on solid acid catalysts. *J. Catal.* **141**, 347–354 (1993).

49. W. J. J. Huijgen, J. H. Reith, H. den Uil, Pretreatment and fractionation of wheat straw by an acetone-based organosolv process. *Ind. Eng. Chem. Res.* **49**, 10132–10140 (2010).

50. Z. Cao, J. Engelhardt, M. Dierks, M. T. Clough, G. H. Wang, E. Heracleous, A. Lappas, R. Rinaldi, F. Schuth, Catalysis meets nonthermal separation for the production of (Alkyl) phenols and hydrocarbons from pyrolysis oil. *Angew. Chem. Int. Ed.* **56**, 2334–2339 (2017).

51. K. R. Graham, C. Cabanetos, J. P. Jahnke, M. N. Idso, A. El Labban, Guy O. N. Ndjawa, T. Heumueller, K. Vandewal, A. Salleo, B. F. Chmelka, A. Amassian, P. M. Beaujuge, M. D. McGehee, Importance of the donor: Fullerene intermolecular arrangement for high-efficiency organic photovoltaics. *J. Am. Chem. Soc.* **136**, 9608–9618 (2014).

52. G. Kresse, D. Joubert, From ultrasoft pseudopotentials to the projector augmented-wave method. *Phys. Rev. B* **59**, 1758–1775 (1999).

53. S. Grimme, J. Antony, S. Ehrlich, H. Krieg, A consistent and accurate ab initio parametrization of density functional dispersion correction (DFT-D) for the 94 elements H-Pu. *J. Chem. Phys.* **132**, 154104 (2010).

54. G. Henkelman, B. P. Uberuaga, H. Jonsson, A climbing image nudged elastic band method for finding saddle points and minimum energy paths. *J. Chem. Phys.* **113**, 9901–9904 (2000).

55. M. Besora, P. Vidossich, A. Lledos, G. Ujaque, F. Maseras, Calculation of reaction free energies in solution: A comparison of current approaches. *J. Phys. Chem. A* **122**, 1392–1399 (2018).

56. X. K. Gu, B. Liu, J. Greeley, First-principles study of sructure sensitivity of ethylene glycol conversion on platinum. *ACS Catal.* **5**, 2623–2631 (2015).

57. L. B. Zhang, L. S. Yan, Z. M. Wang, D. D. Laskar, M. S. Swita, J. R. Cort, B. Yang, Characterization of lignin derived from water-only and dilute acid flowthrough pretreatment of poplar wood at elevated temperatures. *Biotechnol. Biofuels* **8**, 203 (2015).

58. W. Zhao, X. Li, H. Li, X. Zheng, H. Ma, J. Long, X. Li, Selective hydrogenolysis of lignin catalyzed by the cost-effective Ni metal supported on alkaline MgO. *ACS Sustain. Chem. Eng.* **7**, 19750–19760 (2019).

59. S. Wu, D. Argyropoulos, An improved method for isolating lignin in high yield and purity. *J. Pulp Pap. Sci.* **29**, 235–240 (2003).

60. H. Rabemanolontsoa, S. Saka, Comparative study on chemical composition of various biomass species. *RSC Adv.* **3**, 3946–3956 (2013).